

**INTERNATIONAL JOURNAL OF
ENVIRONMENTAL TRENDS**

**I
J
E
N
T**



2019 (3):2 – DECEMBER

<https://dergipark.org.tr/ijent>

International Journal of Environmental Trends (IJENT)

International Journal of Environmental Trends (IJENT) is a journal which was established in November 2017. IJENT is an **internationally peer-reviewed** and indexed journal which has been published regularly in **June, and December** in 2 issues per year, starting from 2017 in the areas of science, engineering and natural sciences. All articles submitted for publication are considered by the editor and editorial advisory board. Scientific studies are published in our journal in the form of original research articles written in **English**.

As the editors of the journal, we aim to provide a unique communication and discussion platform for environmental scientists as well as any discipline of science aiming the protection of the environment.

The main goals of IJENT are

- Presenting current researches being carried out in the environmental engineering area for scientists, scholars, engineers and students from the universities all around the World
- Linking pioneering research with present and emerging/up-coming environmental issues
- Discussing fundamentals of pollutant fate in the environment
- Generating awareness for emerging environmental problems

Providing opportunities for the authors to exchange new ideas and application experiences by article, to establish business or research relations and to find global partners for future collaboration.

Editor in Chief

ISSN 2602-4160 - Period Biannually - Founded: 2017 - Publisher Muhammed Kamil
ÖDEN

EDITOR IN CHIEF

Dr. Muhammed Kamil ODEN (Selcuk University, Turkey)

EDITORS&SCIENTIFIC COMMITTEE

Prof. Dr. Adil K. Al-Tamimi, American University of Sharjah, United Arab Emirates

Pof. Dr. Christopher Imoukhai UNUEVHO, Federal University of Technology, Minna, Nigeria

Prof. Dr. Cristiano Poletto, Federal University of Rio Grande do Sul (UFRGS) - Brazil

Prof.Dr. Gordan BEDEKOVIĆ, University of Zagreb, Croatia

Prof. Dr. Krishna R. Reddy, University of Illinois at Chicago, USA

Prof. Dr. Serkan SAHINKAYA (Nevsehir Haci Bektas Veli University, Turkey)

Assoc. Prof. Dr. Birol KAYRANLI (ILBANK Incorporation, Turkey)

Assoc. Prof. Dr. Ekrem MUTLU (Kastamonu University, Turkey)

Assoc. Prof. Dr. Erkan KALIPCI (Giresun University, Turkey)

Dr. İrfan ÖZER, (Selcuk University, Turkey)

Dr. Oğuzhan GÖK (Aksaray University, Turkey)

Dr. Yasemin PINARKARA (Selcuk University, Turkey)

CONTENTS

Research Articles

Chemical Vapor Deposition of Poly(hydroxyethyl methacrylate-glycidyl methacrylate) Thin Film Coatings for Immobilization of Human Serum Albumin
Fatma SARIİPEK , Esra ÇAĞIL , Mustafa KARAMAN

Pages 96 -119

The Effects of Natural Life Islands Planning on Izmir Bay Ecosystem
Tarık İLHAN, A. Hüsnü ERONAT, Ezgi TALAS, Muhammet DUMAN

Pages 120 - 126

Evaluation of Boron Concentration in Akhüyük (Ereğli) Geothermal Source in terms of Medical Geology
Bilgehan Yabgu HORASAN, Alican ÖZTÜRK

Pages 127 - 141

Variation of Fuel Characteristics of Diesel with the Use of Biodiesel and Alcohols (ethanol, methanol, 2-propanol, 2-butanol)
Ibrahim Aslan RESİTOĞLU

Pages 142 - 150

The Quantitative Effects of Different Growing Media on the Seedling Growth of Aubergine (Solanum melongena L.) and Cucumber (Cucumis sativus L.) in Autumn
Murat DEMİRSOY, Sezgin UZUN

Pages 151 - 158

An Investigation of Gross Error Angle in a Connecting Traverse with a $\pm 200^{gon}$ Difference
Nuri ERDEM, Fazlı Engin TOMBUŞ, Hüseyin İNCE

Pages 159 - 174

Production of Hand Sterilization Fluid of Herbal Origin
Sergen CETEBOZAN , Hatice Kubra OZGUL , Sibel YİĞİTARSLAN

Pages 175 - 184



Research Article

Chemical Vapor Deposition of Poly(hydroxyethyl methacrylate-glycidyl methacrylate) Thin Film Coatings for Immobilization of Human Serum Albumin

Fatma Sariipek¹ , Esra Maltaş Çağır²  and Mustafa Karaman^{1,3} 

¹Department of Chemical Engineering, Konya Technical University, Konya 42030, Turkey

²Department of Basic Pharmacy Sciences, Selcuk University, Konya 42030,

³Advanced Technology Research & Application Center, Selcuk University, Konya 42030, Turkey

Abstract

In this study, poly(2-hydroxyethyl methacrylate-glycidyl methacrylate) (P(HEMA-GMA)) thin films were deposited on crosslinked polyvinyl alcohol (PVA) supports by initiated chemical vapor deposition (iCVD). Use of the tert-butyl peroxide as an initiator allowed very high deposition rates up to 125 nm/min at a filament temperature of 280 °C. FTIR and XPS analyses of the deposited films confirmed that the epoxide functionality of the copolymers increased with increasing glycidyl methacrylate fraction in the reactor inlet. The potential of the glycidyl methacrylate containing copolymer films to act as substrates for protein immobilization was revealed. The immobilization of Human Serum Albumin (HSA), which is the main protein to carry fatty acids and metals to target tissues, was carried out via solid phase extraction. The effects of film composition and thickness on binding capacities of the protein to the polymers were studied. The maximum protein binding for the iCVD synthesized copolymer films was found to be 223 µg.cm⁻². Protein binding was also clarified by FTIR, AFM, and SEM analyses. The mild immobilization conditions, easy and rapid membrane preparation, one-step protein binding at substantially higher levels and membrane reusability make iCVD deposited P(HEMA-GMA) films useful for biomolecules immobilization and for several biochemical processes.

Received

18 September 2019

Accepted

19 November 2019

Keywords

iCVD,
Thin film hydrogel
membrane,
P(HEMA-GMA),
Crosslinked PVA,
Protein immobilization,
HSA.

¹ Corresponding Author Email: fatmasariipek@selcuk.edu.tr

INTRODUCTION

Modification of the surface of supporting materials such as polymers, nanoparticles, nanocomposites and thin films have recently been of major interest for biological applications [1-4]. A number of surface modification techniques have widely been used in order to alter the chemical composition and lead to changes on the surface properties of the materials. Some of the methods are plasma-treatment techniques, binding of the specific ligands for targeting biomolecules, blending with other macromolecules and silanization techniques on the surface [5-6]. Many studies have been reported the adsorption or immobilization of the biomolecules such as DNA, oligonucleotides, different types of proteins, antibodies and enzymes on the polymer surfaces, depending on the type of molecules used and the functional groups on the surfaces such as amine, epoxy and thiol groups [7-8]. Most commonly used protein in immobilization study is albumin which is the most abundant protein in the blood. Albumin which has a molar mass of 66.5 kDa is responsible for the transport fatty acids, metals, vitamins and the drugs to the target tissues [9].

In recent years, PHEMA and PHEMA based materials have been used for a variety of applications including immobilization of proteins and enzymes [10-11], controlled release of drugs [12-13], biosensors [13-15], separation of molecules and cells [16-17], and metal-ion adsorption [18-19]. PHEMA based hydrogel thin films can be prepared by various methods, such as, UV initiated graft-polymerization [20], surface-initiated atom transfer radical polymerization [21-22], electrospinning method [23], sol-gel technique [24] and chemical vapor deposition (CVD) [25-27]. CVD is an all-dry method to produce polymeric thin films with good control over film morphology and stoichiometry. In this method, the substrates with complex geometries can be coated with high uniformity and without solvent related damages, which are observed in conventional wet processes [28-29]. Initiated chemical vapor

deposition (iCVD) is a combination of all-dry CVD technique with free radical polymerization process. In iCVD, resistively heated filaments which are placed a few centimeters above the substrate surface provide the activation energy for polymerization reactions. The technique allows polymerization and surface modification to be completed in a single step and enables very high retention of the functional groups because of the low filament temperatures and the lack of the harmful plasma environment [30-31].

Due to their hydrophilic character, chemical stability, and biocompatibility, PHEMA based polymers and copolymers are attractive in biomaterials area for many years [32-33]. The physical and chemical properties of PHEMA can be modified by copolymerization. The introduction of functional epoxy groups on the PHEMA structure can be provided by copolymerization of HEMA with an epoxy group carrying monomer[34]. GMA is an excellent monomer having a reactive epoxy group, which can be directly coupled with a biological molecule via ring opening reactions or further modified into different functional groups. HEMA is able to form a hydrophilic environment on crosslinked PVA sheet (CPS) [35].

In this work, a copolymer thin film containing functional epoxide and hydroxyl groups was synthesized on a PVA support material using iCVD technique to prepare a PHEMA-based thin film hydrogel membrane. A series of P(HEMA-GMA) thin films with varying compositions were prepared and the as-deposited films were characterized chemically by FTIR and XPS methods. The obtained thin film hydrogel (TFH) membranes were used for the immobilization of human serum albumin. The effects of film thickness and composition on immobilization efficiency were examined.

EXPERIMENTAL

Preparation of Crosslinked PVA Sheets

Polyvinyl alcohol (Alfa Aesar, MW=88000-97000 g/mol, degree of hydrolysis= 98-99%) was dissolved in distilled water and stirred at 95 °C for at least 4 h to obtain 2,0 wt % homogeneous aqueous PVA solution. Then the solution was cooled down to room temperature. 1,0 M hydrochloric acid (Aldrich, HCl, % 37) solution was added dropwise to adjust the pH level of the PVA solution (the target pH is about 1). A glutaraldehyde (Merck, GA, 25 wt% in water) solution was subsequently added to initiate the cross-linking reaction. 4 mL of the PVA/GA solution was cast onto the petri dishes of 6 cm diameter. To complete the cross-linking reaction, the PVA sheet were kept in a humid chamber for 6 h and then washed with distilled water.

Preparation of Poly(2-hydroxyethyl methacrylate-co-glycidyl methacrylate) Film

Films were deposited on silicon wafer (100, p type) and crosslinked poly(vinyl alcohol) (PVA) sheets by initiated chemical vapor deposition method in a custom-built vacuum reactor. The schematic representation and details of reactor set-up is given elsewhere [36]. In this reactor, the reactant gases were thermally activated by heating a tungsten filament array (Alfa Aesar) resistively. The filament array containing 12 parallel tungsten filaments was placed 22 mm above the substrate surface and resistively heated to 210, 240 and 280 °C. The substrates are placed on a backside cooled stage maintained at 27 °C. The filament temperature was measured by directly attaching a K-type thermocouple (Omega) to one of the filaments. Reactor feed consisted of glycidyl methacrylate (GMA, 97%), 2-hydroxyethyl methacrylate (HEMA, 95%), and di-tert-butyl peroxide (TBPO, 98%), which were purchased from Sigma Aldrich, and used as-received. Monomers GMA and HEMA were vaporized in separate jars at 65°C and 67 °C, respectively, and metered into the reactor using needle valves. The initiator TBPO was vaporized in a different jar at room temperature and fed to the reactor

by using a mass flow controller (MKS). The flowrates of TBPO and GMA were kept constants at 1 and 2 sccm, respectively during all experiments, while the flow rate of HEMA was varied between 0 and 2 sccm to synthesize copolymer films of varying compositions. Reactor pressure was kept at 300 millitorrs, which was measured and controlled by a capacitance manometer (MKS Baratron) and a downstream butterfly valve operated by a PID pressure controller (MKS), respectively. The reactor was equipped by a laser interferometry system for real time monitoring of the deposition thickness. During the depositions, silicon wafers were placed next to the crosslinked PVA sheets, for characterization purposes, and for interferometric thickness determination. The chemical structures of the resultant PHEMA and PGMA homopolymers and P(HEMA-GMA) copolymer is given in Figure 1.

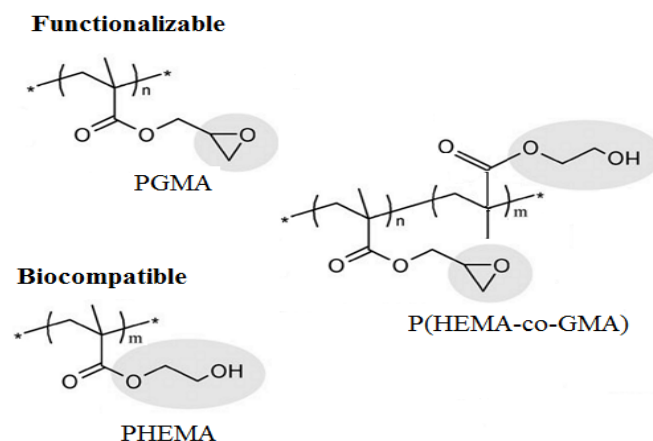


Figure 1. Chemical structures of PGMA, PHEMA, and P(HEMA-GMA).

In the series of iCVD experiments, the only variables were the filament temperature and flow rate of HEMA. For the homopolymers (PHEMA and PGMA, denoted F1-F2 in Table I and copolymer experiments (P(HEMA-GMA), denoted F3 through F7 in Table I, substrate temperature, reactor pressure and flow rates of GMA and TBPO were all kept constant. All runs were carried out to produce films with thickness of 0.5 μm . After iCVD deposition of thin films on crosslinked PVA sheet, the resultant TFH membrane sheets were

cut into 0.6 cm diameter circular discs to be used in the further protein immobilization experiments.

Determination of the swelling rate of the prepared films

The prepared films were allowed to soak in distilled water for 24 h, swollen film were weighed after removing the excess water, dried in vacuum oven at 50 °C for 24 h until constant weight. The swelling rates of the films were calculated as following equation:

Table I. Experimental condition for iCVD of PDPAEMA thin films

sample	temperature (°C)		flow rate (sccm)			reactor	deposition
	Filament	substrate	HEMA	GMA	TBPO	pressure (Torr)	rate (nm/min)
F1	280	27	2		1	0.3	10
F2	280	27		2	1	0.3	25
F3	280	27	0.5	2	1	0.3	54
F4	280	27	1	2	1	0.3	96
F5	280	27	2	2	1	0.3	125
F6	240	27	2	2	1	0.3	78
F7	210	27	2	2	1	0.3	54

$$\text{Swelling rate\%} = \frac{(W_s - W_d)}{W_d} \times 100 \quad (1)$$

where W_s and W_d are the weights of swollen and dry film, respectively

Characterisation of poly(HEMA–GMA) films

Chemical analysis of the as-deposited thin films and TFH membranes was carried out using Fourier Transform Infrared Spectroscopy (FTIR) (Bruker Vertex 70) and X-ray photoelectron spectroscopy (XPS) (Specs spectrophotometer with a monochromatized Al source). FTIR spectra were obtained using a reflectance accessory (Bruker optics) over a spectral range of 800-4000 cm^{-1} at 4 cm^{-1} resolution. All FTIR spectra were baseline corrected and thickness normalized. Film thicknesses during the depositions were monitored by laser interferometry, in which the reflectance of a 633 nm HeNe laser beam (JDS Uniphase) off the polished silicon substrate was monitored by a laser powermeter. In order to check the accuracy of the interferometry, the film thicknesses were also measured ex-situ by a mechanical profiler (AES Nano 500). Surface morphologies of the dried thin films were obtained using scanning electron microscope (JEOL) and atomic force microscope (NtMdt). Contact angle measurements were carried out on a Kruss Easy Drop contact angle goniometer system at ambient temperature. Pure water with a pH close to 7.0 at room temperature was used in static contact angle measurements. A pH-meter (Orion) equipped with a combined glass-Ag/AgCl was used for pH measurements.

Protein Immobilization Experiments

The prepared TFH membranes were mixed with a concentration of 0.15 mg.mL^{-1} of human serum albumin (HSA) in 20 $\text{mM} \times$ Tris, pH 7.4. Each mixture was thumbed for 2 h at 4°C at 0.5654 cm^{-2} of a surface area of TFH membranes. Protein bounded copolymers were separated from supernatant. Albumin bounded particles were also washed with Tris buffer for

chemical characterization. Supernatant was kept at 4°C for analysis of protein concentration. Binding of HSA to copolymers was also confirmed by using fluorescence spectroscopy. For this purpose, intrinsic fluorescence of protein was measured at 280 and 342 nm of excitation and emission wavelengths [37]. Unbounded protein concentration was determined from the equation of calibration curve ($y=29050x+36.882$, $R=0.9943$).

RESULTS AND DISCUSSION

Initiated Chemical Vapor Deposition of P(HEMA-GMA) Thin Films

The deposition rates observed for the PHEMA and PGMA homopolymers are 10 and 25 nm/min, respectively. For iCVD process, the polymerization mechanism is believed to be very similar to the solution phase free radical polymerization, and the polymerization kinetics depends strongly on the surface concentration of species. The fractional saturation ratio, which is the ratio of monomer partial pressure (P_m) to its saturation pressure (P_{sat}) is an important factor to determine the deposition rates. At the given substrate temperature and reactor pressure, P_m/P_{sat} is 0.33 and 0.8 for GMA and HEMA, respectively. The lower deposition rate of PHEMA even at such a high fractional saturation value could be attributed to its low reactivity at the given filament temperature of 280°C. However, when both monomers are fed into the reactor simultaneously; the deposition rates were observed to increase significantly as compared with the homopolymer depositions under similar conditions. The maximum deposition rate for the copolymer is 125 nm/min, which is 12.5-fold higher than the deposition rate of HEMA only polymer. The observed increase in the deposition rate may be due to the interactions between the monomers that have different polarities, which were previously observed in free radical copolymerization reactions[38]. As can be seen in Figure 2, any increase in the HEMA flowrate resulted in higher deposition rates and this dependency is expected for free radical polymerizations.

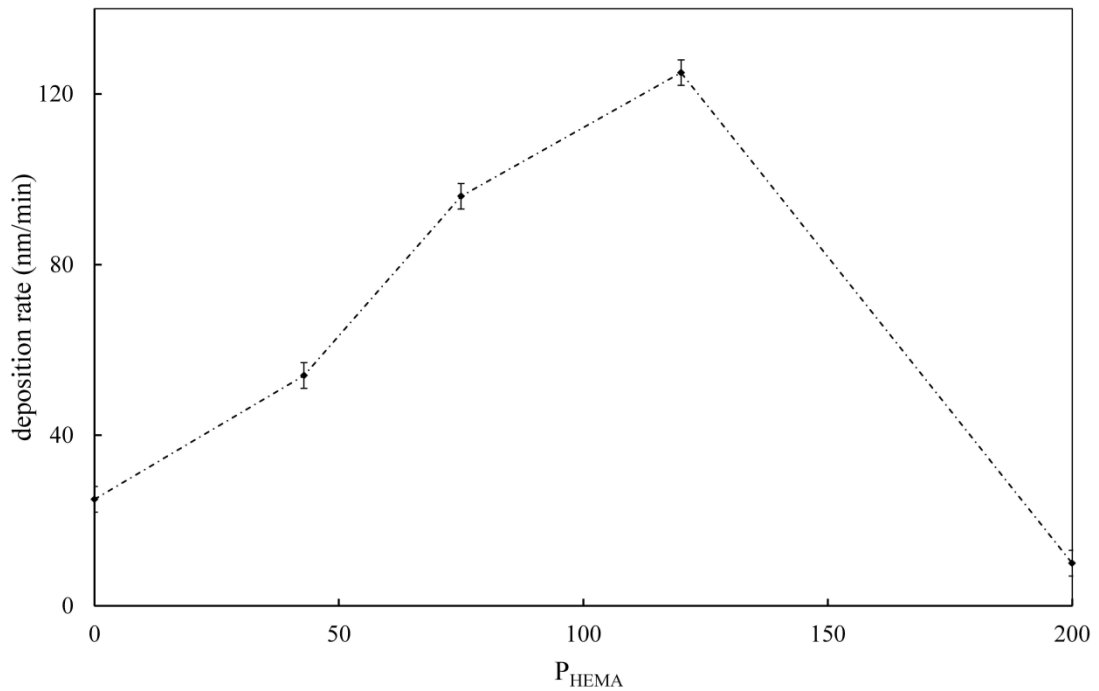


Figure 2. Deposition rate as a function of HEMA partial pressure ($T_f=280$ °C, $P=300$ mtorr, $T_s=27$ °C)

The effect of filament temperature on the deposition rates of copolymers was investigated by keeping any other variables constant in the iCVD depositions. Figure 3 gives the plot of the deposition rate as a function of temperature in an Arrhenius form in the temperature range of 210-280 °C. Apparent activation energy of 26.7 kJ/mol is calculated from the slope of the least squares linear regression to the data. This is a technique widely used in the iCVD literature to estimate apparent activation energy [30-31]. In this calculation the concentration of the monomers in the reactor was assumed to be constant considering low monomer consumption values in iCVD. The observed activation energy is almost 4-times lower than the activation energy observed for iCVD deposition of PGMA [30], meaning that deposition of copolymer is significantly less sensitive to the filament temperature.

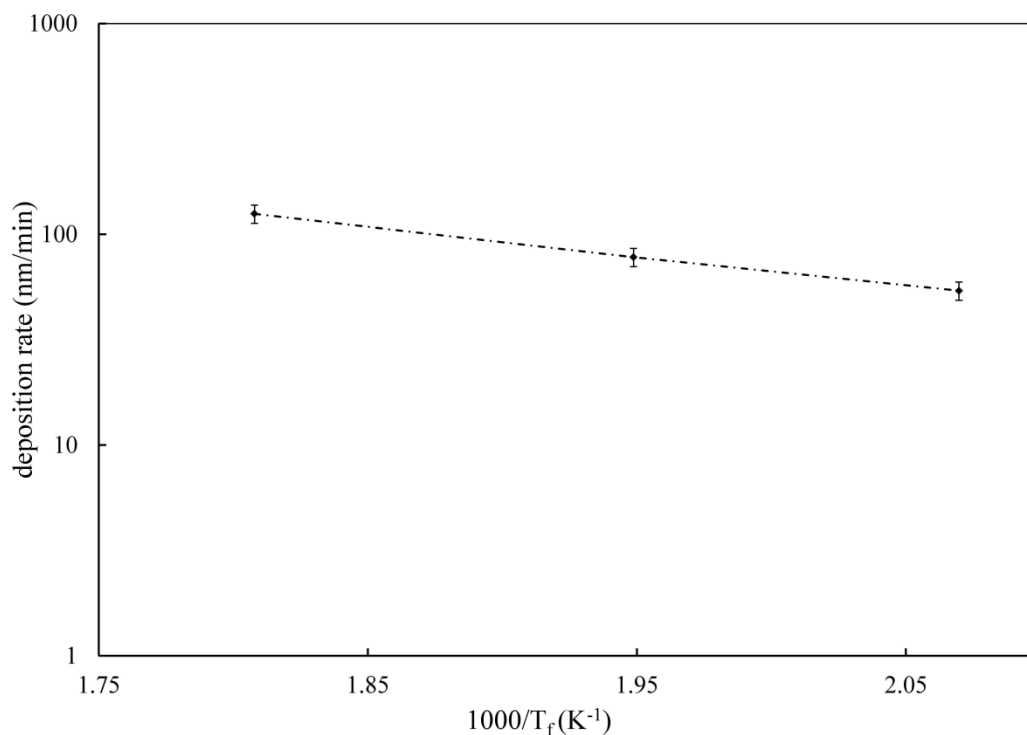


Figure 3. Deposition rate as a function of filament temperature ($P=300$ mtorr, $T_s=27$ °C)

Figure 4 (a-e) shows the FTIR spectra of homopolymers and copolymers with varying compositions. These spectra were thickness-normalized and baseline-corrected, and no other processing was performed. The spectra of iCVD-synthesized polymers do not involve peaks related with C=C bonds that exist only in the monomer spectrum, which proves that the polymerization proceeded through unsaturated C=C double bonds. In the spectrum of PHEMA (Figure 4 (e)), the broad peak between 3700 and 3050 cm^{-1} is related to the characteristic stretching vibration of -OH group. The other main vibrational modes are C-H stretching (3050 - 2700 cm^{-1}), C=O stretching (1750 - 1690 cm^{-1}), C-H bending (1500 - 1350 cm^{-1}), and C-O stretching (1300 - 1200 cm^{-1}). The existences of strong -OH and carbonyl peaks indicate that the chemical functionality of HEMA monomer is well preserved during iCVD polymerization.

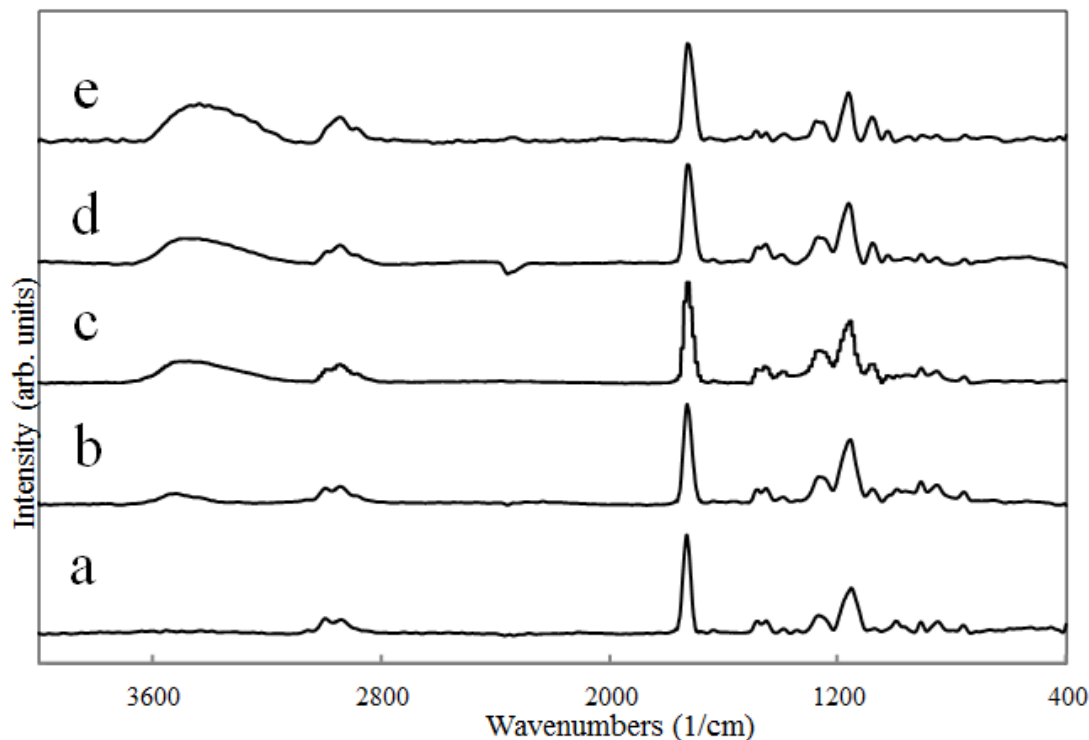


Figure 4. FTIR absorbance spectra of (a) PGMA, (e) PHEMA, and P(HEMA-GMA) with varying compositions ((b) F3, (c) F4 and (d) F5).

In the spectrum of PGMA (Figure 4(a)), the peaks at 907, 848, and 760 cm^{-1} are assigned to the characteristic epoxide group adsorption bands. In the case of spectra belonging to the copolymer films (Figure 4 (b-d)), it was observed that composition of a copolymer film can be tuned by changing the monomer feed ratios. As the flow rate of HEMA at the reactor inlet increases, the intensity of broad hydroxyl peak increases and that of epoxide peaks decrease. An increase in the flow rate of HEMA while keeping the flowrate of GMA constant during the depositions leads to increased partial pressure of HEMA with respect to GMA. Therefore, the concentration of HEMA monomer at the substrate surface becomes higher, which implies that more HEMA monomers can react with GMA monomers to form polymer films with higher hydroxyl functionality. The chemical structures of the copolymer films were also investigated by XPS analysis. According to the XPS survey scan of the copolymer film, for

which FTIR spectrum is given in Figure 4(d), carbon/oxygen atomic ratio was found as 2.25, which is in between the C/O atomic ratios found in GMA 2.33 and HEMA 2.00. High resolution C1s XPS scan was also obtained to investigate the chemical bonding states of the copolymer film.

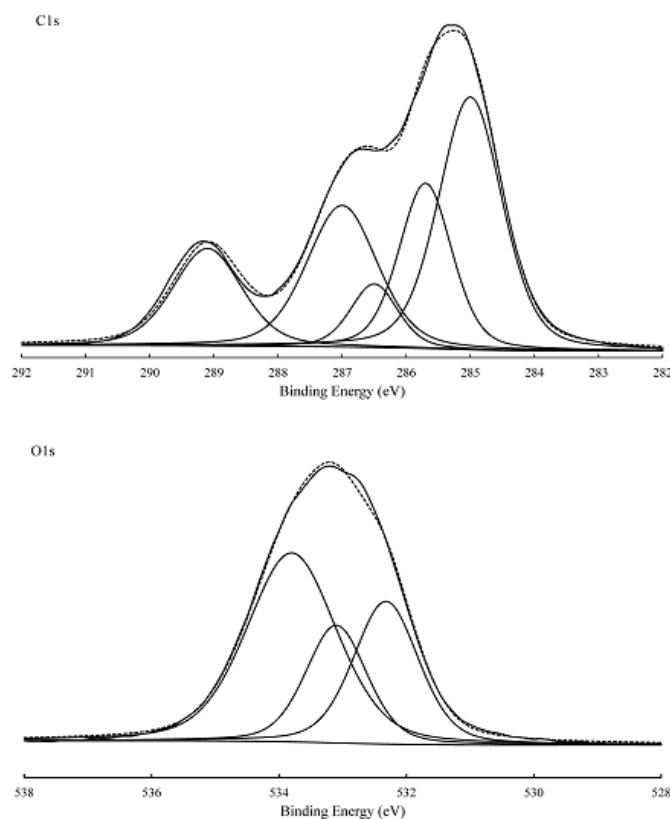
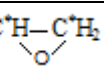
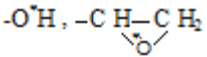


Figure 5. C1s and O1s high-resolution XPS scans of the P(HEMA-GMA) film deposited on PVA sheets by iCVD

Figure 5 shows the high resolution C1s and O1s spectra for P(GMA-HEMA) film together with spectrum deconvolutions. In both spectra, the fitted curves reproduce the experimental spectra with high accuracy. High resolution C1s and O1s spectra can be curve-fitted with five and three peak components, respectively, at binding energy values given in Table II. The peak positions are in good agreements with the previously synthesized PGMA and PHEMA films [21-24,26]. However, the areas of the peaks are different from HEMA or GMA only homopolymers, which can be expected with the copolymer films that contain

functional groups coming from both monomers. Both XPS and FTIR analyses confirm that iCVD produces copolymer thin films that retain essentially high fraction of hydroxide and epoxide functionality.

Table II. High-Resolution XPS Scan Data of the P(HEMA-GMA)

Core level	BE (eV)	Origin
C1s	285.0	$-\text{C}^*\text{H}_3, -\text{C}^*\text{H}_2-$
	285.7	$-\text{C}^*-(\text{CH}_3)-\text{CO}-$
	286.5	$-\text{C}^*\text{H}_2-\text{OH}, -\text{O}-\text{C}^*\text{H}_2$
	287.0	$-\text{O}-\text{C}^*\text{H}_2, -\text{C}^*\text{H}-\text{C}^*\text{H}_2$ 
	289.1	$-\text{C}^*=\text{O}$
O1s	532.3	$-\text{C}=\text{O}^*$
	533.1	$-\text{O}^*\text{H}, -\text{C}^*\text{H}-\text{C}^*\text{H}_2$ 
	533.8	$-\text{CO}-\text{O}^*-\text{CH}_2-$

FTIR spectra were also used to analyze the bulk compositions of the films by using the Beer-Lambert equation [39] assuming that the C=O bond oscillator coefficient is the same in the GMA and HEMA components. The HEMA mole fraction in the film was calculated using the following Equation :

$$f_{HEMA} = 1 - \left(\frac{A_{1730}}{A_{908}} \right)_{PGMA} \left(\frac{A_{908}}{A_{1730}} \right)_{P(GMA-co-HEMA)} \quad (2)$$

where A is the area under the peaks of epoxy (908 cm⁻¹) and C=O (1730 cm⁻¹) absorptions. The results were included in Table III, which show that depending on the partial pressures of HEMA and GMA monomers during the depositions the compositions of the copolymers can be well tuned.

Contact angle measurements were performed to test the hydrophilicity of the thin films synthesized by iCVD. The obtained polymeric thin films have different contact angles as regard to their hydrophilic characters. Compared to the bare or PGMA coated PVA sheets water contact angles of PHEMA and P(HEMA-GMA) coated surfaces were lower due to highly hydrophilic character of -OH functionality. The reported contact angle value of 15° for PHEMA-only film is not stable in time as the linear PHEMA film dissolves gradually with the water droplet placed during the contact angle measurements. The copolymers, on the other hand, were stable. The results showed that the contact angle value is decreased with increasing mole fraction of HEMA, which enhances the hydrophilic character of the deposits.

The swelling rate is of paramount importance when using supports for protein immobilization. The swelling rate of homo and copolymer thin films deposited on cross-linked PVA sheets was determined by weight difference between the water swollen and the dry TFH membrane. The effect of HEMA/GMA mole fraction on the swelling rate of the poly(HEMA-GMA) films given in Table III. Maximum swelling rate was observed in the PHEMA thin film with a swelling rate of 67%. As the molar fraction of HEMA in the structure of deposited copolymer decreased, the swelling rate decreased up to 21% as the amount of -OH groups decreased. Furthermore, considering that HEMA is a more polar

component than GMA, this result was found reasonable. Therefore, the addition of HEMA into the polymer structure caused a increase in the swelling capacity of the polymer.

Table III. Composition of the P(HEMA-GMA) films and amount of the immobilized HSA obtained with these film compositions

Film type	Mole fraction		Contact angle values	Water content (%)	Immobilized protein ($\mu\text{g cm}^{-2}$)
	HEMA	GMA			
F1	1		15°	67	191
F2		1	45°	21	219
F3	0.1204	0.8796	39°	47	213
F4	0.2842	0.7158	31°	51	223
F5	0.397	0.603	26°	58	207

Protein Binding Studies

It is well-known that epoxy, amine and thiol groups on the surfaces of the supporting materials are the efficient functional groups for protein binding and enzyme immobilization due to electron donating character of oxygen and amine [40]. Immobilization mechanism may be covalent and non-covalent such as hydrophobic interactions, hydrogen bond and Van der Waals interactions. In this study, the addition of reactive epoxy group (GMA) in the polymer matrix can improve the covalent interactions with the proteins without the need of further modifications [41]. The epoxy group can combine with amino groups of proteins under neutral and alkaline conditions. The N–C or O–C bonds formed between epoxy containing support and proteins are extremely stable [42]. Hydroxyl group from HEMA have free

electron pairs that may be involved in hydrogen bonding with the ammonium ions in the protein [43-44]. Hydrogen bond contributes to protein immobilization on PVA/P(HEMA-GMA) along with covalent complexation. Some preliminary evaluations were performed to investigate binding efficiencies of the thin polymer films for HSA by using solid-phase extraction. Unbounded HSA was determined at the specific excitation and emission wavelengths of the protein by using fluorescence spectroscopy. After the removal of HSA from copolymers, immobilization amounts of HSA to PVA/P(HEMA-GMA) substrates were measured at 280 and 342 nm of excitation and emission wavelengths by using equation of calibration curve of the protein (Figure 6 (a)).

Determination of binding amount of the protein on all PVA/P(HEMA-GMA) substrates with different compositions was performed by using fluorescence measurements before and after treatment of the protein with copolymers (Figure 6(b)). According to the data, the binding amount of protein to PVA/P(HEMA-GMA) thin film with a GMA concentration of 60.3% (sample F5, Table III) was found to be $193 \mu\text{g}\cdot\text{cm}^{-2}$. Increase of concentration of GMA units in the polymer (samples F3 and F4-1, Table III) keeping the film thickness constant increased the binding amount up to $223 \mu\text{g}\cdot\text{cm}^{-2}$ due to introduction of more epoxy groups on the surface. The effects of film thickness on the binding amount was also investigated (samples F4-1, F4-2 and F4-3, Table III) and data showed that there is no significant difference in the immobilization capacity of the copolymers within a thickness range of 0.1-0.5 μm . The protein binding capacity of PHEMA coated PVA was found to be $198 \mu\text{g}\cdot\text{cm}^{-2}$. PGMA coating on PVA surface was observed to be more effective in protein binding with a capacity of $219 \mu\text{g}\cdot\text{cm}^{-2}$. The immobilization amounts of the protein HSA for both PGMA and P(HEMA-GMA) coatings were observed to be very close. This showed that the molecules having same functional epoxy groups didn't increase binding capacity by just increasing the ratio of the functional groups in the polymer due to stoichiometric ratio of

complexation between protein and the functional groups of copolymer. This data clarified that protein affinity depends on the variation of functional moiety on the surfaces of the polymer rather than molecular structures on the polymer film. However, the synthesis of the copolymer as a thin film provides new chemical properties for biological applications.

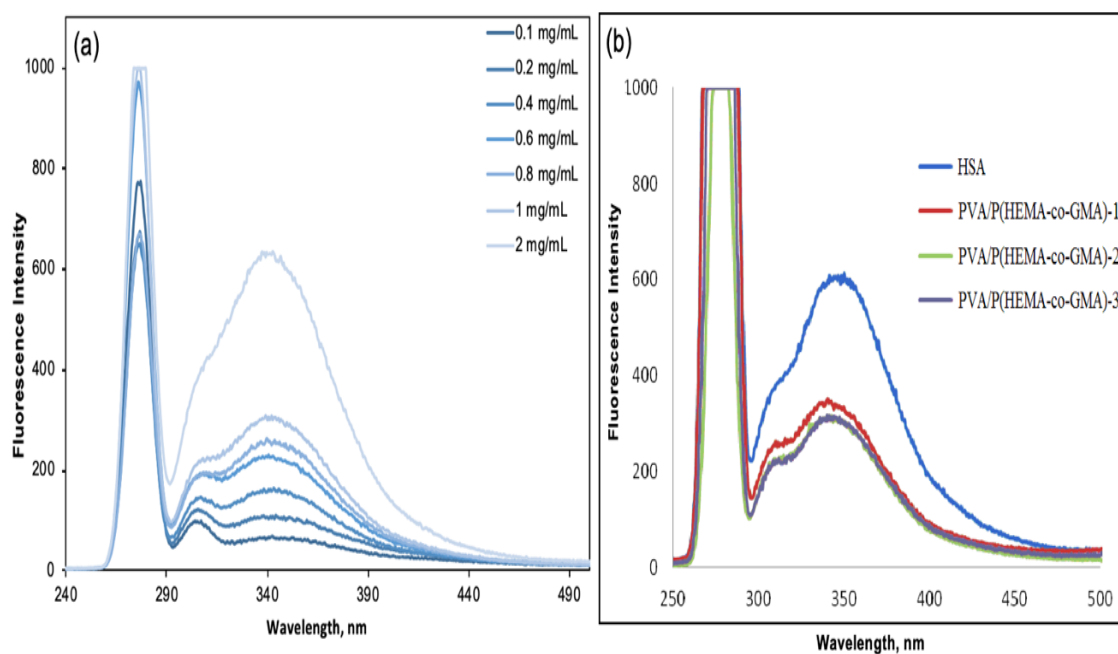


Figure 6. Fluorescence spectra of HSA at a concentration range of $0.001\text{-}0.02 \mu\text{g mL}^{-1}$ (a), Fluorescence spectra of HSA after binding on (PVA/P(HEMA-GMA)) derivatives at 280 and 342 of emission wavelengths (b).

Figure 7 shows the SEM images of P(HEMA-GMA) surfaces before and after protein immobilization. Before the immobilization experiments, the surfaces are smooth and flat, however during the treatment the surface became highly porous which may provide a high internal surface area. After protein binding, globular structure of the protein is clearly seen on the surface. The protein may bind both the external surface of the P(HEMA-GMA) film and within the pore space near the surface. Therefore, this large surface contributes the reaction of substrate with the immobilized protein [45]. The increase in the surface roughness of the films

after the HSA immobilization was also verified by AFM (Figure 8 (a-b)). The RMS roughness value increased from 0.42 nm to 18.33 nm before and after the HSA bindings, respectively.

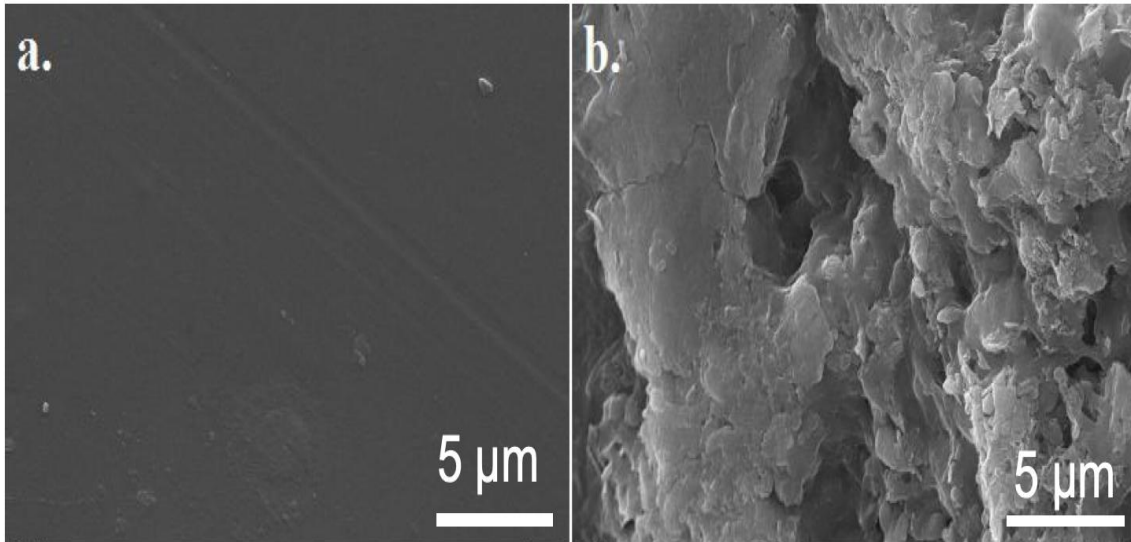


Figure 7. SEM images of PVA/P(HEMA-GMA) before (a) and after (b) HSA binding.

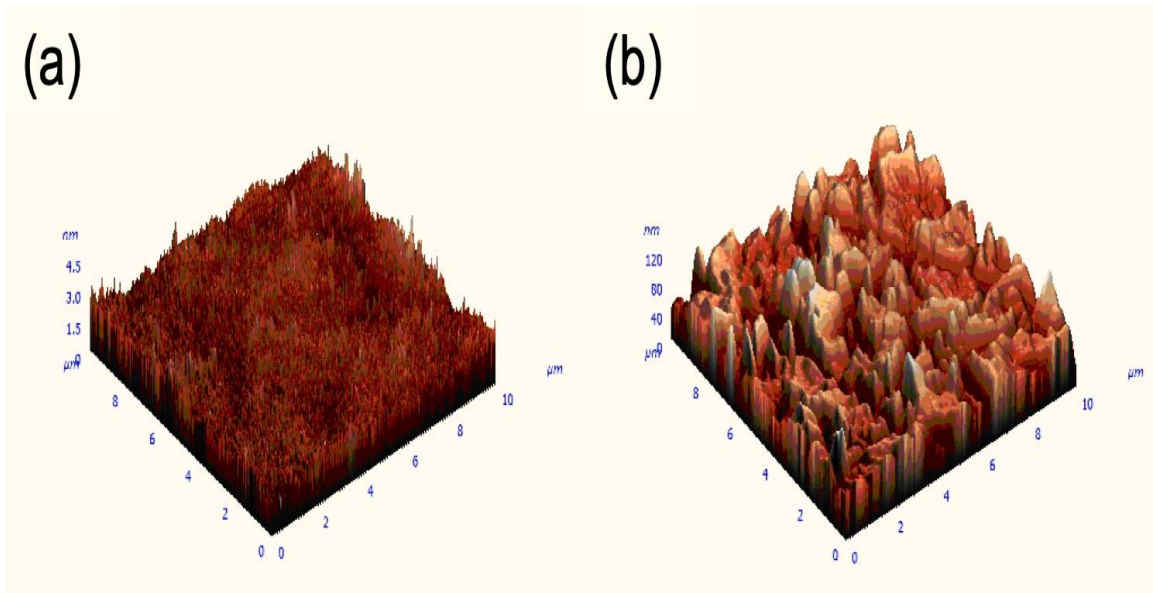


Figure 8. AFM images of PVA/P(HEMA-GMA) before (a) and after (b) HSA binding

Figure 9 (a-b) shows the FTIR spectra of the copolymer film (sample F4 in Table III) before and after the immobilization of HSA. The FTIR spectrum of PVA/P(HEMA-GMA) film have the characteristic stretching vibration band at around 1730 cm^{-1} from ester configuration of both HEMA and GMA. The intensity of that peak obviously decreased after formation of amide bond between ester and amine groups from amino acid residues and N-terminal of HSA, which led to new stretching vibration of Amide I at 1634 cm^{-1} and Amide II at 1526 cm^{-1} . The amide I vibration, absorbing near 1650 cm^{-1} , arises mainly from the C=O stretching vibration with minor contributions from the out-of-phase CN stretching vibration, the CCN deformation and the NH in-plane bending [44]. The amide II mode is the out-of-phase combination of the NH in plane bend and the CN stretching vibration with smaller contributions from the CO in plane bend and the CC and NC stretching vibrations [43-44]. The peak broadening at 1415 cm^{-1} , 1341.5 cm^{-1} and 1057 cm^{-1} may arise from proline and tryptophan residues of the protein [44].

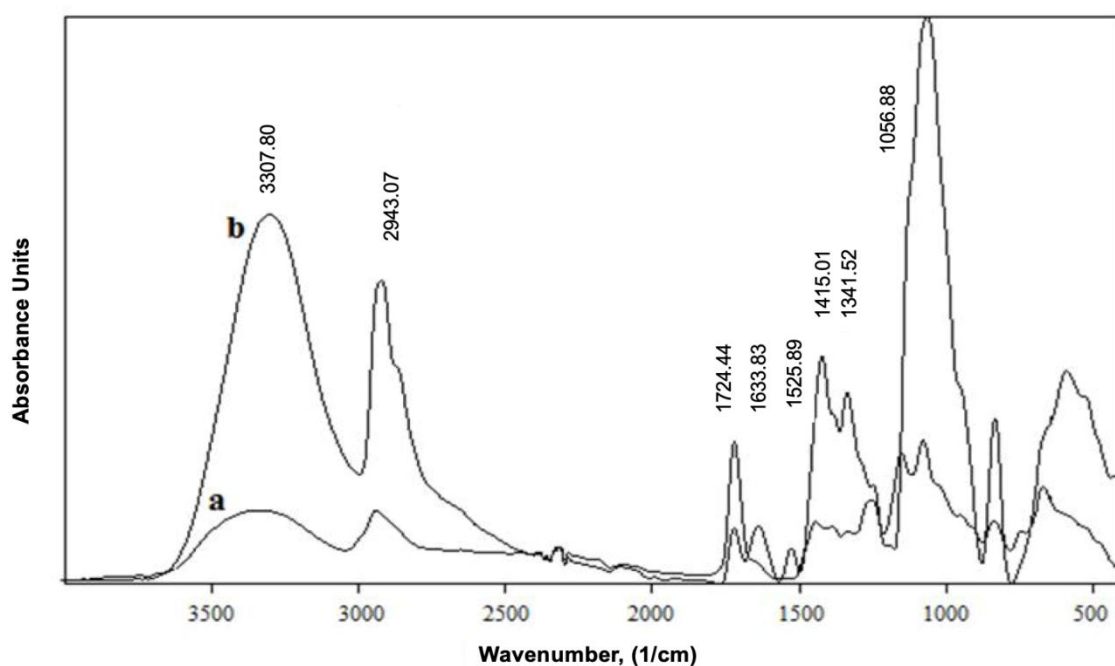


Figure 9. FTIR absorbance spectra of PVA/P(HEMA-GMA) before (a) and after (b) HSA binding

The change of morphology and chemical composition after the addition of HSA was also verified by contact angle measurements, and the results are given in Table III. The water contact angle values of HSA bonded film surfaces increased most probably due to the hydrophobic residues of the proteins such as tryptophan, valine, leucine and isoleucine on the surface. The surface roughness increase may be the other reason behind the contact angle increase.

CONCLUSIONS

P(HEMA-GMA) thin films can be synthesized by iCVD using HEMA and GMA as the monomers. The introduction of tert-butyl peroxide as an initiator allows very high film deposition rates at low filament temperatures. The iCVD, an all dry method, is able to functionalize fragile substrates such as PVA thin membrane sheets. The feasibility of the epoxy and hydroxyl functional groups containing copolymer films to act as substrates for protein immobilization was studied. The covalent protein binding was clarified by FTIR, AFM, and SEM analyses. The mild immobilization conditions, easy and rapid membrane preparation, one-step protein binding at substantially higher levels and membrane reusability make P(HEMA-GMA)/PVA TFH membran having abundant functional groups films useful for biomolecules immobilization and for several biochemical processes.

ACKNOWLEDGEMENTS

This research was supported by Scientific Research Council of Selcuk University (Project No. BAP-12101019).

REFERENCES

1. Cheng, X.; Kondyurin, A.; Bao, S.; Bilek, M. M.; Ye, L. *App. Surf. Sci.* 2017, 416, 686.
2. Kalkan, N. A.; Aksoy, S.; Aksoy, E. A.; Hasırcı, N.; *Jour. App. Poly. Sci.* 2011, 123, 707.
3. Liu, J.; Liang, Y.; Shen, J.; Bai, Q. *Analytical and bioanalytical chemistry.* 2018, 410, 573.
4. Gunasekera, B.; Abou Diwan, C.; Altawallbeh, G.; Kalil, H., Maher, S.; Xu, S.; et al. *ACS applied materials & interfaces.* 2018, 10, 7745.
5. Zhao M, Li H, Liu W, Guo Y, Chu W. *Biosensors and Bioelectronics.* 2016;79:581-8.
6. Calvo JN-M, Elices M, Guinea GV, Pérez-Rigueiro J, Arroyo-Hernández M. *Applied Surface Science.* 2017;416:965-70.
7. Bas SZ, Maltas E, Sennik B, Yilmaz F, Vural HC. *Journal of Applied Polymer Science.* 2014;131(16).
8. Lei Z, Gao J, Liu X, Liu D, Wang Z. *ACS applied materials & interfaces.* 2016;8(16):10174-82.
9. Tong Z, Schiel JE, Papastavros E, Ohnmacht CM, Smith QR, Hage DS. *Journal of Chromatography A.* 2011;1218(15):2065-71.
10. Erol K, Cebeci BK, Köse K, Köse DA. *International journal of biological macromolecules.* 2019;123:738-43.
11. Demir EF, Kuru CI, Uygun M, Aktaş Uygun D, Akgöl S. *Journal of Biomaterials science, Polymer edition.* 2018;29(4):344-59.
12. Vieira AP, Pimenta AF, Silva D, Gil MH, Alves P, Coimbra P, et al. *European Journal of Pharmaceutics and Biopharmaceutics.* 2017;120:52-62.
13. Noein L, Haddadi-Asl V, Salami-Kalajahi M. *International Journal of Polymeric Materials and Polymeric Biomaterials.* 2017;66(3):123-31.

14. Bayramoglu G, Ozalp C, Oztekin M, Guler U, Salih B, Arica MY. *Talanta*. 2019;191:59-66.
15. Çiçek Ç, Yılmaz F, Özgür E, Yavuz H, Denizli A. *Chemosensors*. 2016;4(4):21.
16. Bakhshpour M, Derazshamshir A, Bereli N, Elkak A, Denizli A. *Materials Science and Engineering: C*. 2016;61:824-31.
17. Elkak A, Hamade A, Bereli N, Armutcu C, Denizli A. *Analytical biochemistry*. 2017;525:1-7.
18. Bayramoglu G; Arica, M.Y; Bektas, S; *Journal of Applied Polymer Science*,2007; 106, 169–177.
19. Zeng J, Zhang Z, Dong Z, Ren P, Li Y, Liu X. *Reactive and Functional Polymers*. 2017;115:1-9.
20. Salehi SM, Di Profio G, Fontananova E, Nicoletta FP, Curcio E, De Filpo G. *Journal of Membrane Science*. 2016;504:220-9.
21. Schwellenbach J, Kosiol P, Soelter B, Taft F, Villain L, Strube J. *Reactive and Functional Polymers*. 2016;106:32-42.
22. Bayramoglu G, Senkal BF, Yilmaz M, Arica MY. *Bioresource technology*. 2011;102(21):9833-7.
23. Ramalingam N, Rajiv S. *Journal of Advanced Research in NanoScience and NanoTechnology*. 2018;1(1&2):1-9.
24. Kaya AST, Cengiz U. *Progress in Organic Coatings*. 2019;126:75-82.
25. [M. Gürsoy](#), [T. Uçar](#), [Z. Tosun](#), [M. Karaman](#), *Plasma Process. Polym.* 13 (2016) 438–446.
26. Brian J. McMahon Courtney A. Pfluger Bing Sun Katherine S. Ziemer Daniel D. Burkey Rebecca L. Carrie, *Materials Research A*, 102 (2014) 2375-2382.
27. McMahon BJ, Pfluger CA, Sun B, Ziemer KS, Burkey DD, Carrier RL. *Journal of Biomedical Materials Research Part A*. 2014;102(7):2375-82.

28. Alf ME, Asatekin A, Barr MC, Baxamusa SH, Chelawat H, Ozaydin - Ince G, et al. *Advanced Materials*. 2010;22(18):1993-2027.
29. G. Ozaydin-Ince, A.M. Coclite, K.K. Gleason, *Reports on Progress in Physics*, (2011) 75 016501.
30. Mao Y, Gleason KK. *Langmuir*. 2004;20(6):2484-8.
31. Ozaydin-Ince G, Gleason KK. *Journal of Vacuum Science & Technology A: Vacuum, Surfaces, and Films*. 2009;27(5):1135-43.
32. Hoffman A, Schmer G, Harris C, Kraft W. *ASAIO Journal*. 1972;18(1):10-6.
33. Roointan A, Farzanfar J, Mohammadi-Samani S, Behzad-Behbahani A, Farjadian F. *Int J Pharm*. 2018;552(1-2):301-11.
34. Zhao W, Yang R-J, Qian T-T, Hua X, Zhang W-B, Katiyo W. *International journal of molecular sciences*. 2013;14(6):12073-89.
35. Arica M.Y, Bayramoğlu G, Polyethyleneimine-grafted poly(hydroxyethyl methacrylate-co-glycidyl methacrylate) membranes for reversible glucose oxidase immobilization, *Biochemical Engineering Journal*. 2004, 20 (1); 73-77.
36. Karaman M, Çabuk N, *Thin Solid Films*, 2012;520(21):6484-6488.
37. Buzoglu L, Maltas E, Ozmen M, Yildiz S. *Colloids and Surfaces A: Physicochemical and Engineering Aspects*. 2014;442:139-45.
38. Tenhaeff WE, Gleason KK. *Langmuir*. 2007;23(12):6624-30.
39. Lin-Vien D, Colthup NB, Fateley WG, Grasselli JG. *The handbook of infrared and Raman characteristic frequencies of organic molecules*: Elsevier; 1991.
40. Maltas E, Ozmen M, Yildirimer B, Kucukkolbasi S, Yildiz S. Interaction between ketoconazole and human serum albumin on epoxy modified magnetic nanoparticles for drug delivery. *Journal of nanoscience and nanotechnology*. 2013;13(10):6522-8.

41. Maltas E, Ozmen M, Yildiz S, Ersoz M. Binding affinity of serum proteins to epoxy modified magnetite nanoparticles. *Advanced Science Letters*. 2012;17(1):143-8.
42. Bayramoğlu G, Kaçar Y, Denizli A, Arica MY. Covalent immobilization of lipase onto hydrophobic group incorporated poly (2-hydroxyethyl methacrylate) based hydrophilic membrane matrix. *Journal of food engineering*. 2002;52(4):367-74.
43. Kong J, Yu S. Fourier transform infrared spectroscopic analysis of protein secondary structures. *Acta biochimica et biophysica Sinica*. 2007;39(8):549-59.
44. Barth A. Infrared spectroscopy of proteins. *Biochimica et Biophysica Acta (BBA)-Bioenergetics*. 2007;1767(9):1073-101.
45. Bayramoğlu G, Akgöl S, Bulut A, Denizli A, Arica MY. Covalent immobilisation of invertase onto a reactive film composed of 2-hydroxyethyl methacrylate and glycidyl methacrylate: properties and application in a continuous flow system. *Biochemical Engineering Journal*. 2003;14(2):117-26.



Research Article

The Effects of Natural Life Islands Planning on Izmir Bay Ecosystem

Tarik İlhan*¹ , A.Hüsnü Eronat² , Ezgi Talas³  and Muhammet Duman⁴ 

¹ Institute of Marine Sciences and Technology, Department of Marine Geology and Geophysics, İzmir, Turkey

² Institute of Marine Sciences and Technology, Department of Marine Geology and Geophysics, İzmir, Turkey

³ Institute of Marine Sciences and Technology, Department of Marine Geology and Geophysics, İzmir, Turkey

⁴ Institute of Marine Sciences and Technology, Department of Marine Geology and Geophysics, İzmir, Turkey

Abstract

Izmir is one of the most important trade ports of Turkey, which has hosted many important civilizations through time. Many scientific studies that have been carried out in Izmir Bay for decades point out that the Bay has become by limiting direct pollution of the Bay. However, it is a fact that the present circulation should be increased. For this reason, the Izmir Bay and Port Rehabilitation Project was revealed. The aim of this study is to choose the most suitable place for the proposed "Natural Life Islands", which are to be built from the seabed dredgings from a channel to be built to help increase the circulation in the bay. Hydroacoustic and oceanographic data were collected and evaluated. After post dredging, the future flow pattern and sediment transport model should be investigated. The planned islands are expected to have an impacts on the Izmir Bay ecosystem. Therefore, it is very important to make the right decision as to the placement of the islands. As a result, the effects of the planned islands on the present ecosystem of the bay should be examined in detail.

Received
17 September 2019

Accepted
21 November 2019

Keywords
Izmir Bay
Natural Life Islands
Ecosystem
Seabed Dredging

¹ Corresponding Author Email: tarik.ilhan@deu.edu.tr

INTRODUCTION

Coastal cities in Turkey have naturally developed to the industrial, commercial and tourism activities in particular, in the Mediterranean under the climatic and socio-economic conditions [1]. Izmir Inner Bay is a natural harbor where trade has been active throughout history. The ports of Izmir, Karaburun, Urla and Foça have provided fast and comfortable transportation to the Islands in the Aegean Sea and this has been the most important factor in the rapid development of the city of Izmir [2,3]. In the Ottoman period, durable roads, beautiful and artful bridges were built also increasing transportation. In 19th century, Izmir was the most important and largest city of the western Anatolia region with a population 100,000 [4,5]. Marine transportation in Izmir Bay led to the improvement of surrounding coastal cities such as Ildırı (Erythrai), Foça (Phokaia), Urla (Klozomenai), Sığacık (Theos), Ürkmez (Lebedos) and Menderes (Kolophon) (Fig.1).



Figure 1. The ancient Izmir and important coastal settlements [2]

In Izmir Bay, especially in the last 25 years, the port has become more active in both tourism and trade. The impacts of the Bay, the use of the port and / or the effects are kept under constant control through the Grand Canal Project that began in the 90s. In addition with the Izmir Bay and Port Rehabilitation Project, the improvement in the Bay has been increasing day by day [6]. Izmir Bay is defined as three parts as inner, middle and outer. The rivers flowing into the bay, drain lines and etc. are shown in Fig 2. However, the bathymetric map of the study area was created by adding up-to-date values to the data collected to date and adding the literature to the study.

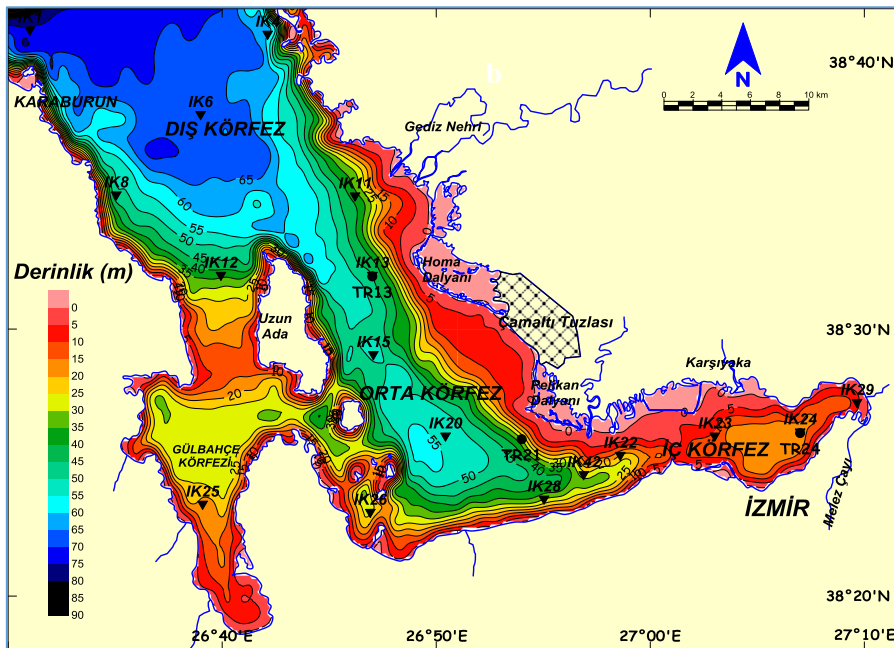


Figure 2. Departments, inputs and bathymetry of Izmir Bay (Atalar, 2012 [7])

The aim of this study is to estimate the effects of the material to be produced as a result of the dredging processes planned in the inner and middle sections and the effects of the planned Natural Life Islands with the use of this material (Fig.3). However, by combining shallow seismic and side scan sonar and physical oceanography data, an example has been tried to be used in such engineering studies. In order to determine the geotechnical properties of the soil forming the seabed, grab sampling stations selected in 1x1 km grid intervals within the boundaries of the study area are shown in Fig 4.

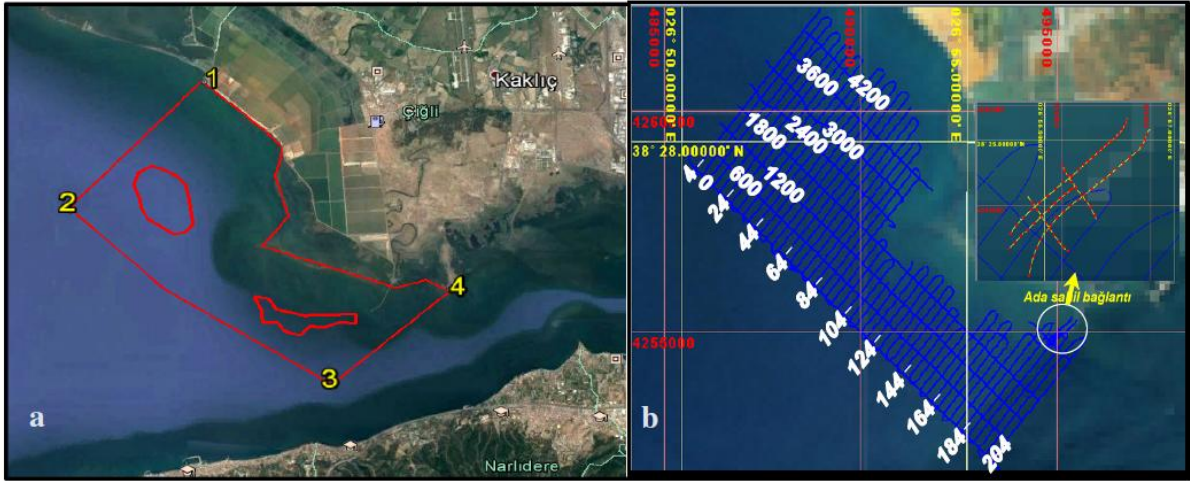


Figure 3. a) Study area and planned natural life islands satellite photo
b) Working lines in the study area

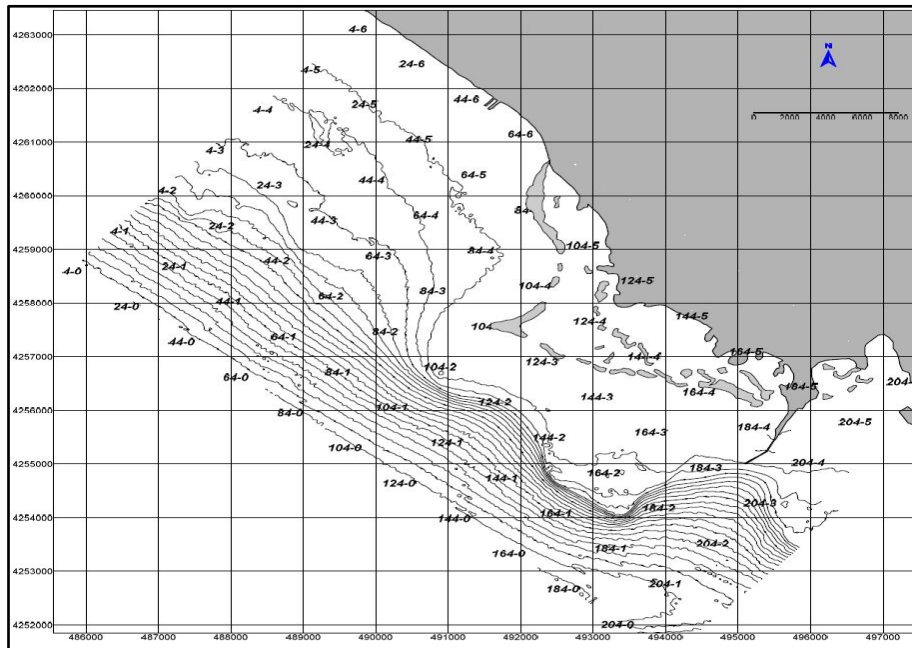


Figure 4. Sediment sampling stations in the study area

MATERIAL AND METHOD

The seismic studies and side scan sonar data, which constitute the basis of this study, were collected from Research Vessel Dokuz Eylül 3 of the Institute of Marine Sciences and Technology in 2016-2017. Data were recorded and processed using Strata-Box 3510 Dual Frequency Seismic System with Cmax CM2 Side Scan Sonar. Side Scan Sonar (SSS) records, Sub-bottom Profiler (SBP) data were collected to

provide full coverage and high resolution maps with high discrimination capacity among the characteristics of the different seabed. Oceanographic data were collected continuously with Teledyne Mariner 600 kHz Acoustic Doppler Current Profile (ADCP) in each working line along the working area. Data were collected from 40 km² coastal area for Izmir Bay, up to 50 m water depth. During the study, the speed of the research vessel was chosen as 3-3,5 knots. The reason for keeping the speed within this range is the acoustic systems used to record data with maximum efficiency at these speeds. Since the recorded data can only be taken under appropriate meteorological conditions the work was interrupted due to strong winds and sea wave lengths exceeding 1.5 meters.

RESULTS AND DISCUSSION

When all shallow seismic data are interpreted, the unit contains the A-unit (fine-grained sediments) with fine-grained sediment and the B-unit (fine and coarse-grained sediments) underneath. The upper seismological unit (A) on the acoustic foundation consists of up- to- date sediments such as clay, conglomerate-silty sand ranging in thickness from 0 to 10 m. The acoustic base (B) unit, which has thicknesses of more than 10m, consists of sedimentary layers composed of different stacks from thin to massive. Potential gas deposition sites have been observed in some areas of seismic sections (Fig.5a and 5b).

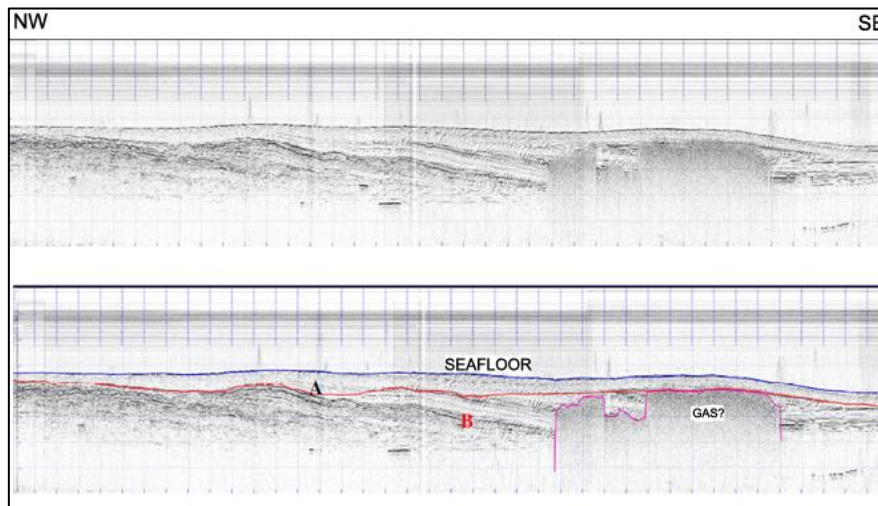


Figure 5a. NW-SE (NorthWest-SouthEast) seismic section from north of study area

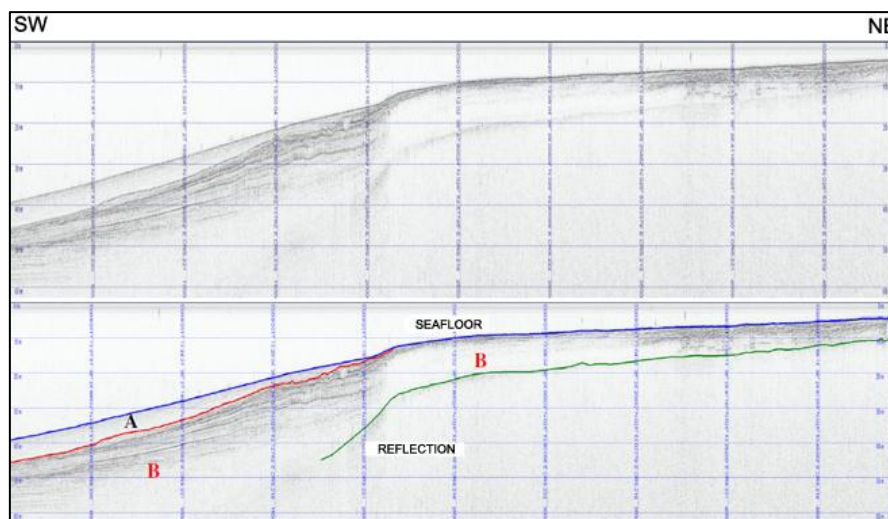


Figure 5b. SW-NE (SouthWest-NorthEast) seismic section from south of study area

The mosaic map in Fig.6 was drawn from the SSS data in the study area. The drawn map shows traces of possible small-scale trawl scans. In addition, cylindrical apparatuses such as closures and cages are frequently observed. The reflection records of other structures on the seafloor were observed in the sonar.

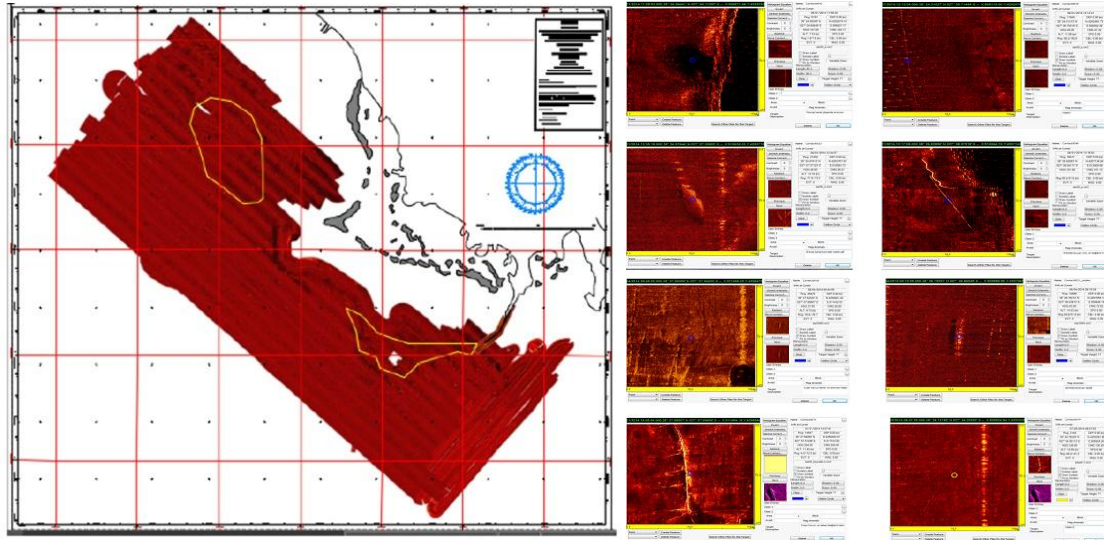


Figure 6. Side scan sonar mosaic map (left) and visual information about objects and structures (right) (wrecks, cable, rope and screening marks etc...)

The current directions and velocities in the study area vary depending on the seasonal conditions and the seabed morphology. The direction of current in the northern part of the region is northwest, and the common stream in the south is the south-southeast (Fig.7). The average current velocity in the north is 7 cm/s and the average current velocity in the south is 11 cm/s. Especially in coastal areas where water circulation is limited, high values (such as in station 064-6, 144-4, 184-4) were observed (Table 1). The maximum value of %18.91 organic material (station 204-6) was observed near the wastewater treatment plant. The fact that the maximum values were observed in the deep sections as storage areas and in the areas close to the wastewater treatment plant indicate the possible wastewater discharge effect.

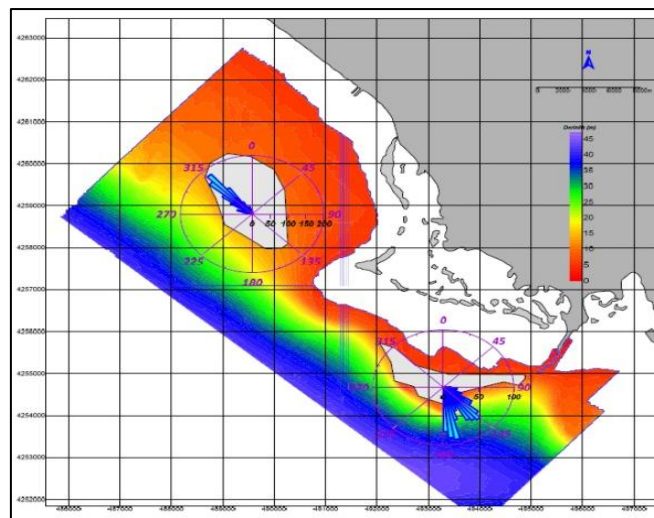


Figure 7. Current survey stations directions

Table 1. Organic materials content in some stations

Sample ID	Dry Weight (g)	Absorption Value	Organic Material (%)	Organic Carbon (mg/gr)	Organic carbon (%)
004-0	0,9541	0,197	3,08	15,99	1,60
004-3	1,0790	0,123	1,92	8,83	0,88
024-2	1,0006	0,153	2,39	11,84	1,18
024-6	0,9743	0,242	3,78	19,24	1,92
044-1	1,0201	0,211	3,30	16,02	1,60
044-4	1,0828	0,138	2,16	9,87	0,99
064-5	0,9454	0,133	2,08	10,90	1,09
064-6	0,9203	0,453	7,08	38,12	3,81
084-2	0,9648	0,171	2,67	13,73	1,37
084-3	1,1371	0,135	2,11	9,20	0,92
104-0	1,0346	0,217	3,39	16,24	1,62
104-1	0,9788	0,200	3,13	15,83	1,58
124-2	0,9829	0,146	2,28	11,50	1,15
124-3	1,0710	0,143	2,23	10,34	1,03
144-2	0,9414	0,162	2,53	13,33	1,33
144-4	1,0182	0,292	4,56	22,21	2,22
164-2	1,0193	0,186	2,91	14,13	1,41
164-3	1,1482	0,181	2,83	12,21	1,22
184-0	1,0010	0,268	4,19	20,74	2,07
184-4	0,9940	0,425	6,64	33,12	3,31
204-5	0,9393	0,295	4,61	24,32	2,43
204-6	0,9258	1,210	18,91	101,23	10,12

CONCLUSION

The consequences of changes in the water circulation and subsequently in the ecosystem of Izmir Bay need to be thoroughly researched and evaluated. It is estimated that approximately 25 million m³ of material, which is seen as mainly soft clay and sand, will be extracted from the dredging stage to be conducted in the north of the middle bay. However, the projected size of the proposed two natural life islands will require 53 million m³ of dredging material. For this reason, only the planning of the circulation channel, to be built at -8 m elevation, should be examined and the bathymetric map of the bay should be reviewed at present. When we look at the bathymetric structure of the inner bay, there is a trench deeper than 20 meters in the middle bay, isolated from the outer bay. There is no study on the effect of the channel which is planned to be opened to the water movements in this trench zone. The contribution of the channel that will be opened without any modeling on all these features to the Izmir Bay should be discussed. Even though all the data obtained in this study does not indicate the possible effects to Izmir Bay, which is an important wetland habitat and port in Turkey, a more accurate inference for Izmir Bay may be reached with further studies.

ACKNOWLEDGMENT

This study was funded by Izmir Metropolitan Municipality Project No: DBTE-231

REFERENCES

- [1]. Burak, S., Doğan, E. and Gazioğlu, C., 2004. Impact of urbanization and tourism on coastal environment. *Ocean & Coastal Management*, 47, 515-527.
- [2]. Yıldırım, R. and Oban, R., 2011. The importance of heritage roads on the development of Western Anatolia and Izmir. *Procedia Social and Behavioral Sciences* 19, pp.90-97.
- [3]. Kefeli, E., Taşagil, A., Karagül, N.S., 2008. Dünden Bugüne İpek yolu, Beklentiler ve Gerçekler, Ötüken Yayınları. İstanbul.
- [4]. French, D. and Mitchel, S., 1977. Roma İmparatorluğu'nun İlk Devirlerinde Pisidia'da Yollar ve Ulaşım, *Türk Arkeoloji Dergisi*, Ankara, Sayı XXIV-I, pp. 214–221.
- [5]. Baykara, T., 1982. Osmanlı Tarihi, Anadolu Uygarlıkları, Görsel Anadolu Tarihi Ansiklopedi, İstanbul, p.p. 832-842.
- [6]. Yılmaz, T., Özbaş, G., İşgenç, M.F., and Molva, M., 2018. İzmir Körfezi ve Limanı Rehabilitasyon Projesi. 9. Kıyı Mühendisliği Sempozyumu, pp.413-420.
- [7]. Atalar, M., 2012. İzmir Körfezi'nin Sedimantolojik, Mineralojik ve Sismik İncelemesi. Dokuz Eylül Üniversitesi, Fen Bilimleri Enstitüsü Yüksek Lisans Tezi.



Research Article

Evaluation of Boron Concentration in Akhüyük (Ereğli) Geothermal Source in terms of Medical Geology

Bilgehan Yabgu HORASAN*^{1,2} , Alican ÖZTÜRK³ 

¹ Selçuk University Sarayönü Vocational High School Department of Environmental Protection and Control Konya

² Selçuk University Advanced Technology Research Center Selçuklu Konya

³ Konya Technical University, Geological Engineering Department, Selçuklu, Konya, Turkey

Abstract

Some of the thermal waters are used for drinking, some in bath cures and some in both. In addition to the elements that will benefit the living organisms of the thermal waters, the negative consequences of the toxic elements above the limit values are inevitable. The historical and scientific structure of medicine and geology has created a common field of work related to humanitarian activities and problems that arise naturally with modernization. This requirement led to the emergence of medical geology. The study area is in Ereğli - Bor Neogene basin. In the scope of this study, the boron concentration of the water was determined in the geothermal area at the Ereğli District. In the scope of this study, the boron concentration of the water in the geothermal area at the Ereğli District was determined. The results of the analysis of the water found in the study area by the General Directorate of Mining Inspection, results of the analysis made by Ereğli Municipality, and water sample results from this study were evaluated. The effect of boron concentration on living things has been interpreted in terms of Turkish standards and the maximum boron concentration values recommended by the World Health Organization.

Received
07 September 2019

Accepted
28 November 2019

Keywords
Medical Geology,
Boron,
Thermal waters,
Konya,
Ereğli

¹ Corresponding Author Email: bilgehanyabgu@gmail.com

INTRODUCTION

Boron is the element with more than one hundred minerals on the earth that can be used for different purposes [1]. Boron is the first element in the 3A group with atomic number 5 and is indicated by “B” on the periodic table [2]. For the first time in the world, the elemental boron was found in 1808 by Thenard, Gay-Lussac and Davy at the same time. Boron compounds with long history are widely used in a wide range of applications such as agriculture, health, energy, computer, cosmetics, cleaning, whitening, ceramics, glass, metallurgy, nuclear and aircraft industry. Thus, a very wide range of boron products come into our daily life [3]. Boron element, which has a very large reserve within the borders of our country, is very important in terms of health sciences as well as production-based real sectors such as industry, technology and agriculture. The historical and scientific structure of medicine and geology has created a common area of work related to the problems arising from the products of human and natural processes that emerge along with the modernization. This study was evaluated in terms of medical geology which investigates the relationship between the elements, minerals, rocks, soil, water emerged as the natural results of geological environments and these processes and environmental health, the use of boron compounds in the treatment of diseases is thought to become as important as industry and technology in the following years. Boron compounds are also used in the medical field. Uses of boron compounds in medicine are; the treatment of osteoporosis and rheumatoid arthritis, Boron Neutron Capture Therapy (BNCT) used to treat brain tumors, burn treatments, wound healing, antiseptic lens solutions, ointments, mouthwashes and eye drops. Along with all these, the drug named “Bortezomib” which contains boron is accepted by the Food and Drug Administration (FDA) for the treatment of multiple myeloma. [4]. In this study, the results of chemical analyzes on the water samples taken from Akhüyük geothermal source in Ereğli district of Konya province were evaluated. Some of the hot spring waters which emerge from geothermal sources is used for drinking, some for bath cures and some for both. In addition to providing benefits to the living organisms, the excess of toxic elements found in thermal waters above the limit values can cause harm. People take boron compounds into their bodies by means of breathing, contact and digestion. Studies conducted on animals, adults and young children have shown that long-term contacts with boron damage skin [5]. According to the chemical analysis of the water samples

taken from the geothermal source from the study area, the boron value was compared with the previous years' studies and its effect on the body was investigated.

MATERIAL AND METHOD

For this study, field study was started after evaluation of previous studies conducted in the region. The region was examined geologically and the boundaries of the existing formations in the study area were checked. The study area was examined in detail in terms of whether there is another geothermal source (Figure 1). Ridge or conical formations caused by old hot water outlets were detected in the field. There are two geothermal wells in the field and KEA-2 well where water samples are not available. For this reason, a water sample was taken from the KEA-1. Both the sample of this study and the water sample taken by Ereğli Municipality were taken by a commission established by the provincial public health directorate during the spring. In the previous study, the water sample was taken in the fall period. In this study, water samples were taken into special containers with a sampling capacity of 500 and 1000 ml, which were gamma sterile, with a 50 mm wide mouth, and a leak-proof seal inside to prevent leakage. The water samples were taken into the cooled carrying bags and delivered to the laboratory. Water samples were analyzed with ICP-OES model in Envirolab Measurement and Analysis Services (ind.trade.co.ltd.) and inductively coupled plasma-optical emission spectrometry (PerkinElmer ICP - OES) was performed by three replications with EPA 200.7 method. The results of the analysis in this study and the results of the analysis found in previous studies were compared and are subjected to evaluation in terms of Turkey and World drinking and using water standards. For the geological evaluation of the region, the physical properties of the travertine in the area, formation boundary relations and the physical properties of the alluvium unit were investigated in detail. The thickness of the travertine unit has been determined by the mirrors in the open travertine quarry which is already produced in the field and by the drilling of the borehole made from this quarry.

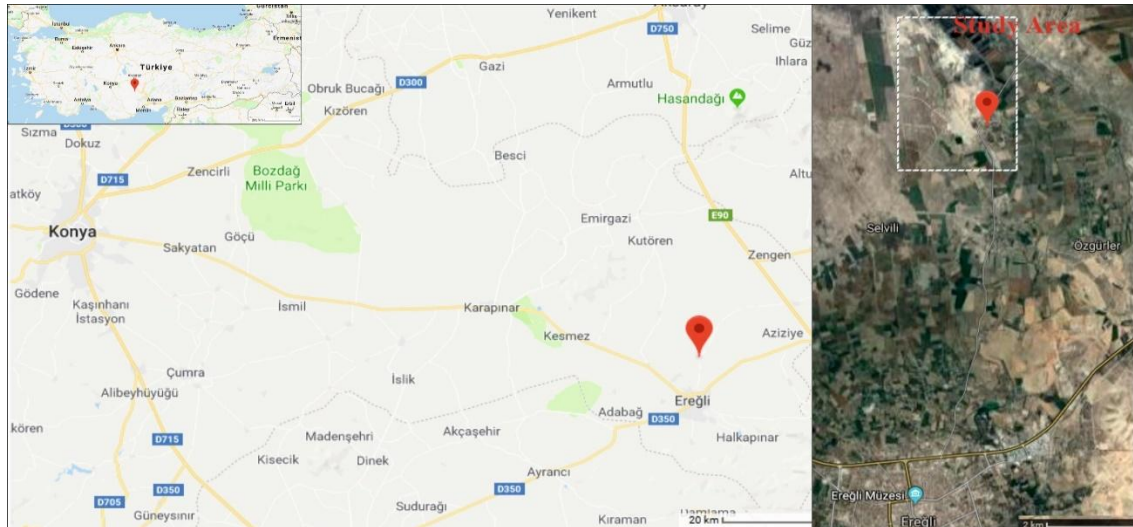


Figure 1: Location of the Study Area

EFFECTS OF BORON ON HEALTH

In terms of boron compounds, research and development has been made in our country in previous years mostly for industry and technology. The acceptance of boron mineral as an essential supplement for humans is towards the middle of 1980. According to the previous studies the amount of boron required to be taken for healthy and balanced diet is 1-13 mg / day which is sufficient and necessary. The human body is tolerant to the amount of boron at a level of 0.4 mg / kg body weight and the minimum amount of boron coming from food should be 1.2 mg. [5-6]. It was stated that males take more boron than females, and boron uptake increases as age progresses. Boron amount to be taken in daily nutrition varies according to age groups; 548 μg in 0 - 2 year old children, 594 μg in 14 - 16 age girls, 853 μg in boys, 690 μg in women aged 25 - 30, 890 μg in men, 754 μg in 60-65 years old females and 883 μg in males. The amount of boron should be taken from various foods per day varies between 600-1200 μg [7-8]. In order to understand the importance of boron in terms of bone health, 12 women received a diet with a low boron ratio (0.25 mg / day) during the postmenopausal period of 119 days and in addition, a supplementary capsule containing 3 mg boron was added to the diet for 28 days. As a result of the tests performed at the end of the study, it was found that the calcium content in the urine decreased by 44% with the support of the boron element and it was concluded that the boron could prevent osteoporosis in the postmenopausal period [9]. In a different study conducted on men, calcium excretion in urine decreased whereas calcium uptake in bone increased by 17% in males supplemented with 10 mg boron

every day over a 4-week period [10]. Boron has an important function in the metabolism of calcium and magnesium, which is the basic need for joint movements and bones. In addition to activation of calcium and Vitamin D, it is stated that it is effective in protecting bone tissue and preventing demineralization, and strengthening immunity and hormonal system [11,12,13]. It has been argued that boron can be effective in human brain functions and mental performance, and when people are receiving low amounts of boron through nutrition, deterioration in hand-eye coordination, decrease in attention and perception, and significant deterioration in short and long term memory have been observed [14]. It is known that the amount of blood hemoglobin increases significantly when supplemented with boron [15]. There are some findings suggesting that boron has a protective effect against some types of cancer. In the areas where boron minerals are present, it is determined that the values of prostate cancer decreased in the region with the introduction of minerals into the body and nutrient content, and the boron can be very effective in the prevention of prostate cancer [16,17]. It has been determined that the risk of prostate cancer, lung cancer and abnormal cervical cytopathology, which are common type of cancer diseases in humans, decrease due to the increase in boron intake. In a study conducted on 763 women with lung cancer and a control group of 853 people, it was observed that the risk decreased with the increase of boron intake [18,19]. According to the studies, it can be stated that boron is effective against prostate cancer [15,16,17,20]. In another study investigating the effect of boron on prostate cancer, 8720 healthy individuals were compared in 95 cases and it was found that low amount of boron intake increased the risk of prostate cancer [20]. Critical threshold values vary in different countries and regions of the world. In the study conducted by EFSA (European Food Safety Authority), it is known that the amount of boron contained in drinking water is 0.2-0.6 mg / day [21]. The different countries of the world, especially the US and European Union countries, have announced various studies and opinions on the amount of boron daily intake requirement. While the maximum acceptable limit for adults set by the United States Medicine and Food and Nutrition is 20 mg / day, World Health Organization announced the amount as 0.4 mg per 1 kg of body weight. On the other hand, the European Union determined the limit of 10 mg / day as the recommended maximum daily intake of boron. The EFSA 2013 panel announced that the daily maximum level of boron intake should be 0.16 mg kg / day [5,22,23]. The lowest lethal dose of boric acid is 640 mg / kg when entered into the

body via the oral route, 8600 mg / kg when it penetrates through the skin and 29 mg / kg when it is injected. If more than 500 mg of boron is taken signs of poisoning observed in a healthy person are; nausea, vomiting, head and abdominal pain, diarrhea, muscle contractions, shock, fatigue, digestion and central nervous system disorders, disruption of the functioning of the glands, and skin lesions. In children, toxic effects of boron causes brain membrane destruction such as referral and coma. The characteristic sign of boron poisoning is the pink color seen at the fingertip which is the most distinctive and distinguishing indication of boron poisoning [24,25]. The way the boron is removed from the body is the same in humans and animals. The tolerable amount of boron entering the body through nutrients, breathing, etc. is excreted by 90-95% directly from the body through the urinary tract without any accumulation. Boron accumulates only in organs such as bone, hair, nail, spleen and liver [5,26,27]. Drinking water with high boron minerals content causes disturbances in the digestive system and may cause serious problems such as liver growth and swelling [28]. According to the studies conducted in our country and in the world besides its possitive effects in treatment, overdose exposure of boron may cause serious health problems. In general, the therapeutic effects of boron minerals are; regulate steroid hormone metabolism, help the bones to grow and strengthen, antioxidant effects, help the immune system to strengthen,short the healing process, regulate energy metabolism, play a protective role against different types of cancer and reduce the possibility of their occurrence, increase brain function and performance, treat blood cancer and slow down excess weight gain [29].

AKHÜYÜK GEOTHERMAL FIELD

The geothermal area within the boundaries of the Akhüyük neighborhood of Ereğli district of Konya province is 158 km to Konya and 12 km to Ereğli. In the research area where continental climate is dominant, the most rainy season is spring and the driest season is summer. The vegetation also consists of steppe species depending on these climatic conditions. Tree and shrub formations on the field is less than the dominant plant species in herb formation [30]. The site was first discovered by the General Directorate of Mineral Research and Exploration. There are two geothermal wells in the field.

Regional Geology

Many researchers have performed geological studies related to the study area and its surroundings [31,32,33,34,35]. In this study the regional geology was evaluated by using the previous studies conducted by the researchers (Fig. 2).

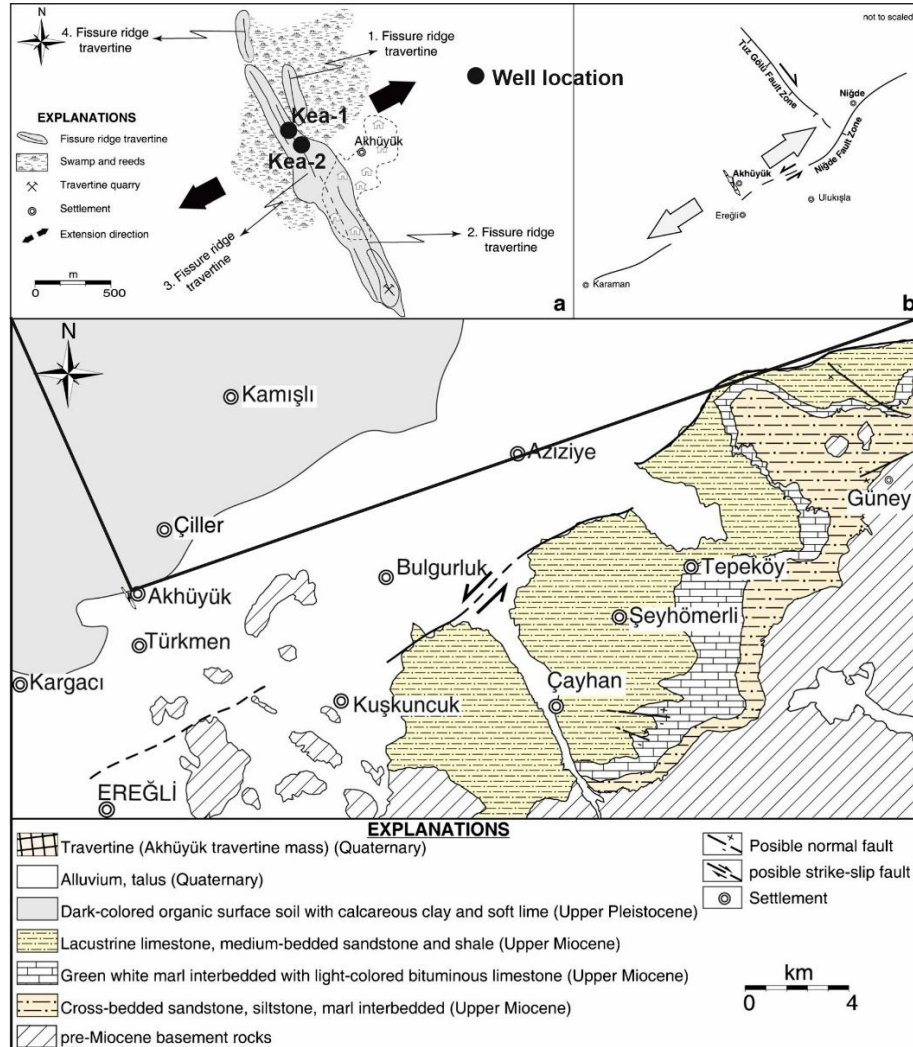


Figure 2. Regional geology and location map [36]

The study area lies within the Ereğli - Bor Neogene basin and consists of the Lower Paleozoic Nigde Group rocks. This unit was cut by Upper Cretaceous Sineksizyle Metagabros and Üçkapılı Granodiyrite. Ulukışla - Çamardı group consists of limestone blocks, Paleocene-Eocene volcanics, siltstone, sandstone and conglomerate of volcanic rocks. This unit was cut by Köyderesitepe trachytes. The Upper Paleocene-Eocene aged Başmakçı limestone, which is a reactive nummylitic limestone, overlies the Serenkaya formation. All these units were cut by Cehritepe syenite (Lower Eocene). This unit is overlain by Karatepe limestone. The volcanic

effect ended in the Central Lutetian and the South formation consisting of gray-beige colored siltstones began to precipitate. Due to the orogenic movements in Upper Lutetian, angular unconformity occurs between these rocks and the overlying units. As a result of the shallow marine - lagoon environment of the basin which began to occur in the Upper Eocene - Oligocene, an evaporitic deposit, Zeyvegediği anhydrite, was formed. Zeyvegediği anhydrite begins with light colored and stratified anhydrite at the bottom and then proceeds to upper levels with brownish, thin stratified sandstone-limestone and green marl. It consists of white colored stratified anhydrite and brownish clayey gypsum to upper levels. The lacustrine units were precipitated by sedimentation after this evaporitic sequence. The abundant presence of living organisms in this period has caused the abundance of organic material to be transported to the lake setting. Transported organic materials formed bituminous shales in an oxygen-free environment where the lake was deepened. This unit, which is called Katrandede Tepe formation, begins with green, white colored marls, followed by clayey limestone and marl. This unit contains bituminous shale levels in between. These bituminous shale levels continue alternately with evaporitic units. Above this unit, Beştepeler formation consisting of the clayey limestones and white, gray, dark gray, dirty white hard thin and smooth layers and conglomerate and sandstone-like clastic units formed due to re-shallower formation of the lake exists. To the north of the basin in the Tuz Gölü basin, volcanic activity from Upper Miocene-Pliocene to Quaternary has taken place. These activities affected the basin in terms of salinity. In the Upper Miocene-Pliocene, Melendiz and Hasandağı volcanism, which are formed on the large tectonic lines, form the elevations in the plain. The lavas of the Ojit-Andesite, Pyroxene-Andesite species belonging to the Melendiz volcanics were followed by the Hasan Mountain volcanism of the Andesite-Basalt type in Quaternary and finally the alkaline type volcanism in the plain [31,32,33,34].

Geology of the Study Area

The study area lies within the Ereğli - Bor Neogene basin. The definition and border relations of the formations were examined in detail in the field studies with the help of previous studies. Quaternary alluvial and travertine units were observed in the area.

Travertine

The unit developed due to the fossil geothermal outlet is a long slender zone which is depending on the topography 2.2 km long and has a thickness ranging between 13 and 16 meters and is approximately 120 meters wide, with Akhüyük village in the middle. Travertines have dirty white, cream and white colored smooth layers and are located between black and green colored layers. From the drilling of the travertine quarry located in the study area and the visible mirrors observed in the plant, the thickness of the travertine was determined. In the study area, back shaped travertine is generally observed but very little cone or dam shaped ones. Travertines on the field were precipitated as a result of loss of CO₂ gas in fluids rising up through the opening cracks. The smell of H₂S is felt and the current sulfur formations were observed.

Alluvium

Alluvium covering a very large area in the study region; consists of untied clay, silt, sand and gravel which unconformably covers other older units.

Evaluation of Chemical Analysis

In this study, the geology of Konya Ereğli Akhüyük geothermal field and its close vicinity were investigated and the two wells drilled in the field for geothermal purposes were examined in May 2018. Water samples were taken from one of these wells (KEA-1) for chemical analysis. The sample was placed in special plastic sterile container and brought to Envirolab measurement and analysis services (ind.trade.co.ltd.). Boron concentration was found to be 174 mg / lt. In previous studies, boron concentration was measured in water samples taken from that geothermal field. In 2012, [31] stated that, according to the chemical analysis of water samples taken, boron concentration is 251 mg / l in KEA-1 well and 254 mg / lt in KEA-2 well. As a result of the chemical analysis of the study carried out in the KEA - 1 well of the Ereğli municipality in 2017, the amount of boric acid found is 2118,41 mg / lt. For many years boron has not been considered as a toxic element. In 1958, 1963 and 1971, the International Standards on Drinking Water prepared by the World Health Organization have not been mentioned about boron.

Table 1. Boron concentration measured in water samples taken from wells

	MTA	Ereğli municipality(boric acid)	This Study
KEA-1	251 mg/lit	2118.41 mg/lit	174 mg/lit
KEA-2	254 mg/lit		

It was accepted that boron did not have any toxicological effect at the limit values published by the World Health Organization for drinking water in 1958-63 and 1973. In 1984, for the first time in this year's published articles, the boron element was mentioned and it was explained that there was no need for a study to reduce the boron value in drinking water. In 1993, for the first time in laboratory studies, harmful effects on animals were understood and the boron upper limit value in drinking water was stated as 0.3 mg / l. In 1998, it was increased to 0.5 mg / lt. Then, the maximum accepted upper limit value of the boron was increased to 2.4 mg / lt by taking into consideration the daily intake within limit values [37,38]. Table 2 shows the permissible upper limit concentrations of boron in drinking water of different countries. As it is understood from the table, many countries do not adhere to the recommendations of the World Health Organization. Saudi Arabia and Israel are the only countries that comply with these decisions. In the US, there is no regulation on the amount of boron concentration in drinking water, while Canada and Australia have set limits above the recommended upper limit. The first of two reasons for higher limit value is; there is not enough concrete information to prove its negative effects on human. Secondly, boron removal methods from waters are difficult and it is costly to reduce the boron concentration below standards [38]. According to Water Intended for Human Consumption Regulation published in Turkey, the upper limit of boron concentration which can be permitted was identified as 1 mg / L.

Table : 2 Permitted drinking water concentration in different regions of the World [37]

Regions	Max Boron Concentration mg / lt
Saudi Arabia	0.5
United States of America	-
Minnesota	0.6
New Hampshire	0.63
Florida	0.63
Maine	0.63

Wisconsin	0.9
European Union	1
South Korea	1
Japan	0.2
New Zeland	1.4
Israel	0.5
Australia	4
Canada	5
Turkey	1
WHO's recommended value	0.5

DISCUSSIONS

Boron element is frequently seen in scientific studies related to industry, food and agriculture, cleaning and health services. In recent years, studies of health sciences showed that daily intake of boron is different [5,6,7,8] in diets of children, young people, adults and elderly people depending on the gender. In a study conducted on postmenopausal women in terms of bone health, it was found that the amount of calcium in urine decreased by 44% at the end of the study with boron supplementation for 119 days [9]. In another study conducted on males, it was determined that calcium excretion in urine decreased 17% with the increase of daily boron intake [10]. Low levels of boron uptake have led to temporary memory losses in human brain functions and mental performance [14]. It was stated that Boron has preventive and protective effects in some types of cancer [15,16,17,18,19,20]. According to all these studies, boron element, used in proper amounts, has protective and preventive effects in terms of health related issues, while it is known to have toxicological effects in living organisms at high doses [5,24,27,28]. The present study evaluated the boron concentration of the sample from geothermal sources according to the chemical analysis performed and it was found that the limit values is above the limit values of standards set by Turkey and the World Health Organisation drinking water guidelines [38].

CONCLUSIONS

In this study, analysis results of water sample collected were evaluated according to Turkey and the World drinking water standards. According to the results obtained in this study; it was determined that boron concentration was above the drinking and potable water standards. When it is evaluated in terms of medical geology, according to the studies mentioned above related to health and food; it is

known that boron contributes to bone development, decreases the risk of cancer, increases mental performance and can benefit in human in many ways [15,16,17,18,19,20]. A total amount taken more than 500 mg per day may cause toxicity symptoms such as nausea, vomiting, headache, abdominal pain, diarrhea, muscle contraction, shock, weakness, digestive and central nervous system irregularities, impaired functioning of the glands and skin lesions as reported in different studies. The effect of boron concentration in thermal waters on people who are exposed to it in spa cure applications should be investigated in detail.

Thanks

In this study, I thank Envirolab Measurement and Analysis Services (ind.trade.co.ltd) and Geology Engineer Buğra SUCU for their support in water analysis. The authors declared that there was no conflict of interest.

REFERENCES

- [1] Çalık, A., 2002, Turkey's Bor Mining and Features, Engineer and Mechanical Magazine, 508, 36-41.
- [2] Nielsen F., 1998, Boron An Overlooked Element Of Potential Nutritional Importance Nutrition Today, 4-7 January/February 1988.
- [3] Yünlü, K., 2016, Boron, 1st ed. Ankara, Değişim Yayınları, 2016.
- [4] National Boron Research Institute Web Site: <http://www.boren.gov.tr/Access>, 29.12.2016.
- [5] WHO, 1998, Boron Environmental health criteria No. 204. A WHO monograph., World Health Organization, Geneva-Switzerland, 201p.
- [6] Barr, R.D., Clarke, W.B., Clark, R.M., Venturelli, J., Norman, G.R., ve Downing, KG., 1993, Regulation of lithium and boron levels in normal human blood, Environmental and Generic Considerations. J. Lab. Clin. Med., 121, 614-619.
- [7] Meacham, S.L., and Hunt, C.D., 1998, Dietary boron intakes of selected populations in the United States, Biol. Trace Elem. Res., 66, 65-78.
- [8] Rainey, C.J., ve Nyquist, L.A., 1998, Multicountry estimation of dietary boron intake, BioL. Trace Elem. Res., 66, 79-86.
- [9] Nielsen, F.H., Hunt, C.D., Mullen, L.M., Hunt J.R., 1997, Effect of dietary boron on mineral, estrogen, and testosterone metabolism in postmenopausal women, FASEB J., 1: 394-7.

- [10] Naghii, M.R., Samman, S.,1997, The effect of boron supplementation on its urinary excretion and selected cardiovascular risk factors in healthy male subjects, *Biol Trace Elem. Res.* 56: 273-86.
- [11] Chapin, R.E., and Ku, W.W.,1994, The reproductive toxicity of boric acid *Environ Health Persp.*, 102 (suppl. 7), 87-91.
- [12] Newman, R.E.,1994, Essentiality of boron for healthy bones and joints *Environ Health Persp.*, 102(7), 83-85.
- [13] Anonymous, Boron and Health, complete handbook of information, From the World WideWeb: <http://healthhelper.com/vitamins/minerals/boron.htm>., 2000.
- [14] Penland J.G.,1994, Dietary boron, brain function and cognitive performance, *Environ Health Perspect*, 102: 65-72.
- [15] Nielsen F.H., Mullen L.M., Nielsen E.J.,1991, Dietary boron affects blood cell counts and hemoglobin concentrations in humans, *J Trace Elem Exp. Med.*, 4: 211-23.
- [16] Bakirdere, S., Orenay,S., Korkmaz M.,2010,The effect of boron on human health, *The Open Mineral Processing Journal*, 3-1.
- [17] Müezzinoğlu, T., 2008, Boron Mineral Prevents Prostate Cancer? www.frm.tr.com/1442-159.
- [18] Hunt, C.D., Boron In: Coates P.M., Blackman M.R., Cragg G.M., Levine M., Moss J., White J.D.,2010, *Encyclopedia of Dietary Supplements* 2nd ed., New York, Marcel Dekker, p: 55-65.
- [19] Nielsen F.H., 2014,Update on human health effects of boron. *J Trace Elem Med and Biol.*, 28: 383-7.
- [20] Cui Y., 2004, Winton M.I., Zhang Z.F., Rainey C., Marshall J., De Kernion J.B., et al. Dietary boron in take and prostrate cancer risk, *Oncol Rep.*, 11: 887-92.
- [21] European Food Safety Authority. Opinion of the scientific panel on dietetic products, nutrition and allergies on a request from the commission related to the tolerable upper intake level of boron. *EFSA J* 2, 1-9, 2004.
- [22] Trumbo, P., Yates, A.A., Schlicker, S., Poos M., 2001,Dietary reference intakes for vitamin A, vitamin K, arsenic, boron, chromium, copper, iodine, iron, manganese, molybdenum, nickel, silicon, vanadium, and zinc, *J Am Diet Assoc.*, 101, 294-301.
- [23] European Food Safety Authority Scientific Opinion on the re-evaluation of boric acid (E 284) and sodium tetraborate (borax) (E 285) as food additives. *EFSA J.*, 11, 1-52, 2013.

- [24] Dogan, G., Sabah, E., Erkal, T.,2015, The scientific research in Turkey on the environmental impacts of the boron, the 19th International Mining Congress, Izmir, p. 425-31, 9-12 June 2015.
- [25] Tosun, E.,2010, Spectrophotometric determination of boron in various samples, E.Ü. Institute of Science and Technology, Master Thesis, 2010.
- [26] Şaylı, B. S.2000, Human Health and Boron Minerals, Ankara University Faculty of Medicine and A.Ü.Tıp Fakültesi - Eti Holding Projects Manager, Ankara, (www.bıgadic.gov.tr), May 2000.
- [27]Mastromatteo, E., and Sullivan, F.,1994, Summary; International Symposium on health effects of boron and its compounds Environ. Health Persp., 102(7), 139-141, 1994.
- [28] Cantürk M.,2002, Effects of Boron. TUBITAK Journal of Science and Technology, 2002. (www.biltek.tubitak.gov.tr/merakettikler)), 22.06.2017.
- [29] Kuru R., Yarat A.,2017, A Current View of Boron and Its Effects on Health Clin Exp Health Sci., 7 107-14.
- [30] Gülaçar, G.,2006, Geographical Survey of Ereğli Environment, Selcuk University Institute of Social Sciences.
- [31] Durdu, M., Karzaoğlu,H., Karzaoğlu, G., 2012, Konya Ereğli Akhüyük Field Geology - Geophysics - Study Report, MTA Report, 2012.
- [32] Kadıncık, G., Pekgöz, M., Karakaş, M., Murat, A.,2017, Tertiary Katrandedetepe Formation of Sodium Sulphate (Glauberite-Bloedite) - The Association of Khaled, Ereğli-Bor Basin, Turkey, Mineral Research and Exploration Journal, , 154, S:137-158, 224.
- [33] Oktay, F.,1982, Stratigraphy and geological evolution of Ulukisla and its surroundings. Turkey Jeol, Kur, Bült., 25, 15-24.
- [34] Dönmez, M., Türkecan, A., ve Akcay., A.E., 2003, Kayseri-Niğde-Nevşehir Region Tertiary Volcanites, MTA Report.
- [35] Altay, T., 2010, Investigation Of Mineralogic-Geochemical Properties and Industrial Raw Material Potential Of Neogene Aged Sedimentary Units Between Bor-Ulukisla Towns Selcuk University Graduate School of Natural and Applied Sciences PhD Thesis, p 286 (unpublished).
- [36] Temiz, U. u.; Savaş, F. 2015, Relationship between Akhüyük fissure ridge travertines and active tectonics: their neotectonic significance (Ereğli-Konya, Central Anatolia). Arab J Geosci., 8:2383–2392. DOI 10.1007/s12517-014-1353-7

[37] Başkan, Bilici, M., Atalay, N., 2014, Boron Pollution And Boron Removal Methods In Drinking And Irrigation Waters, Pamukkale University Engineering Sciences Degr., Vol. 20, Number 3, pp 78-84.

[38] Hilal, N., Kim, G.J., Somerfield, C., 2011, Boron removal from saline water: A comprehensive review, Desalination, 273 (1), 23-25.



Research Article

Variation of Fuel Characteristics of Diesel with the Use of Biodiesel and Alcohols (ethanol, methanol, 2-propanol, 2-butanol)

Ibrahim Aslan RESITOGLU*¹ 

¹ Mersin University, Department of Automotive Technology, Mersin, Turkey

Abstract

Many researches have been focused on alternative fuels in internal combustion engines because fossil-based fuels have many negation not only environmental aspects but also economical aspects. Especially, Diesel engines need alternative fuels because of their widespread use and harmful emissions mainly Nitrogen Oxides and Particulate Matter. Alcohols and biodiesel are the main alternative fuels to diesel fuel. They can be used in diesel engines as additive without any modification of engine. In this study, the effect of blending alcohols (ethanol, methanol, 2-propanol, 2-butanol) and biodiesel with diesel fuel on the diesel fuel properties was investigated experimentally. The alcohols were blended as 15% and biodiesel as 20%, 40% and 60% with diesel fuel. The results showed that the use of alcohols with diesel fuel as alternative fuels leads to a decrease in density, viscosity, calorific value, flash point and Cetane number values. On the other hand, biodiesel led to an increase in density, viscosity and flash point values, and a decrease in Calorific value and Cetane Number.

Received
1 November 2019

Accepted
4 December 2019

Keywords
Diesel
Alternative Fuels
Alcohols
Biodiesel
Fuel Specifications

¹ Corresponding Author Email: aslanresitoglu@gmail.com

INTRODUCTION

Nowadays, most of the energy needs are met by fossil fuels. In the transport sector, particularly diesel and gasoline vehicles, fossil fuels are commonly used energy sources [1]. However, instability in the prices of these fuels, increases in energy consumptions, environmental factors and the limited availability of these resources have led to the search for alternative energy sources [2]. Biodiesel and alcohols, which are biomass energy sources, are among the alternative energy sources for diesel fuel [3].

Biodiesel is the name given to esters formed by the reaction of oils in the presence of any alcohol and catalyst. Many types of edible or non-edible oil can be used in biodiesel production. Soybean, canola, sunflower are the most common vegetable oils used in biodiesel production [4]. Apart from these vegetable oils, animal fats and waste oils is widely used in the production of biodiesel. In particular, the use of waste oils results in significant reductions in biodiesel production costs [5]. Many scientific studies on the production of biodiesel and the use of biodiesel in compression ignition (CI) engines are being carried out by researchers [6-9]. In these studies, it is seemed that the biodiesel has a positive effect for diesel engines. Compared to diesel fuel, oxygen content in its structure, high flash point, improvement effect of engine emission characteristics and production with domestic resources are generated the main advantages of biodiesel [10]. On the other hand, the high viscosity and density is the main drawback against to use of biodiesel in diesel engines [11].

Alcohols are the most common sources of energy used as alternative fuels in diesel engines after biodiesel [12]. Alcohols obtained from vegetable wastes and renewable biological sources can be used as alternative fuels in CI engines by blending with diesel fuel in certain ratios. Thanks to the oxygen content, it improves the combustion efficiency and creates a catalyst effect on the engine characteristics [13]. The disadvantages of alcohols can compile as miscibility, low calorific and Cetane value and poor lubricating properties [14].

Compared to biodiesel, alcohols have lower density and viscosity values, which make it advantageous to use alcohols with biodiesel [15]. The higher density and viscosity is an important disadvantage for biodiesel. The use of combination of alcohols and biodiesel in diesel fuel is an effective way to prevent the drawbacks of biodiesel and alcohols. Many researchers have been approach to use together biodiesel and alcohols with diesel fuel [16-18]. Thus, the deficiencies of both biodiesel and diesel are eliminated.

The properties of fuels provide preliminary information on fuel efficiency and quality. Considering the various standards developed on fuel properties, it is possible to make comments on the similarity of alternative fuel types to diesel fuel and their usability in diesel engines. In this study, the effect of blending biodiesel and 4 different alcohol types with diesel fuel on the diesel fuel properties was investigated experimentally. After the alternative fuels were blended with diesel fuel in certain ratios, the basic fuel properties as density, viscosity, calorific value, flash point and Cetane number of each mixture were determined. The obtained values were compared with the fuel standard values.

MATERIAL AND METHODS

This section clearly describes the process of preparing fuels and determining the properties of fuels.

Preparation of Fuels

The biodiesel used in the study was obtained from a commercial company. Ethanol, Methanol, 2-Butanol and 2-Propanol were got commercially from Merck.

In this study, 7 different fuel mixtures were prepared by blending biodiesel and alcohols

with diesel fuel in different ratios. Biodiesel was blended as 20%, 40% and 60% and 4 different types of alcohol (ethanol, methanol, 2-propanol, 2-butanol) as 15% with diesel fuel. High rates of blending of alcohols with diesel fuel have a negative effect on diesel fuel properties and combustion efficiency [14]. Therefore, the ratio of alcohols in diesel was determined as 15%. Mixture fuels are named as indicated in the table below, taking into account the fuel content in them (Table 1).

Table 1. The blends

Fuel Code	Fuel rates
D	%100 Diesel
BI20	%20 Biodiesel + %80 Diesel
BI40	%40 Biodiesel + %60 Diesel
BI60	%60 Biodiesel + %40 Diesel
ET15	%15 Ethanol + %85 Diesel
ME15	%15 Methanol + %85 Diesel
PR15	%15 2-Propanol + %85 Diesel
BU15	%15 2-Butanol + %85 Diesel

Determination of Fuel Properties

In determining the properties of fuels, 5 different property values (density, viscosity, calorific value, Cetane number and Flash Point) were measured. Each measurement was performed 3 times and the values averaged.

In the measurement of density, Kyoto Electronic DA-130 Density Meter was used. The measuring range is 0-2 g/cm³ and 0-40 °C. The device is measured according to TS 6311 and ASTM D 4052-96 standards.

In determining viscosity values, Saybolt Universal Viscometer was used. It consist mainly a heater, fuel cup and fuel spill part. In the measurements carried out at 40 °C, the flow times of the samples were determined and these values were used in the conversion table and the viscosity values of each mixture were determined. Measurements were made in accordance with TS EN 14214 standard.

IKA-Werke C2000 calorimeter was used for the measurement of calorific values of fuels. Measurements can be made in TS1740, ASTM 240D, ISO1928, DIN51900, BSI standards.

TANAKA Flash Point Detection Device was used to determine the flash point of fuels, while ZX-440 Analyzer was used to determine Cetane numbers.

RESULTS AND DISCUSSION

In this section, the comparison of the density, viscosity, calorific value, flash point and cetane number values of the mixtures and diesel with each other and also with the EN 590 and EN 14214 standards are discussed in detail.

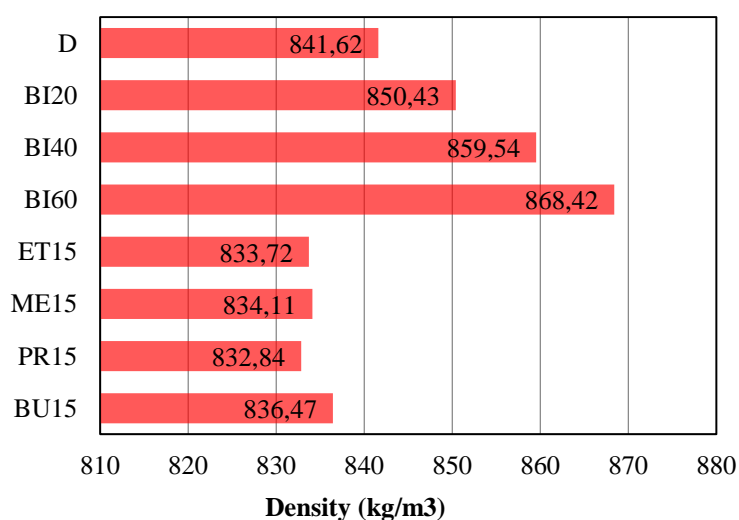
EN 590 and EN 14214 are the standards published by the European Committee for Standardization that describes the physical properties of diesel fuel and biodiesel respectively (Table 2).

Table 2. EN 590 (Diesel) and EN 14214 (Biodiesel) Standards

	EN 590	EN14214
Density at 15 °C (kg/m ³)	820-845	860-900
Viscosity kinematic at 40°C (mm ² /s)	2.0-4.5	3,5-5
Calorific value (MJ/kg)	-	-
Flash Point (°C)	Min 55	Min 101
Cetane number	Min 51	Min 51

Density

Density is defined as the weight of the unit volume. Figure 1 shows the density values for the mixtures. Density values increased with the use of biodiesel and decreased with alcohol use. The lowest density value was obtained with PR15 fuel using 15% propanol with 832.84 kg/m³. The highest density value was obtained with BI60 fuel. Compared to density of diesel, the densities of BI20, BI40 and BI60 were increased as 1.04%, 2.11% and 3.18%, while the densities of ET15, ME15, PR15 and BU15 were decreased as 0.91%, 0.89%, 1.04% and 0.61% respectively. Considering the EN 590 standard, it was found that all alcohol mixtures were in compliance with the standard. Due to the high-density values of biodiesel, density values of biodiesel mixtures were obtained higher than EN590 standard.

**Figure 1.** Density value of blends

Viscosity

Viscosity is the strength of fluids to flow and is an important factor for diesel engines, especially fuel supply and injection systems. Temperature and pressure significantly affect viscosity. The viscosity of diesel fuel directly affects the injector spray characteristics and consequently the combustion in the cylinder.

The viscosity values of the mixtures are shown in Figure 2. Similar to density values, viscosity values decreased with the use of alcohols and increased with the use of biodiesel. The lowest viscosity value was obtained with ME15 fuel as 2,348 mm²/s, while the highest viscosity value was measured as 3,732 mm²/s with BI60 fuel. All the viscosity values of the mixtures comply with EN590 standard. Compared to viscosity of diesel, the viscosities of BI20, BI40 and BI60 were increased as 13.06%, 26.01% and 39.30%, while the viscosities of ET15, ME15, PR15 and BU15 were decreased as 9.63%, 12.35%, 4.36% and 1.26% respectively.

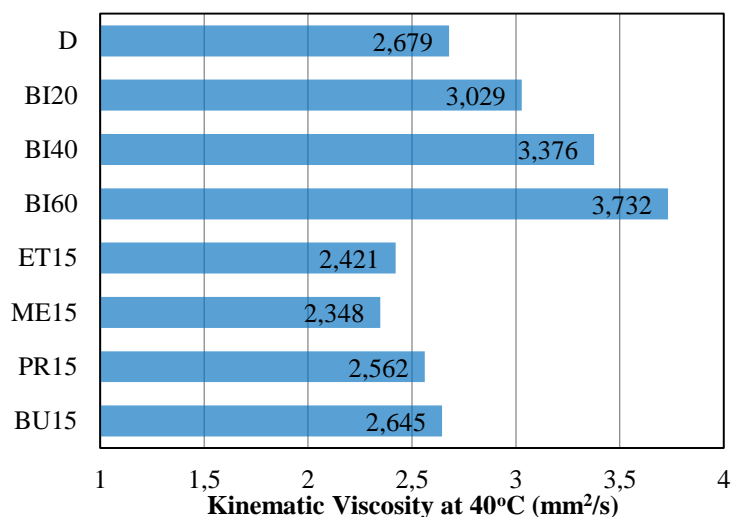


Figure 2. Viscosity value of blends

Calorific Value

The calorific value is equal to the thermal energy given to the environment when the fuel is fully burned in a continuous flow open system and the end-products are converted into combustion products. In other words, the calorific value of a fuel is equal to the absolute value of the combustion enthalpy of the fuel. The calorific values of fuels are usually given by the energy of the unit mass (kJ/kg or kcal/kg).

The calorific value depends on the phase of H₂O in the end-products. Thus, it is called as the higher calorific value (HHV) in the liquid phase of the H₂O at the end-combustion products and the lower calorific value (LHV) in the vapor phase of the H₂O at the end-combustion products.

The calorific value or combustion enthalpy of a fuel can be calculated from the enthalpy of formation of compounds involved in the combustion process. The higher calorific value of a fuel is equal to the lower calorific value and the latent heat of evaporation of the water vapor in the post-combustion products. Since the water is always present as steam at the end of combustion temperatures in the engines, the calorific value should be given as the lower calorific value. The calorific value is desired to be large because it indicates the amount of fuel energy.

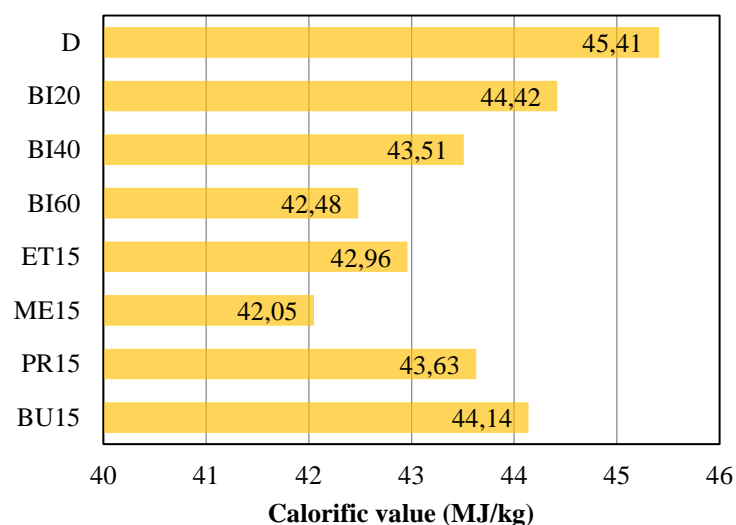


Figure 3. Calorific value of blends

The calorific value of each mixture is shown in Figure 3. The calorific values of all of the mixtures were measured at a lower value than that of fossil based diesel fuel produced from crude oil. Compared to calorific value of diesel, the calorific values of BI20, BI40, BI60, ET15, ME15, PR15 and BU15 were decreased as 2.18%, 4.18%, 6.45%, 5.39%, 7.39%, 3.91% and 2.79% respectively.

Calorific value is the most important indicator of fuel performance. However, although the use of biodiesel and alcohol causes a decrease in calorific value, it improves combustion performance. The main reason for this is that biodiesel and alcohols contain oxygen in the content and this has a catalytic effect on combustion.

Flash Point

In order for a liquid fuel to burn, the vapor of fuel must be mixed with the air in certain proportions. The easier a fuel can become vapor, the easier it is to form a flammable mixture with air. This easily combustible property of the fuel is determined by the flash point. The flash point of a flammable object is the lowest temperature at which it emits a vapor, which forms a flammable mixture with air. The flash point is not a fuel feature directly related to engine performance. Rather, it is measured to determine the safe handling and storage of fuels.

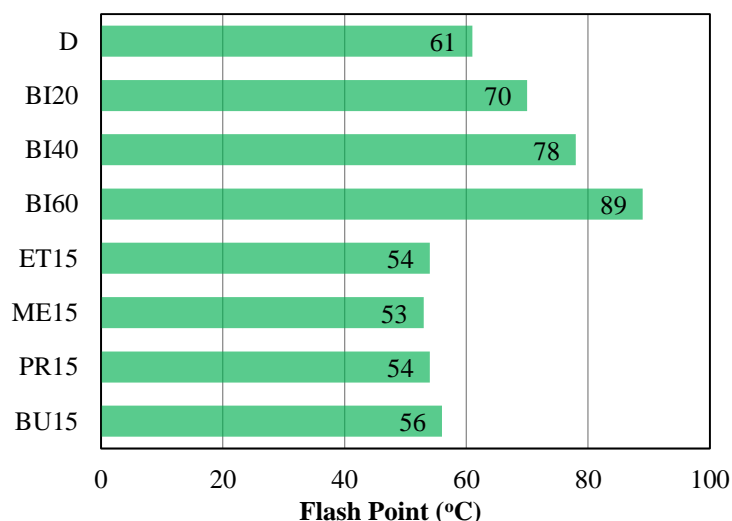


Figure 4. Flash Point value of blends

Figure 4 shows flash point values for mixtures and diesel. Significant increases in flash point values have been achieved with the use of biodiesel fuel. This is very useful for safer storage and transfer of diesel fuel. The flash point values of alcohol-containing mixtures were lower than those of diesel. The lowest flash point value was measured with a methanol-containing fuel mixture. Compared to flash point of diesel, the flash points of BI20, BI40 and BI60 were increased as 14.75%, 27.86% and 45.90%, while the flash points of ET15, ME15, PR15 and BU15 were decreased as 11.47%, 13.11%, 11.47% and 8.19% respectively. Compared to EN 590 standard, ME15 has a flash point of 2 °C, ET15 and PR15 of a flash point of 1 °C lower. This has a limiting effect on the further use of alcohol-containing fuels by 15%.

Cetane Number

In diesel engines, the measure showing the fuel's self-ignition capability is called the Cetane number. It is one of the most important features of diesel fuel. The increase in the number of Cetane reduces the ignition delay time, which forms the most important part of the

combustion process in the diesel engine, and therefore reduces the amount of fuel accumulated in the combustion chamber before sudden combustion. This leads to a decrease in the pressure increase rate during the sudden combustion phase.

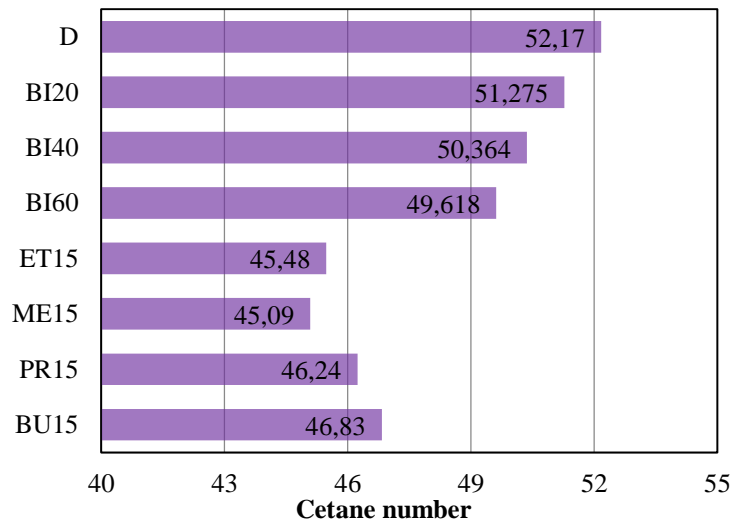


Figure 5. Cetane Number of blends

Figure 5 shows the values of the Cetane number of fuels. The use of biodiesel and alcohols with diesel fuel caused a decrease in the Cetane number values. The lowest Cetane number was measured as 45.09 with ME15 fuel. Compared to Cetane number of diesel, the Cetane numbers of BI20, BI40, BI60, ET15, ME15, PR15 and BU15 were decreased as 1.71%, 3.46%, 4.89%, 12.82%, 13.57%, 11.36% and 10.23% respectively.

CONCLUSION

As a result of the diesel blending of biodiesel and alcohol fuels which are alternative to diesel fuel, significant changes have been made on the fuel properties. Density and viscosity values increased with the use of biodiesel fuel compared with diesel fuel, but decreased with the use of alcohol fuels. The use of biodiesel and alcohols has led to some reductions in calorific value. However, oxygen content of biodiesel and alcohols completely prevents the decrease in combustion performance due to the decrease in calorific value. The flash point values of biodiesel-containing mixtures are higher than those of diesel fuels. This situation makes biodiesel storage and transfer processes safer. Some decrease in Cetane numbers was observed with the use of biodiesel and alcohols. In conclusion, compared the blends, B20 between biodiesel-diesel blends and B15 between alcohol mixtures, showed more similar fuel properties to diesel.

ACKNOWLEDGEMENTS

This study was supported by Mersin University Scientific Research Projects Unit. (Project Code: 2018-2-AP3-2964)

REFERENCES

- [1] Barreto, R. A., 2018. Fossil fuels, alternative energy and economic growth. *Economic Modelling* 75:196-220.
- [2] Ugurlu, A. and Oztuna, S., 2015. A comparative analysis study of alternative energy sources for automobiles. *International Journal of Hydrogen Energy* 40:11178-11188.
- [3] Erdiwansyah, Mamat, R., Sani, M. S. M., Sudhakar, K., Kadorahman, A., Sardjono, R.E., 2019. An overview of Higher alcohol and biodiesel as alternative fuels in engines. *Energy*

Reports 5:467-479.

- [4] Hosseinzadeh-Bandbafha, H., Tabatabaei, M., Aghbashlo, M., Khanali M., Demirbas, A., 2018. A comprehensive review on the environmental impacts of diesel/biodiesel additives. *Energy Conversion and Management*, 174:579–614.
- [5] Hajjari, M., Tabatabaei, M., Aghbashlo, M., Ghanavati, H., 2017. A review on the prospects of sustainable biodiesel production: A global scenario with an emphasis on waste-oil biodiesel utilization. *Renewable and Sustainable Energy Reviews* 72:445-464.
- [6] Abed, K. A., Gad, M. S., El Morsi, A. K., Sayed, M. M. Abu Elyazeed, S., 2019. Effect of biodiesel fuels on diesel engine emissions. *Egyptian journal of petroleum* 28(2):183-188.
- [7] Goga, G., Chauhan, B. S., Mahla, S. K., Cho, H. M., 2019. Performance and emission characteristics of diesel engine fueled with rice bran biodiesel and n-butanol. *Energy Reports* 5:78-83.
- [8] Asokan, M. A., Prabu, S. S., Bade, P. K. K., Nekkanti, V. M., Gutta, S. S. G., 2019. Performance, combustion and emission characteristics of julfiflora biodiesel fuelled di diesel engine. *Energy* 173:883-892.
- [9] Manigandan, S., Gunasekar, P., Devipriya, J., Nithya, S., 2019. Emission and injection characteristics of corn biodiesel blends in diesel engine. *Fuel* 235:723-735.
- [10] Singh, D., Sharma, D., Soni, S. L., Sharma, S., Kumari, D., 2019. Chemical compositions, properties, and standards for different generation biodiesels: A review. *Fuel* 253:60-71.
- [11] Sing, D., Sharma, D., Soni, S. L., Sharma, S., Sharma P. K., Jhalani, A., 2020. A review on feedstocks, production processes, and yield for different generations of biodiesel. *Fuel* 262:116553.
- [12] Yusri, I. M., Mamat, R., Najafi, G., Razman, A., Awad, O. I., Azmi, W.H., Ishak, W. F. W., Shaiful, A. I. M., 2017. Alcohol based automotive fuels from first four alcohol family incompression and spark ignition engine: A review on engine performance and exhaust emissions. *Renewable and Sustainable Energy Reviews* 77:169–181.
- [13] Tutak, W., Lukacs, K., Szwaja, S., Bereczky, A., 2015. Alcohol-diesel fuel combustion in the compression ignition engine. *Fuel* 154:196-206.
- [14] Zaharin, M. S. M., Abdullah, N. R., Najafati, G., Sharudin, H., Yusaf, T., 2017. Effects of physicochemical properties of biodiesel fuel blends with alcohol on diesel engine performance and exhaust emissions: A review. *Renewable and Sustainable Energy Reviews* 79:475–493.
- [15] Emiroğlu, A. O. and Şen, M., 2018. Combustion, performance and exhaust emission characterizations of a diesel engine operating with a ternary blend (alcohol-biodiesel-diesel fuel). *Applied Thermal Engineering* 133:371-380.
- [16] Bencheikh, K., Atabani, A.E., Shobana, S., Mohammad, M. N. and et al., 2019. Fuels properties, characterizations and engine and emission performance analyses of ternary waste cooking oil biodiesel–diesel–propanol blends. *Sustainable Energy Technologies and Assessments* 35:321–334.
- [17] Yesilyurt, M. K., Eryılmaz, T., Arslan, M., 2018. A comparative analysis of the engine performance, exhaust emissions and combustion behaviors of a compression ignition

engine fuelled with biodiesel/diesel/1-butanol (C4 alcohol) and biodiesel/diesel/npentanol (C5 alcohol) fuel blends. *Energy* 165:1332-1351.


- [18] Mahalingam, A., Devarajan, Y., Radhakrishnan, S., Vellaiyan, S., Nagappan, B., 2018. Emissions analysis on mahua oil biodiesel and higher alcohol blends in diesel engine. *Alexandria Engineering Journal* 57: 2627–2631.




Research Article

The Quantitative Effects of Different Growing Media on the Seedling Growth of Aubergine (*Solanum melongena* L.) and Cucumber (*Cucumis sativus* L.) in Autumn

Murat Demirsoy¹, Sezgin Uzun²

¹Sarayönü Vocational School, Selçuk University, Konya, 42003, Turkey, 

²Ondokuz Mayıs University, Faculty of Agriculture, Department of Hort., Samsun, Turkey. 

Abstract

The objective of this study was to examine the availability of some materials namely, forest soil, ash (firewood), charcoal, chicken manure, sheep manure, cow manure (decomposed), which can be easily found in Turkey. The vegetable crops tried were aubergine (Aydın siyahı) and cucumber (Beta 309 F1). The effect of growing media on the growth of seedling was found to be different depending on the species. In the study with forest soil and peat (GM1 and GM3) was ascertained that leaf dry weight (LDW), root dry weight (RDW), plant dry weight (PDW), total leaf area (TLA), leaf weight ratio (LWR), root weight ratio (RWR), stem weight ratio (SWR) and leaf area ratio (LAR) increased for aubergine during autumn season. This is similar to the increased in leaf dry weight (LDW), stem dry weight (SDW), root dry weight (RDW), plant dry weight (PDW), total leaf area (TLA) and leaf area ratio (LAR) of media named GM1 and GM3 applied for cucumber during autumn season. The results obtained from the present study showed that the most suitable growing media were the media named GM1 (forest soil) and the media named GM3 (a mixture of forest soil and peat) for aubergine and cucumber during autumn season.

Received

13 February 2019

Accepted

30 November 2019

Keywords

Growing Media,
Seedling quality,
Seedling cultivation,
Growth

¹Corresponding Author Email: mdemirsoy@selcuk.edu.tr

1. INTRODUCTION

One of the most important issues affecting the success of vegetable growing to produce quality seedlings [1, 2, 3]. The substrate composition is very important for seedlings. The physical properties and chemical composition have both a considerable effect on plant growth rate of young plants [4]. Although seedling production is commonly used many countries, the desired level of seedling production in terms of the appropriate media and mixtures have not been reached. The researchers focused on the usefulness of seedlings growing regional organic waste [1, 5]. Growing media is usually made from a mixture of organic materials and inorganic materials [6, 7]. Peat, due to favorable physical characteristics and high cation exchange capacity is used widely [8]. Farmers sometimes produce seedlings growing medium. However, they cannot take adequate measures against weed seeds, diseases and pests [9]. However, began to search for alternative materials due to major damage to the natural environment and the limited supply of peat [10, 11].

In our country, it could not develop an appropriate fee to the standards for the production of vegetable seed and seedling mortars, constitutes one of the major problems manufacturers. For this purpose, a seedling growing medium mixture prepared by different researchers, in the cultivation of different types of vegetables. Plant growth, earliness, yield and growing media were determined to make a positive impact on the quality of advice to the producers [12]. As a result of mistakes made in the preparation of seedlings grown in medium; seedlings, seeds, time, labor and causes a loss of product [7].

Quality seedlings; must have a balanced stem-root ratio, should have a high degree of total dry matter, nodes interval should be short, stem should be thick, leaves should be green and thick, it must have sufficient root growth, all parts must be strong and healthy, such as specific color characteristics must be evident, should not be too young or old and all the seedlings should be homogenous [13, 14, 15, 16]. Quantitative indicators of these criteria have been examined in our study. Therefore, the seedlings of vegetables growing medium should be the ideal mix enough to meet the request. Prepared seedlings growing media can be useful for others, although it is useful for a plant. In this respect to meet the demands of the majority of vegetables by making various preparations are needed to determine the ideal seedling growing media or separately optimal growing media for each type of seedling. This study; preparing seedlings of different environments, with different types of vegetables the growing medium (aubergine and cucumber) seedling quality, by determining their effects on seedling growth and development were studied to determine the most appropriate medium.

2. MATERIAL AND METHODS

In this study, the plant material "Aydin siyahı" aubergine and "Beta 309 F1" cucumber varieties were used. The type of material on the properties of seedling growing media and grain size is effective. Therefore, selecting one group of various materials in the desired size and mixed in suitable proportions multiple materials can be accessed on the intended properties. As the seedling growing media; forest soil ready for commercial peat, natural peat, wood ash, coal dust, chicken manure, sheep manure, cow manure, garden soil, hazelnut husk slag, pine needle and perlite materials were used. Commercial peat was used as control application. Also, fertilization was not performed on seedlings growing medium. The material used seedling growth medium mixture and the mixture ratios are given in Table 1.

Table 1. Mixing ratio of the seedling growth mediums used in the experiment.

Media	Material mixtures
GM1	Forest Soil (Pine forest)
GM2	Commercial Peat (Control)
GM3	1 Part Forest Soil + 1 Part Commercial Peat
GM4	1 Part Garden Soil + 2 Part Cow Manure
GM5	1 Part Forest Soil + 1 Part Sheep Manure + 1 Part Cow Manure + 1 Part Chicken Manure + 1 Part Ash + 1 Part Coal + 1 Part Pine Needle + 1 Part Hazelnut Husk Slag
GM6	1 Part Forest Soil + 1/3 Part Ash + 1/3 Part Coal + 1/2 Part Pine Needle + 1/2 Part Hazelnut Husk Slag
GM7	1 Part Forest Soil + 1/3 Part Sheep Manure + 1/3 Part Cow Manure + 1/3 Part Chicken Manure + 1/3 Part Ash + 1/3 Part Coal + 1/2 Part Pine Needle + 1/2 Part Hazelnut Husk Slag
GM8	1/3 Part Ash + 1/3 Part Coal + 1/2 Part Pine Needle + 1 Part Hazelnut Husk Slag
GM9	1/3 Part Sheep Manure + 1/3 Part Cow Manure + 1/3 Part Chicken Manure + 1/3 Part Ash + 1/3 Part Coal + 1/2 Pine Needle + 1 Part Hazelnut Husk Slag
GM10	1 Part Garden Soil + 2 Part Cow Manure + 1 Part Perlite
GM11	1 Part Garden Soil + 2 Part Cow Manure + 1/2 Part Hazelnut Husk Slag + 1/3 Part Ash + 1/3 Part Coal + 1/3 Part Sheep
GM12	1 Part Natural Peat + 1 Part Commercial Peat
GM13	1 Part Natural Peat + 1/3 Part Sheep Manure + 1/3 Part Cow Manure + 1/3 Part Chicken Manure
GM14	Natural Peat
GM15	1 Part Natural Peat + 1/2 Part Perlite + 1/3 Part Sheep Manure + 1/3 Part Cow Manure + 1/3 Part Chicken Manure

Seedlings were raised in module seed trays (45 cells 5*5 cm). Both plant species were the seed planting date 27 July. 50% shading were applied to seedlings until the date of planting. Nine seedlings have 4-5 true leaf is removed for analysis in each application and then plant dry weights were determined. Drying process was performed in the incubator (Nüve FN 500) at 80 °C for two days to determine the dry weight of different part of the plant (leaf, stem and root). The dry weights of the materials taken from the incubator were determined by weighing them on a precision scale (Chyo JL-180 (0,000lg)). Leaf areas of plant were measured by digital planimetry (Placom). Experiments were conducted in randomized blocks design with 3 replications and 9 plants in each replication. As a result of quantitative analysis, the formulas given in Table 2 were used in the calculation of plant growth parameters [17].

Table 2. The plants growth parameters for quantitative analysis.

Leaf weight ratio (LWR) = Total leaf dry weight (g)/Total plant dry weight (g)
Stem weight ratio (SWR) = Total stem dry weight (g)/Total plant dry weight (g)
Root weight ratio (RWR) = Total root dry weight (g)/Total plant dry weight (g)
Specific leaf area (SLA) (cm^2g^{-1}) = Total leaf area (cm^2)/Total leaf dry weight (g)
Leaf area ratio (LAR) (cm^2g^{-1}) = Total plant leaf area (cm^2)/Total plant dry weight (g)

The seedling health index was determined using the following equation [18] :

$$\text{Seedling Health index} = (\text{Stem diameter}/\text{Stem height}) * \text{Dry weight}$$

3. RESULTS AND DISCUSSION

For evaluation of research results, the highest results of seedling media are compared only.

3.1. Total plant dry weight (PDW)

Change of total plant dry weight of aubergine and cucumber seedlings of different growth media are given in Fig. 1, respectively. GM1 application for aubergine (0.66 g) and cucumber (2.01 g) showed the highest TPDW values (Fig. 1). Control application has reached a higher value than most of the growing medium in aubergine (Fig. 1a). Adding of mixtures of forest soil, seedling growing media was very effective in significantly increasing plant dry weight than the control plants in cucumber (Fig. 1b). In aubergine and cucumber showed significant increases in forest soil plant development. The results were notifications; Wang and Lin [19], adding half strength of 50% fertilizer to a mixture of 50% soil plus 50% compost was very effective in significantly increasing plant dry weight. According to Babaj, et al. [4] the cucumber seedlings grown in vermin compost had a higher dry matter compared with peat grown seedlings. It was reported by Uzun, et al. [20], the highest plant dry weight was obtained from the mixtures in the mixtures for decomposed farmyard manure, sieved garden soil, hazelnut husk, rice hull, sand of 2 mm, decomposed pine leaves, tobacco waste, coal ash and coal dust as ratios of 2:1:1:1:1/3:1:1/2:1/2:1/4. The highest leaf dry weight in aubergine was obtained from the plants grown in the mixture of decomposed farmyard manure, sieved garden soil and sand (2 mm) used in a ratio of 1:1:1.

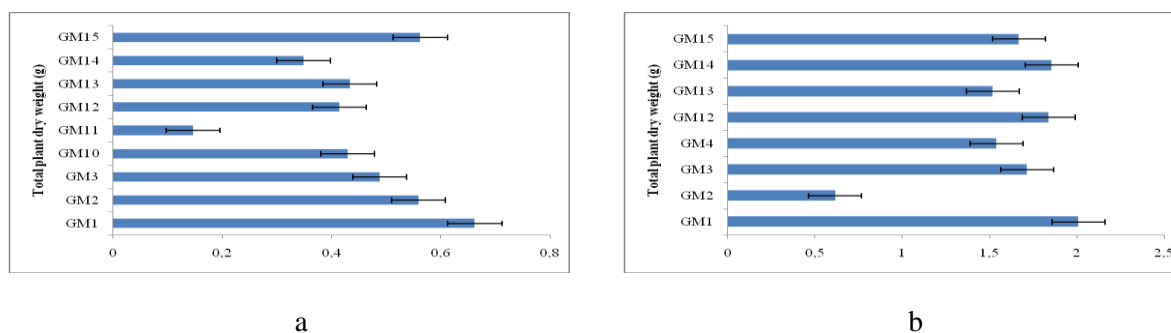


Fig. 1. According to different seedling growing media the changes of total plant dry weight (TPDW) for aubergine (a) and cucumber (b).

3.2. Total leaf area (TLA)

Total leaf area of aubergine and cucumber seedlings of different growth media are given in Fig. 2. GM3 application showed the highest TLA values (99 cm²) in aubergine (Fig. 2a). GM1 application showed the highest TLA values (312.53 cm²) in cucumber. Similar to the total dry weight of the cucumber plant total leaf area value is quite high compared to the control (Fig. 2b). According to Jankauskienė and Brazaitytė [21], seedlings grown in peat are higher, have bigger leaf area than the seedlings grown in peat-perlite, peat-zeolite substratum, but in leaves and roots they accumulate less dry matter and plant fresh weight also is smaller.

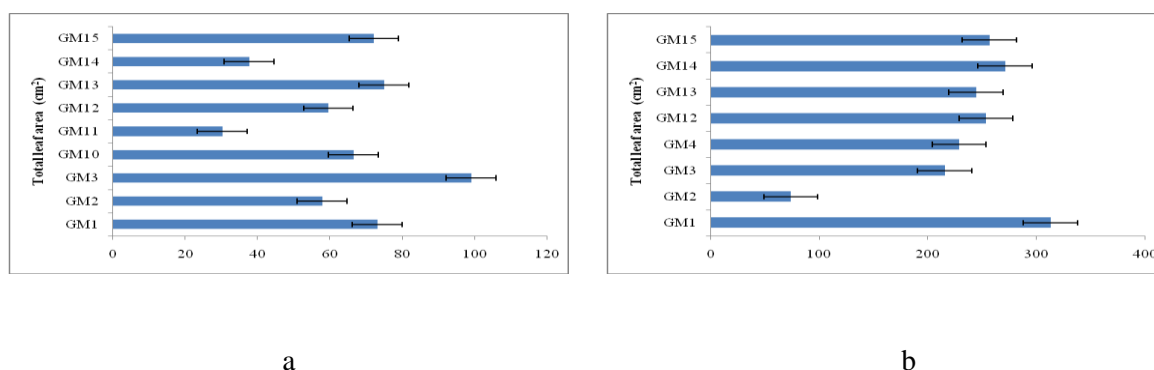


Fig. 2. According to different seedling growing media the changes of total leaf area (TLA) for aubergine (a) and cucumber (b).

3.3. Evaluation of Plant Growth Parameters

3.3.1. Leaf weight ratio (LWR), Root weight ratio (RWR) and Stem weight ratio (SWR)

When Fig. 3a is examined, it is observed that the highest LWR, RWR and SWR were seen from the seedlings of the GM3, GM1 and GM2 mediums, respectively. As seen in Fig. 3b, the highest seedling LWR, RWR and SWR were obtained from the seedlings of the GM4, GM2 and GM1 mediums, respectively. According to Kandemir, et al. [22], the highest leaf weight ratio and root weight ratio was measured as 0.56, 0.15 from the seedlings respectively. These results were found similar for cucumber.

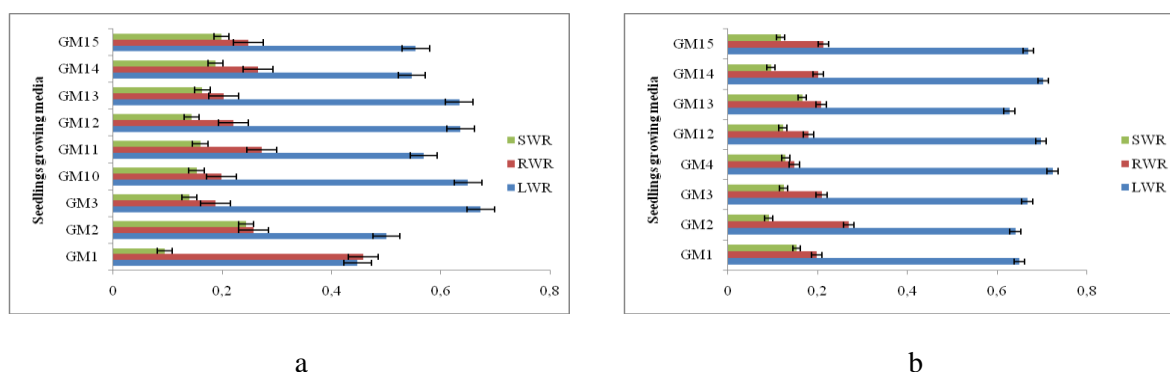


Fig. 3. According to different seedling growing media the changes of leaf weight ratio (LWR), root weight ratio (RWR) and stem weight ratio (SWR) for aubergine (a) and cucumber (b).

3.3.2. Specific leaf area (SLA)

The highest aubergine seedling specific leaf area was determined in the GM11 medium as 362.65 cm²/g, whereas the highest cucumber seedling specific leaf area was determined in the GM13 medium as 256.58 cm²/g (Fig. 4). According to Kandemir, et al. [22], the highest specific leaf area (276.82 cm²/g) were determined from the cucumber seedlings of the farmyard manure and garden soil (FYM+S) medium.

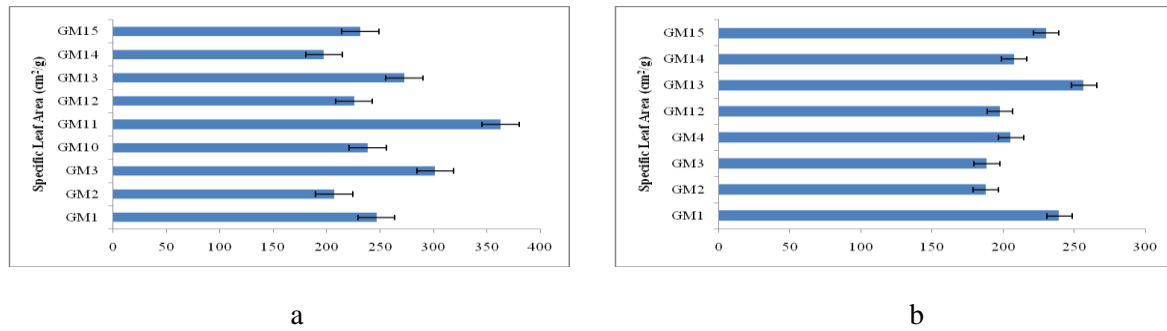


Fig. 4. According to different seedling growing media the changes of specific leaf area (SLA) for aubergine (a) and cucumber (b).

3.3.3. Leaf Area Ratio (LAR)

The highest leaf area ratio (206.23 cm²/g) for aubergine was determined from the seedlings of the GM11 medium (Fig. 5a). This value was obtained from GM13 medium for cucumber (Fig. 5b). According to Kandemir, et al. [22], the highest leaf area ratio (154.77 cm²/g) were determined from the cucumber seedlings.

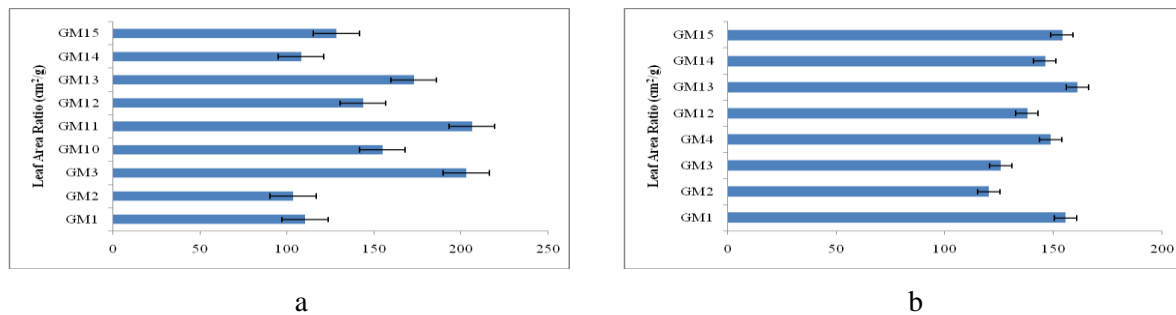


Fig. 5. According to different seedling growing media the changes of leaf area ratio (LAR) for aubergine (a) and cucumber (b).

3.4. Seedling Health Index (SHI)

When Fig. 6a is examined, it is observed that the highest seedling health index of 0.5 was determined from the seedlings of the GM1 medium. This medium was followed by medium GM3. The lowest seedling health index of 0.09 was obtained from the seedlings of the GM11 medium. As seen in Fig. 6b, the highest seedling health index was obtained from the seedlings of the GM14 medium. Seedling health index is an important indicator of quality seedlings [18]. According to Jankauskienė and Brazaitytė [21], cucumber seedlings grown in peat-zeolite and peat-perlite substratum accumulated in leaves and roots more dry matter than the seedlings grown only in peat.

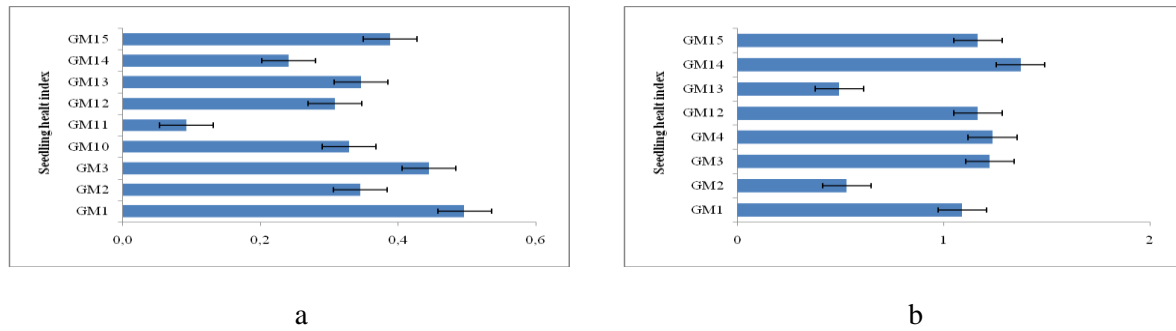


Fig. 6. According to different seedling growing media the changes of seedling health index (SHI) for aubergine (a) and cucumber (b).

4. CONCLUSION

It was reported that the proportion of quality seedlings obtained from quality seeds and suitable seedling media mixtures were found to be 20-30% higher than those of the seedlings produced with less and seedling media quality [22, 23]. The mixture used at the beginning of seedling production is preferred that the light structured. In this regard, the seedling production the use of materials such as perlite, sand or peat is more appropriate. Potting mix materials should be different according to usage. In vegetable production will start with quality seedlings; Increasing the product yield and quality will be achieved. As a result of this study, it can be said that the seedlings produced in the medium which were the media named GM1 (forest soil) and the media named GM3 (a mixture of forest soil and peat) for aubergine and cucumber during autumn season.

Information: This study is a part from master thesis of Murat DEMİR SOY. In addition, dear academic researcher Prof. Dr. Sezgin UZUN died in 2014.

References

1. Sevgican A. Örtüaltı Sebzeçiliği. Cilt IE Ü. Ziraat Fakültesi Yayınları No: 528. ISBN 975-483-384-2, İzmir; 1999.
2. Sevgican A. Topraksız Tarım. 3. Sebze Tarımı Sempozyumu. 2000:11-13.
3. Yanmaz R, Duman İ, Yaralı F, Demir K, Sarıkıymış G, Sarı N, . . . Özalp R. Sebze üretiminde değişimler ve yeni arayışlar. Türkiye Ziraat Mühendisliği VIII Teknik Kongresi. 2015:579-605.
4. Babaj I, Kaçiu S, Sallaku G, Balliu A. The Influence of Different Substrate Composition on Growth Parameters and Dry Mass Partitioning of Cucumber (*Cucumis sativum* L.) Seedlings. IV Balkan Symposium on Vegetables and Potatoes 830; 2008.
5. Gül A. Topraksız Tarım Uygulamaları. Türkiye V Seracılık Sempozyumu, s. 1990:411-419.
6. Atiyeh R, Subler S, Edwards C, Bachman G, Metzger J, Shuster W. Effects of vermicomposts and composts on plant growth in horticultural container media and soil. *Pedobiologia*. 2000;44(5):579-590.
7. Bunt B. Media and mixes for container-grown plants: a manual on the preparation and use of growing media for pot plants. Springer Science & Business Media; 2012.
8. Raviv M, Wallach R, Silber A, Bar-Tal A. Substrates and their analysis. Embryo

- Publications, Athens; 2002. p. 25-105.
9. Beckett KA, Beckett K, Carr D, Stevens D. The contained garden: the complete guide to growing outdoor plants in pots. frances lincoln ltd; 1999.
 10. Alexander P, Bragg N, Meade R, Padelopoulos G, Watts O. Peat in horticulture and conservation: the UK response to a changing world. *Mires and Peat*. 2008;3(8).
 11. Barkham J. For peat's sake: conservation or exploitation? *Biodiversity and Conservation*. 1993;2(5):556-566.
 12. Uzun S. Sıcaklık ve Işığın Bitki Büyüme, Gelişme ve Verimine Etkisi (III. Verim). *OM Ü Ziraat Fak Dergisi*. 1999;15(1):105-108.
 13. Álvarez S, Navarro A, Nicolás E, Sánchez-Blanco MJ. Transpiration, photosynthetic responses, tissue water relations and dry mass partitioning in *Callistemon* plants during drought conditions. *Scientia horticulturae*. 2011;129(2):306-312.
 14. Davis AS, Jacobs DF. Quantifying root system quality of nursery seedlings and relationship to outplanting performance. *New Forests*. 2005;30(2-3):295-311.
 15. Peter-Onoh C, Ngwuta A, Obiefuna J, Ogoke I, Orji J, Nwokeji E, . . . Abana P. Influence of growth media on the rate of emergence, growth parameters.
 16. Sa'id A, Lere G, Yahqub M, Abdullahi H, Hamma I. Influence of nursery media and age of cutting on the performance of moringa (*Moringa oleifera* (L.) in Samaru, Zaria. *Nigerian Journal of Agriculture, Food and Environment*. 2015;11(3):70.
 17. Uzun S. Sıcaklık ve ışığın bitki büyüme, gelişme ve verimine etkisi (I. Büyüme). *OMÜ Ziraat Fak Dergisi*. 1997;12:147-156.
 18. Fan X-X, Xu Z-G, Liu X-Y, Tang C-M, Wang L-W, Han X-l. Effects of light intensity on the growth and leaf development of young tomato plants grown under a combination of red and blue light. *Scientia Horticulturae*. 2013;153:50-55.
 19. Wang SY, Lin S-S. Composts as soil supplement enhanced plant growth and fruit quality of strawberry. *Journal of Plant Nutrition*. 2002;25(10):2243-2259.
 20. Uzun S, Balkaya A, Kandemir D. The effect of different mixtures of organic and inorganic materials and growing positions on vegetative growth of Aubergine (*Solanum melongena* L.) grown in bag culture in greenhouse. *Anadolu Journal of Agricultural Sciences (Turkey)*. 2007.
 21. Jankauskienė J, Brazaitytė A. The influence of various substratum on the quality of cucumber seedlings and photosynthesis parameters. *Sodininkystė ir daržininkystė*. 2008;27(2):285-294.
 22. Kandemir D, Özer H, Özkaraman F, Uzun S. The Effect of Different Seed Sowing Media on the Quality of Cucumber Seedlings. *The European Journal of Plant Science and Biotechnology* 2013;7 (Special Issue 1).
 23. Günay A. Sebze Yetiştiriciliği. Cilt I. Meta Basımevi, 502s İzmir. 2005.



Research Article or Review Article

An Investigation of Gross Error Angle in a Connecting Traverse with a $\pm 200^{gon}$ Difference

Hüseyin İnce^{1a}, Nuri Erdem², Fazlı Engin Tombuş^{1b}

^{1a,b}High School of Mapping and Land Survey, Hitit University, Çorum, Turkey,

²Engineering Faculty, Department of Geomatic Engineering, Osmaniye Korkut Ata University, Osmaniye, Turkey

Abstract

The Global Navigation Satellite System (GNSS) cannot always be used efficiently in city surveys because of the effect of obstructions such as high-rise building and high trees in the city discussed in. In this situation the measurements of angles and lengths have to be carried out with the conventional (classical) traversing methods. Since geodetic surveys can be tedious and time consuming, it is inevitable that systematic errors, unsystematic errors and gross errors occur despite the care that is taken. An angle measured in a traverse with an error margin can be used in the calculation of traverse.

If there is an error in the measurement of a traverse angle of $\pm 200^{gon}$ and this is then used in the manual traverse calculation, then the identification of this gross error is not possible in the calculation. In this case, the gross error is noticeable when the α_n control bearing is checked. However, the Brönnimann formula can be used in manual calculations to determine the point where gross error occurred. After a wide literature survey it was found that there is no such study with concerning special case of gross error is seen in the literature. In this study a simple formula which can replace the Brönnimann formula is presented for the case where the error is $\pm 200^{gon}$. A new formula is created to calculate easier and simpler than classical formula for this special case. A flow chart of the program for scientific calculators and computers are given together with numerical examples.

Received
21 July 2019

Accepted
09 December 2019

Keywords

Connecting traverse,
blunder angle (gross error angle),
single calculation method 1

1. Introduction

The Global Navigation Satellite System (GNSS) cannot always be used efficiently in city surveys because of the effect of obstructions such as urban canyon¹ and high trees discussed in [1, 2]. In this situation the measurements of angles and lengths have to be carried out with the conventional (classical) traversing methods. Since geodetic surveys can be tedious and time consuming, it is inevitable that systematic errors, unsystematic errors and gross errors occur despite the care that is taken. In this study, a method is proposed for the special case of gross error that can occur in angle surveys. This is when the error is to $\pm 200^{gon}$ of the normal value of a traverse angle. After a wide literature survey it was found that there is no such study with concerning special case of gross error is seen in the literature [3-7].

A single calculation method has been developed by many researchers [8-13] to investigate the gross error angle and it is possible to use the formula developed by [14].

If there is an error in the measurement of a traverse angle of $\pm 200^{gon}$ and this is then used in the manual traverse calculation, then the identification of this gross error is not possible in the calculation. In this case, the gross error is noticeable when the α_n control bearing is checked (Fig. 1). However, the Brönnimann formula can be used in manual calculations to determine the point where gross error occurred. In this study a simple formula which can replace the Brönnimann formula (Brönnimann, Study On The Gross Error Angles Of Traverse Calculations (in German: Auffindung eines groben Winkelfehlers in einem Polygonzug), submitted to the *Zfv.*, 1888) is presented for the case where the error is $\pm 200^{gon}$. A new formula is created to calculate easier and simpler than classical formula for this special case.

¹ An urban canyon is community of very high buildings in a city

Currently the calculations of traverse coordinates, the search for gross angular error and gross error length are carried out by computer using CAD programs. If software used in traverse calculation has been coded without taking into consideration this special case give in this study, then the program application will fail this happens in Turkey with software such as Netcad [15]. This study will present the programming that is required to prevent the failure of certain programs when facing a gross error of $\pm 200^{gon}$. The flow chart of the program has been developed, which will even run on scientific calculators and computers.

This paper outlines the background to the study, then the evaluation of the gross error and gross error angle with the flow chart of the program are presented. Finally, sample numerical examples are given.

2. Investigation of Gross Error and Gross Angle Error Angle on a Traverse

2.1. Investigation of the Gross Angle in Checking of the Control Bearing

Where, $\beta_0, \beta_1, \dots, \beta_n$ are the measured angles and $\alpha_0, \alpha_1, \dots, \alpha_n$ are the bearings. The angular misclosure error (f_β) in Figure1 is calculated as shown in equation (1).

$$f_\beta = \alpha_n - \alpha'_n \quad (1)$$

α'_n is calculated from equation (2).

$$\alpha'_n = \alpha_0 + [\beta] - k * 200^{gon} \quad (2)$$

The k value is determined to be a positive integer to calculate α_n approximately from $\alpha_0 + [\beta]$ in equation (2) and it is not a constant. The tolerable limit (F_β) of the angular misclosure determined by equation (1) is calculated according to the Regulations of Map Making used in Turkey. If $f_\beta < F_\beta$, d_β is computed the correction factor is as follows:

$$d_{\beta} = \frac{f_{\beta}}{n} \quad (3)$$

Thus, f_{β} is distributed over the angles using d_{β} as shown in equation (4).

$$\begin{aligned} (B1) &= \alpha_0 + \beta_0 + d_{\beta} \pm 200^{gon} \\ (12) &= (B1) + \beta_1 + d_{\beta} \pm 200^{gon} \\ (3C) &= (23) + \beta_3 + d_{\beta} \pm 200^{gon} \end{aligned} \quad (4)$$

Then, as shown in Figure 1 using the formula given in equation (4), all the bearings (azimuths) are calculated for all points starting from where the traverse is initially connected. The bearing from C to D is calculated with the first basic geodetic rule using the arctangent function (equation (5)).

$$(CD) = \arctan \left(\frac{Y_D - Y_C}{X_D - X_C} \right) \quad (5)$$

(CD) is also controlled by the relationship in equation (6).

$$(CD) = (3C) + \beta_n + d_{\beta} \pm 200^{gon} \quad (6)$$

If one of the angles in this traverse route is mistakenly taken as $\pm 200^{gon}$, (CD) calculated using equation (6) will be $\pm 200^{gon}$ different than when calculated using equation (5). An angular error of $\pm 200^{gon}$ to an angle cannot be detected in normal traverse calculations.

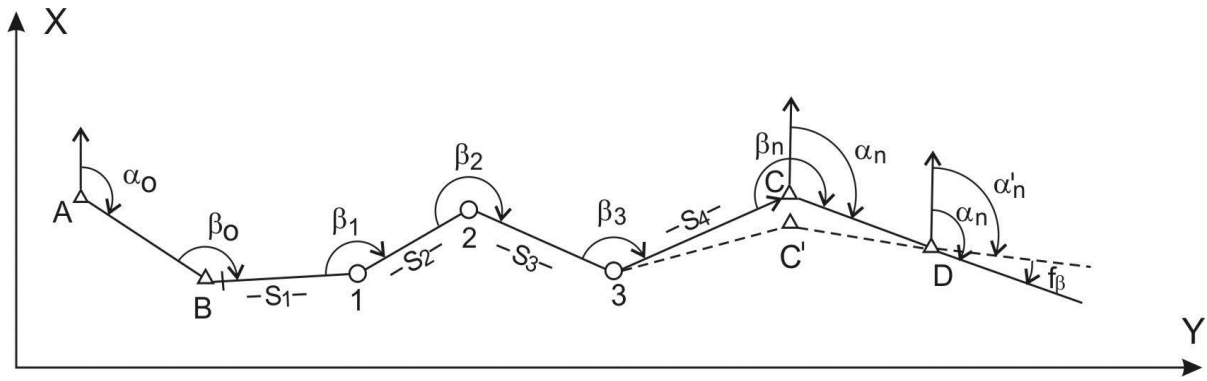


Figure 1. Locations of a connecting traverse route without a gross angular error (α_0 : starting bearing, α_n : control bearing, β : traverse angles at the points).

2.2. Investigation of Gross Error Angle Using Single Calculation Method

The investigation of the gross angular error will be explained in two stages, theoretically and practically.

2.2.1. Theoretical Investigation of The Point Where a Gross Error Angle Measurement is made

Taking the situation shown in Figure 2 where the error is applied to the angle at station 1. Thus, $\beta'_1 = \beta_1 - 200^{gon}$ this error will cause points 2 and C to be located at 2' and C' respectively. Drawing a line from C to C', two similar triangles are formed, namely C'2'1 and C21. M is the midpoint on the line and its position coincides with the position of point 1. From these similar triangles, the following relationships exist:

$$C'2' = 2'C, 12' = 12, C'2' \parallel 2C \text{ and } \beta_2 = \beta'_2 \text{ then } C'1 = 1C$$

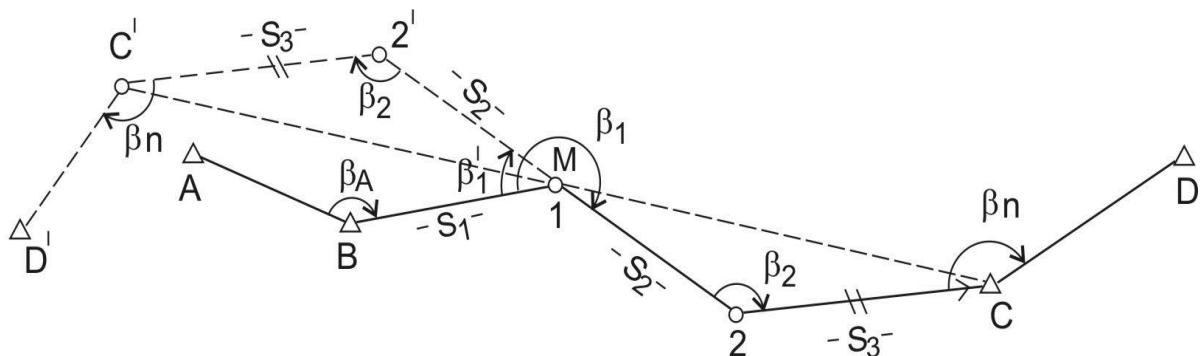


Figure 2- The effect of the error on the location of the following points when the angle on the connecting traverse route is taken as $\beta_1' = \beta_1 - 200^{gon}$ at point 1.

Taking the situation shown in Figure 3 where the error is applied to the angle at station 3. Thus, $\beta_3' = \beta_3 + 200^{gon}$ this error will cause points 4 and C to be located at 4' and C' respectively. Drawing a line from C to C', two similar triangles are formed, namely 34'C' and 34C triangles. M is the midpoint on the line and its position coincides with the position of point 3. From these similar triangles, the following relationships exist:

$$C'4' = 4C, 34' = 34, C'4' \parallel 4C \text{ and } \varepsilon = \varepsilon' = 400 - \beta_4 \text{ then } C'3 = 3C$$

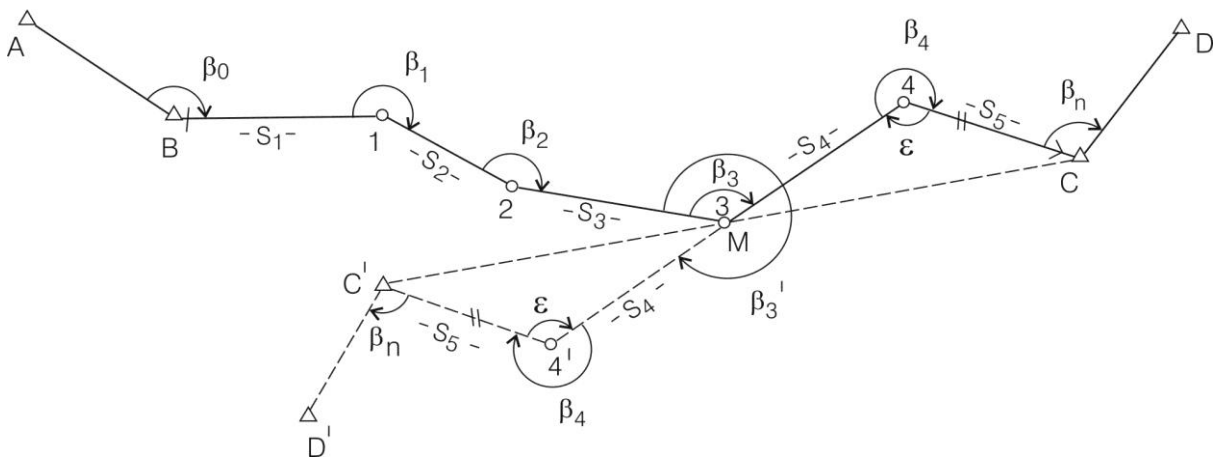


Figure 3- The effect of the error on the location of the following points when the angle on the connecting traverse route is taken as $\beta_3' = \beta_3 + 200^{gon}$ at point 3.

The M coordinate of midpoint of CC' line is obtained from following equations.

$$Y_M = \frac{Y_{C'} + Y_C}{2}, \quad X_M = \frac{X_{C'} + X_C}{2} \quad (7)$$

To find the angle that is given in any value, the single calculation method developed by various researchers [5, 8-11, 14] is expressed as follows:

$$Y_P = Y_M - 0.5*(X_{C'} - X_C)/\tan(f_\beta/2) , \quad X_P = X_M + 0.5*(Y_{C'} - Y_C)/\tan(f_\beta/2) \quad (8)$$

2.2.2. Practical Investigation of The Point Where a Gross Error Angle Measurement is made (Manual Calculation)

According to Figure 3, when the direction of calculation is taken from B to C , and after the (CD) value calculated for control purposes using equation (6) is determined to be $\pm 200^{gon}$ different from that calculated using equation (5), corrections made on angles using equation (3) are deleted. In the traverse calculation table, all bearings between the first and last connection points are calculated from following relationship.

$$(B1)' = \alpha_0 + \beta_0 \pm 200^{gon}$$

$$(12)' = (B1)' + \beta_1 \pm 200^{gon}$$

.

(9)

.

$$(3C)' = (23)' + \beta_3 \pm 200^{gon}$$

$$(CD)' = (3C)' + \beta_n \pm 200^{gon}$$

Using the calculated bearing and length values, the ΔY and ΔX values are calculated, as follows:

$$\begin{aligned} \Delta Y_1 &= S_1(B1)', & \Delta X_1 &= S_1 \cos(B1)' \\ \Delta Y_2 &= S_2(12)', & \Delta X_2 &= S_2 \cos(12)' \\ &\vdots & &\vdots \\ \Delta Y_4 &= S_4(3C)', & \Delta X_4 &= S_4 \cos(3C)' \end{aligned} \quad (10)$$

Then the traverses and point of the C' coordinates are calculated as follows:

$$\begin{aligned}
 Y_1 &= Y_B + \Delta Y_1, & X_1 &= X_B + \Delta X_1 \\
 Y_2 &= Y_1 + \Delta Y_2, & X_2 &= X_1 + \Delta X_2 \\
 &\vdots & &\vdots \\
 Y_{C'} &= Y_3 + \Delta Y_4, & X_{C'} &= X_3 + \Delta X_4
 \end{aligned}
 \tag{11}$$

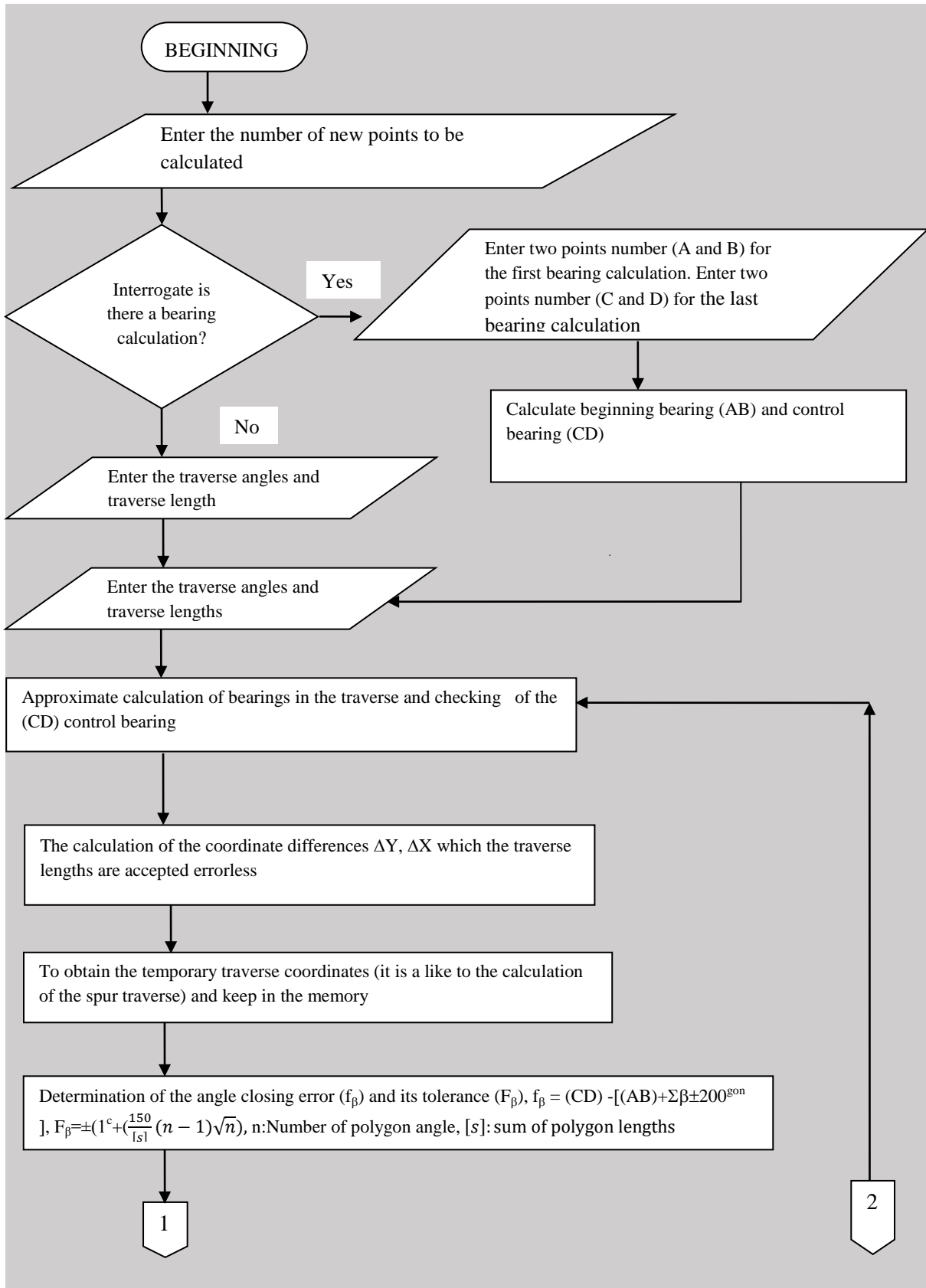
In the evaluation of the point at which the gross error angle is measured using the developed single calculation method (Figure 2 and Figure 3), equation (7) is used. The point coordinate value in the traverse calculation table, which is, nearly equal the values obtained from equation (7) is considered to be the point where the coarse error angle was measured.

3. The Flow Chart of the Program

Recently the calculation of the traverse has been performed with CAD software. However, this software appeared on the market, the calculation of traverse and the researching of gross error angle and gross error length was achieved by programs written by researchers [16, 17] in Turkey in Basic or FORTRAN.

The investigation of gross error angle was carried out in two ways in this study. The first way was to use the classical formula (8) to calculate the coordinate of the point with a measured gross error angle of any value (8). The second way was to find the coordinate of the point with measured angle with a $\pm 200^{gon}$ after the incorrect formula (7) was used. In addition another study [18-20] concerning the investigation of the gross error length was taken into the consideration.

The flow chart for the program was originally created for scientific calculators and it is given below (Fig. 4).



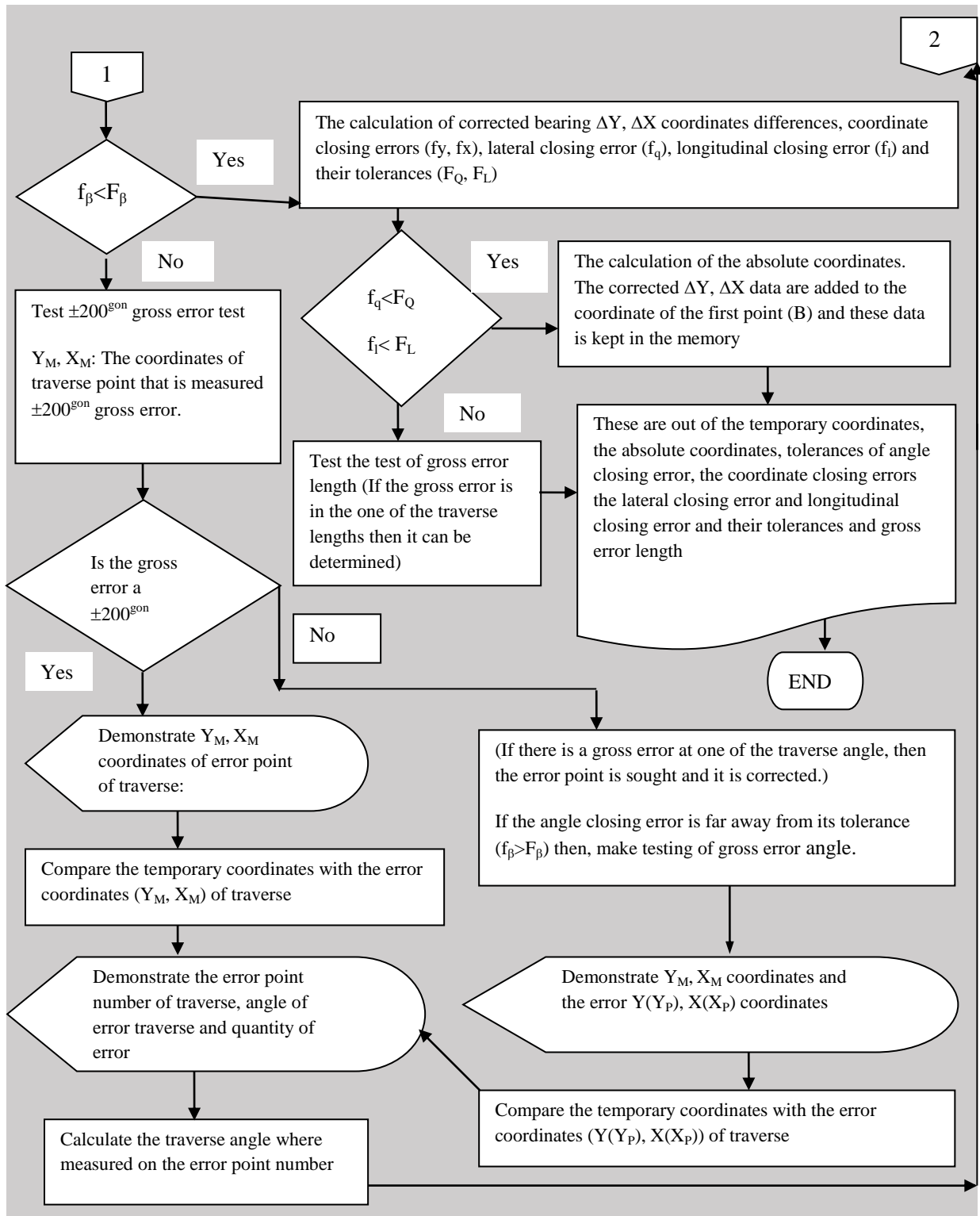


Figure 4- Flow chart of the program

4. An Application

For a numerical application, the traverse route without a gross error in which the lateral and longitudinal closing errors are smaller than their tolerances was taken into the consideration. The data of traverse route is given in Table 1. Assuming that the angle at point 2 in Figure 5 is measured as 115.2756^{gon} by mistake;

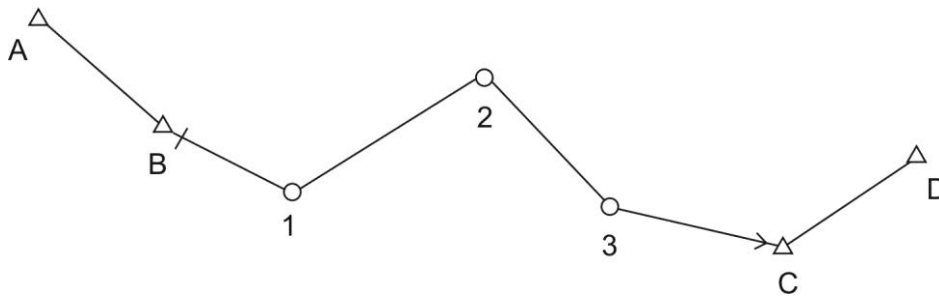


Figure 5- A traverse route placed without gross error

Table 1. The data of the traverse net without gross error angle

Point Number	Y	X	Traverse Angles (gon)	Lengths (meter)	Bearings (gon)
A	2701.38	4945.10	$\beta_0=175.4253$	B1=150.27	$\alpha_0=(AB)=185.9613$
B	2750.62	4725.43	$\beta_1=101.3347$	12=180.56	$\alpha_n=(CD)=84.1350$
C	3140.10	4382.63	$\beta_2=315.2756$	23= 195.42	
D	3383.10	4444.47	$\beta_3=185.4877$	3C=160.90	
			$\beta_n=120.6385$		

Manual Calculation;

Table 2. Calculation of the coordinates of the traverse without a gross error angle

Point Num.	Traverse Angles (^{gon})	Bearing (^{gon})	Length (m)	Y (m) ΔY (m)	X (m) ΔX (m)
A		$\alpha_0=185.9613$			
B	175.4253^{+23cc}			2750.62	14725.43
1	101.3347^{+24}	161.3889	150.27	85.65^{-3cm}	-123.47^{-2cm}
				2836.24	14601.94
2	315.2756^{+24}	62.7260	180.56	150.49^{-3}	99.78^{-2}
				2986.70	14701.70
3	185.4877^{+24}	178.0040	195.42	66.18^{-4}	-183.87^{-2}
				3052.84	14517.81
C	120.6385^{+24}	163.4941	160.90	87.29^{-3}	-135.16^{-2}
				3140.10	14382.63
D	$\alpha_{0+\Sigma\beta}= 1084.1231$ -1000.0000 $\alpha_n'=84.1231^{gon}$	$\alpha_n= 84.1350$ $-\alpha_n'=-84.1231$ $f_\beta=0.0119^{gon}$ $F_\beta= \pm 0.0295^{gon}$		$\Delta Y=389.48$ $-[\Delta Y]=-389.61$ $f_y = -0.13 m$ $f_q=0.15m$ $F_Q= \pm 0.17 m$	$\Delta X=-342.80$ $-[\Delta X]=-(-342.72)$ $f_x = -0.08 m$ $f_l=0.04m$ $F_L= \pm 0.23 m$

Table 3. Calculation of the coordinates of the traverse with a gross error angle of $\pm 200^{gon}$ value

Point Num.	Angle (^{gon})	Bearing (^{gon})	Length (m)	Y (m) ΔY (m)	X (m) ΔX (m)
A		$\alpha_0=185.9613$			
B	175.4253			2750.62	14725.43
1	101.3347	161.3866	150.27	85.66	-123.47
				2836.28	14601.96
		62.7213	180.56	150.48	99.79

2	115.2756			2986.76	14701.75
3	185.4877	377.9969	195.42	-66.20	183.86
				2920.56	14885.61
C	120.6385	363.4866	160.90	-87.31	135.15
				3140.10	14382.63
D	$\alpha_{0+\Sigma\beta}=884.1231$ 800.0000	$\alpha_n= 84.1350$ $\alpha_n' = (284.1231)$ $f_\beta=200.0119^{\text{gon}}$		$Y_C'=(2833.25)$	$X_C'=(15020.76)$

The coordinate of the midpoint, M , were computed with equation (7) as follows.

$$Y_M = (2833.25 + 3140.10) / 2 = 2986.67 \text{ m.}$$

$$X_M = (15020.76 + 143.63) / 2 = 14701.70 \text{ m.}$$

These Y_M and X_M values are similar to the coordinate values for point 2, indicating that the gross angular error occurred at point 2.

5. Results and Discussion

a) The investigation of gross error angle can be done in two ways:

- In the first way, the classical formula (8) can be used to calculate the coordinate of an angle with any value.
- As a second way, the formula (7) was developed to calculate the coordinate of a point with an angle with an error of $\pm 200^{\text{gon}}$ from the normal value.

b) The formulas in equation (7) are easier to use and simpler than classical formula given in equation (8) for this special case.

c) If software used to calculate the traverse has been coded without taking into consideration this special case, then the program application fails. This means that a special program must be created to cope with this error situation.

d) A study of gross error angle and gross error length on the traverse have been investigated used the software developed in this study. This software can even be used with scientific calculators such as Casio calculators.

e) To use the formula (7) in manual calculations, the following points should be noted:

- The use of $\pm 200^{gon}$ different value of an angle on calculation of the traverse coordinate appears when checking the control bearing.
- The corrections on the traverse angles have to be cancelled to find the gross error point and the coordinates of the points must be calculated using temporary bearings.
- The gross error point has to be determined by comparing the calculated value obtained by formula (7) with the coordinates calculated on the traverse calculation table.

REFERENCES

- [1] Bullock, B., (2004). GPS Antenna Placement Analysis for Receivers, www.commsdesign.com/main/9802fe.3htm
- [2] Tsakiri M. and Stewart M., (1998). A Future Vehicle Positioning System For Data Capture In The Urban Canyon, *Cartography- The Journal*, June, Vol.27, No.1.
- [3] Allan, A. L., Hollwey, J. R. and Maynes, J. H. B., (1968). *Practical Field Surveying and Computations*, Heinemann, London.
- [4] Bannister, A., Raymond, S. and Backer, R., (1992). *Surveying*, John Willey & Sons. Inc. 605 third Avenue, New York.
- [5] Kavanagh, B.F. and Bird, S. J. G., (2000). *Surveying Principles and Applications*, Upper Saddle River, New Jersey 07458.
- [6] Kissam. P., (1966). *Surveying Practice the Fundamentals Of Surveying*, McGraw- Hill, New York.
- [7] Uren, J. and Price, W.F., (1986). *Surveying For Engineers*, Second Edition, ELBS Macmillan and London.
- [8] Pinkwart,, (1941). Study On The Gross Error Angles Of The Conecting Traverse Calculations (in German: Die Auffindung eines groben Winkelfehlers im Polygonzug ohne Abschlurichtung.) *Zfv*. p. 227.
- [9] Rennebach,, (1941). The Determination of Gross Error Angles And Error Points In The Traverse Calculation (in German: Ermittlung eines groben Winkelfehlers und des Fehlerpunktes im Streckenzuge (Polygonzuge) ohne Abschlurichtung). *Zfv*, p.81.
- [10] Hamacher, W., (1963). Study on the Error Point of the Gross Error Angels of the Traverse Calculation (in German: Das Auffinden des Fehlerpunktes bei einem groben Winkelfehler im Polygonzug), *Zfv*, Nr, 3/1963, p.130-132.
- [11] Kavanagh, B. F., (2003). *Geomatics*, Pearson Education Inc., New Jersey.
- [12] Wolf, P. R., and Ghilani, C. D., (2008). *Elementary Surveying an Introduction to Geomatics*. 12th Edition, Upper Saddle River, New Jersey: Pearson Prentice-Hall.
- [13] Kavanagh, B. F., (2009). *Surveying principles and application*. 8th ed. Columbus: Pearson Education Inc.,

- [14] Brönnimann,, (1888). Study On The Gross Error Angles Of Traverse Calculations (in German : Auffindung eines groben Winkelfehlers in einem Polygonzug) Zfv. p.524.
- [15] URL_1:www.nedcad.com.tr
- [16] Banger, G., (1995). Basics of Computer Programming, Basic As Programming, Language, General Programming Structures, Sample Programs Volume 2 (in Turkish), K.T.Ü. Faculty of Engineering & Architecture, Faculty Press No: 52, Trabzon, Turkey.
- [17] Pektekin, A., (1978). Calculating The Coordinates Of A Traverse By Computers And Searching of Gross Error Angle And Length (in Turkish), Y.T.Ü. Text Nots / Monographies, İstanbul, Turkey.
- [18] İnce, H., (1999). The Proposals In The Researching By Calculation Method Of The Length Which Has Gross Error On The Dependent Traverse And Series Triangulation (in Turkish) K.T.Ü. Faculty of Engineering & Architecture, Faculty Press No: 24, Trabzon, Turkey.
- [19] Mao, Y., et al. Model of Gross Error Elimination for Monitoring Data Collected by A Surveying Robot, Journal of Engineering Science and Technology Review 7 (4) (2014) 13-17.
- [20] Mao Y. et al. A new method data caper method for rejecting the deformation monitoring data with the gross errors, Journal of Northeastern University, 2011(7), pp.1020-1023.



Research Article

Production of Hand Sterilization Fluid of Herbal Origin

Sergen Cetebozan^{1,1} , Hatice K. Ozgul^{1,2}  and Sibel Yigitarslan^{*1,3} 

¹ Suleyman Demirel University, Department of Chemical Engineering, Isparta, Turkey

Abstract

When the body is exposed to microorganisms of daily life, their negative effects on human health will be observed. Industrial disinfection gels especially used for effective and rapid hand disinfection, contain ethyl or isopropyl alcohol. Due to the presence of alcohol, they cause some allergic reactions on the skin. The aim of this study was to investigate the usability of flavonoids obtained from horse chestnut shells as hand disinfection gel material. Single and multi-parameter optimizations were applied to obtain the maximum amount of flavonoids from the material by ultrasonic extraction. In single optimization, it was determined that the application of 50°C, 2g-plant/100ml-water, 10 min-continuous sound waves increased the extraction efficiency. To determine the optimum values of parameters in multiple optimization, the Response-Surface Method including Box-Benkhen design was used via the Design-Expert program. As a result of the numerical solution, the application of ultrasonic extraction to 2.44g of horse chestnut and 100ml of water at 40.1°C for 14.89 minutes produced the highest flavonoid content. The amount of antioxidant in extracts was analyzed spectrophotometrically by DPPH method. The Addition of 9.6ml of the extract to mixed microorganism culture media resulted in successful inhibition. Thus, it was concluded that the disinfection liquid containing the same concentration produced by thickening it with sodium alginate was found as an alternative to the existing product containing synthetic chemicals.

Received

4 October 2019

Accepted

13 December 2019

Keywords

Aesculus hippocastanum
Ultrasonic extraction
Disinfection
DPPH

* Corresponding Author Email: yildizsibel@sdu.edu.tr

INTRODUCTION

It is a known fact that various microorganisms on the materials used in daily life cause serious diseases, especially infectious diseases, which may adversely affect human health, when entered into the human body [1]. Therefore, it is necessary to pay attention to environmental cleanliness and individual sterilization. In order to provide a faster and exact solution to disinfection of microorganisms, hand disinfectant gels contain 45-95% of ethyl alcohol or isopropyl alcohol [2]. Alcohol content of it is one of the main disadvantages of the product that causes some allergic reactions. Infection-related diseases and deaths, which are common problems from past to present, are increasing day by day. New methods have been tried to develop every day to prevent and/or treat them. Therefore, it has been suggested that in the field of pharmacology, the products obtained from antimicrobial plants may provide an advantage to human health compared to the products containing alcohol.

Basic compounds having antimicrobial effect in various plants and spices are declared as phenolics, phenolic acids, flavonoids, tannins, alkaloids and coumarins [3]. The sources of antimicrobial effect of plants are essential oils and extracts obtained from their seeds, leaves, flowers etc. The extracts contain alcohols, phenols, acids, aldehydes and esters and the combinations of these molecules. Due to their anticancer, antiseptic, antiallergenic and antimicrobial properties, they have been used as functional compounds in many drugs [4, 5]. Flavonoids are defined as a group of polyphenolic compounds and are known to decrease free radical formation [6]. The high efficiency of these compounds depends on the determination of the optimum conditions of the parameters such as solvent, solid-to-liquid ratio, time and temperature to be used during extraction [7]. Phenolic compounds are known to dissolve better in alcohol due to their hydrophilic nature. Thus, extraction of these compounds has been carried out with methanol, ethanol, water, acetone or combinations [8, 9]. In some academic researches, different types of essential oils (pinene, tujil alcohol, cineol flask and geraniol) have been extracted from the plants, and these essential oils have been declared to have antimicrobial properties against many bacteria and fungi [10]. In addition the usage of plants for medicinal purposes is not new. Positive effects of *Aesculus hippocastanum* plant and *Bunium paucifolium* on urinary tract inflammation, *Linum nodiflorum* on ulcers, *Centauria kurdica* on neural removal, *Echium italicum* on edema removal, *Salvia verticillata* on cell regeneration, *Ranunculus constantinopolitanus* on rheumatoid and ulcers have been announced in literature studies [11-14]. Erkaç and Yığıtarıslan obtained an extract from horse chestnut shells by using various solvents. They showed that this extract could prevent the growth of undesirable microorganisms during fermentation of olives in the table olive production [15]. *Aesculus hippocastanum* L. (*Hippocastanaceae*), also known as horse chestnut, grows on trees at temperate climates. From the past to the present, the extract of horse chestnut bark, flowers and seeds has been used on venous insufficiency diseases, varicose veins, hemorrhoids, phlebitis (inflammation of the veins), skin diseases, and for the treatment of body pain [16,17]. Application of horse chestnuts to cosmetic products such as scalp, oral care, facial, body hygiene started in 1980s. Recently, horse chestnut extracts have been added to enhance the health effects of many commercial products like body lotions, hair shampoos, creams and the like [16].

The aim of this study was to investigate the use of flavonoids derived from horse chestnut (*Aesculus hippocastanum*) shells as hand disinfection gel raw material. To achieve this, the extraction conditions of the horse chestnut were optimized by using response surface methodology and the efficiency of the extracts obtained under optimum conditions on microbial growth was investigated by analyzing the growth of specific microorganisms chosen.

MATERIAL AND METHOD

In this study, ultrasonic extraction method was used to obtain phenolic compounds of horse chestnut shells. This method was preferred because of performing both a faster and more efficient extraction process based on the observance of particles breakage to be extracted by mechanical shaking and the cavitation effect provided by the ultrasonic energy by applying acoustic vibrations at certain frequencies to the material that creates bubbles [18]. In the extraction experiments of the powdered horse chestnut shells, the single and double effects of the parameters such as temperature, solid-to-liquid ratio, time, wavelength, solvent type were optimized. In order to determine the optimum values of the parameters with the minimum number of experiments, the procedure in Balcı and Yigitarslan [19], in which flavonoid extraction by the ultrasonic extraction method from *Cinnamomum zeylanicum* was optimized, were applied in parallel. Box-Behnken experimental design (Table 1.) containing the response surface method was used with Design -Expert program to express surfaces representing the extraction process.

Table 1. Box-Behnken design parameters used in the study

Parameter Code	-1	0	+1
x ₁ : Temperature (°C)	40	50	60
x ₂ : Solid/Liquid (g/ml)	2/100	5/100	8/100
x ₃ : Time (min.)	5	10	15

The Total amount of antioxidant in the extracts was determined by DPPH (1,1-diphenyl-2-picryl-hydrylase) method. It is based on the reduction reaction between the antioxidant and the oxidant materials. The degree of the color change in the oxidizing agent (DPPH) depends on the concentration of antioxidants in the sample [20-22]. In this study, 1.4 ml phosphate buffer (pH 7.4), 100 µl sample and 1ml DPPH solution were mixed for 30 minutes to perform the reaction. The total amount of antioxidant is expressed by the percent of absorbance values calculated by the following equation due to the linear relationship between them.

$$\%ABS = \frac{ABS\ Blank - ABS\ solution}{ABS\ blank} \times 100$$

In the experiments which examined the efficacy of the extracts on microbial growth, horse chestnut extracts were prepared at optimum conditions determined by the Response Surface Method. Three different microorganisms and/or microorganism combinations were studied (No 1: *Saccharomyces boulardii*; No 2: *Lactobacillus casei*, *Lactobacillus acidophilus*, *Bifidobacterium animalis ssp lactis* B94; and No 3: *Lactobacillus acidophilus*, *Lactobacillus rhamnosus*). Samples were prepared in the laminar cabinet (ESCO), by addition of the inoculated microorganisms and aqueous solution of hand samples taken from the volunteers (500µl) into a sterilized MRS broth (100 ml), followed by addition of the extracts (9 ml) when the microbial growth in the medium reached to the log phase. Samples without extract were used as control groups for each microorganism colonies. Microbial growth in control groups and samples was analyzed spectrophotometrically at 600nm.

RESULT AND DISCUSSION

In this study, in order to determine the multiple optimization parameters of the ultrasonic extraction process, single optimization was applied by working with parameters including

temperature, solid per liquid ratio, duration and type of wave. In this process, the optimum values of each parameter were determined as 50°C, 2gr/100ml, 10 minutes and continuous sound waves, respectively. 15 experiments were carried out in accordance with the extraction parameters given in (Table 1), which were found to be the most effective ones on extraction efficiency, and antioxidant contents of extracts at those conditions were analyzed by DPPH method (Table 2). The proposed functions were analyzed statistically by using Design Expert program. The criteria used to determine the best function were as follows: the compatibility of the function proposed by the program must be “significant”, the difference between predicted R^2 and adjusted R^2 values must be less than 0.2, and the regression values must be close to 1.0 and close to each other. In the functions proposed by the computer program, the function providing these conditions was determined to be a reduced cubic model (Table 3). P values less than 0,0500 indicate that the model terms are significant. Values greater than 0.1000 indicate that the model terms are not meaningful. The parameter having the highest F value and the lowest p-value is the most effective parameter of the process. When the reduced cubic model data were examined, it was decided that the most important model terms were A, B, BC, C^2 and the most effective parameter was A (Table 3). As a result of multiple optimization, it was determined that the extract with the highest antioxidant content would be obtained by extraction of 2.44 g horse chestnut by using 100 ml of water, and at 40.1°C, and with continuous ultrasonic wave application during 14.89 minutes.

In the literature studies, different alcohol or alcohol combinations have been used as a solvent in the extraction processes [15, 23]. In terms of the intended material, the usage of alcohol was found to increase the extraction efficiency [15]. In this study, water was used as a solvent, because aiming to determine the antimicrobial properties of the *Aesculus hippocastanum* shell were resulted from the antioxidant components of the extract, not from the alcohol; and because of intending production of a non-alcoholic and thus not allergenic product to the human body.

Table 2. Radical scavenging activity of the extracts at conditions determined by Design Expert Program

Experiment No	x_1	x_2	x_3	ABS %
1	-1	-1	0	92.71
2	+1	-1	0	84.24
3	-1	+1	0	92.23
4	+1	+1	0	80.44
5	-1	0	-1	93.69
6	+1	0	-1	88.99
7	-1	0	+1	92.79
8	+1	0	+1	84.90
9	0	-1	-1	91.13
10	0	+1	-1	91.75
11	0	-1	+1	94.50
12	0	+1	+1	84.19
13	0	0	0	86.81
14	0	0	0	89.01
15	0	0	0	87.52

Table 3. ANOVA for Reduced Quadratic model

Source	Sum of Squares	df	Mean Square	F-value	P-value	
Model	226,44	5	45,29	21,08	0,0001	significant
A-Temperature	134,89	1	134,89	62,79	< 0.0001	
B-Solid/Liquid	24,40	1	24,40	11,36	0,0083	
C-time	10,53	1	10,53	4,90	0,0541	
BC	29,87	1	29,87	13,90	0,0047	
C ²	26,75	1	26,75	12,45	0,0064	
Residual	19,33	9	2,15			
Lack of Fit	16,81	7	2,40	1,91	0,3868	not significant
Pure Error	2,52	2	1,26			
Cor Total	245,77	14				

$R^2=0.9213$; predicted- $R^2=0.7701$; adjusted $R^2=0.8776$; standart deviation=1.47; CV=1.65%

Considering the studies in the literature, it is seen that even if the desired component and extraction parameters are the same, different optimum values are obtained for different plants [15, 18, 23]. For example, in the study conducted by Wang et al., the optimum time for the extraction was determined as 30 minutes, whereas in the study of Stanisavljević et al. 40 minutes was found, and in this study, 14.89 minutes were determined to reach maximum yield. Although both studies used ultrasonic methods and in both phenolic components were extracted, the optimum values of extraction parameters, and thus the extraction yields, in the plants of *Inula helenium* and *Echinacea purpurea L.* were quite different from each other [18, 23]. Therefore, as the extraction conditions and yields are highly dependent on both the plant and the method, comparison of the study findings with the literature data is not possible because there is no match.

In this study, it was found that the extract components obtained at determined optimum conditions inhibited the growth of whole microorganisms (Figures 1, 2 and 3), when they were added to the media prepared with mixed microorganism cultures and palm microflora. Approximately 70% of inhibition in the pathogenic microorganism-predominant medium in 780-1260 minutes, approximately 84% in non-pathogenic microorganism medium between 600-900 minutes, and 55% in probiotic microorganism medium in 900-1140 minutes were determined. Finally, in the study, extracts with the same concentration, hand disinfection gel produced by thickening with sodium alginate were produced.

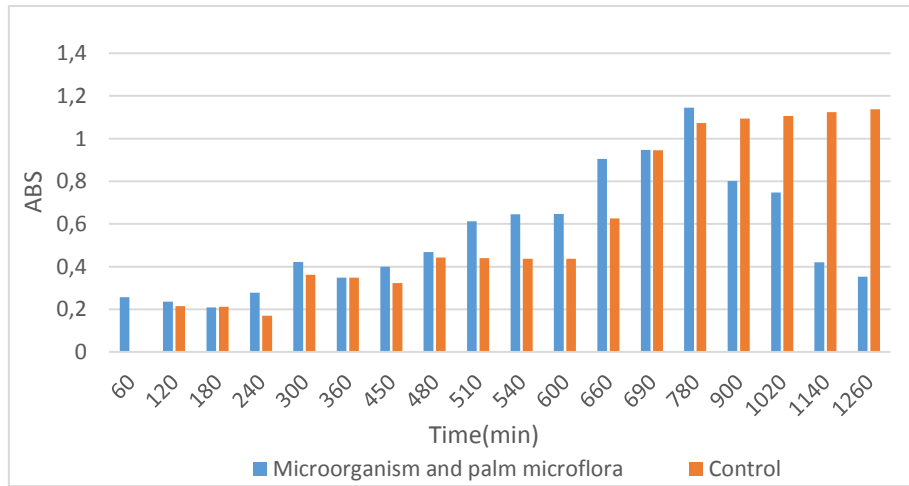


Figure 1. The effect of extracts on the growth of *Saccharomyces boulardii*-palm microflora

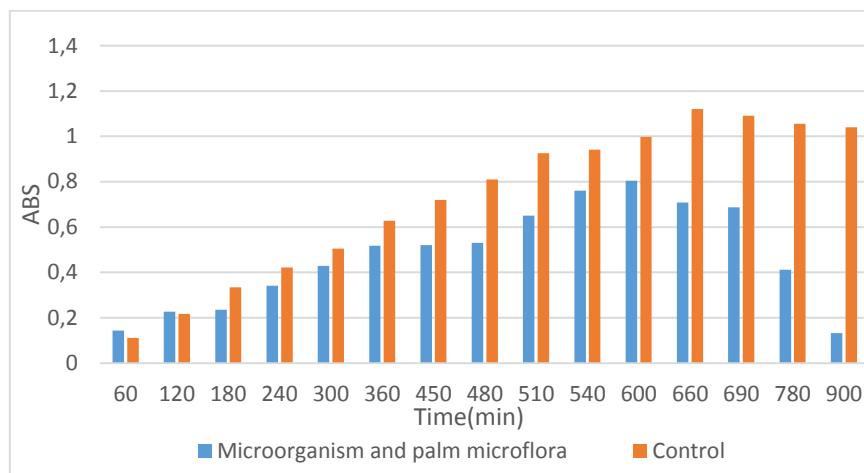


Figure 2. The effect of extracts on the growth of *Lactobacillus casei*, *Lactobacillus acidophilus*, *Bifidobacterium animals ssp lactis* B94 –palm microflora

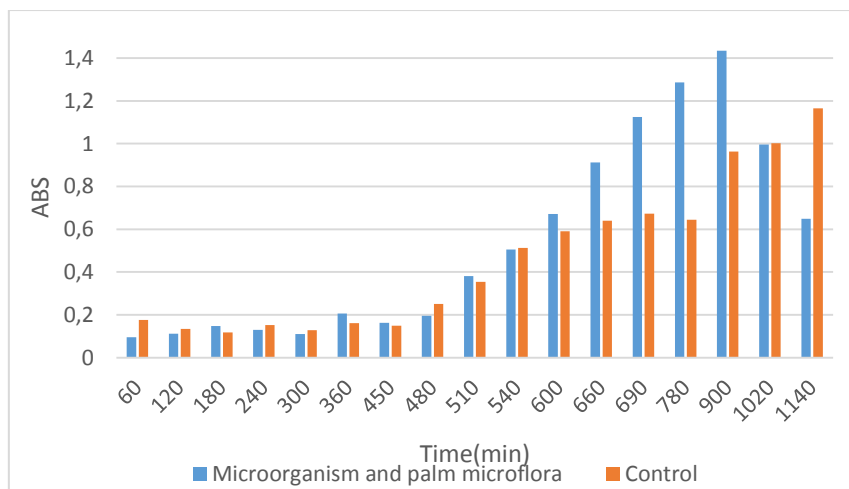


Figure 3. The effect of extracts on the growth of *Lactobacillus acidophilus*, *Lactobacillus rhamnosus* – palm microflora

In the study, when multiple optimization techniques were applied to the parameters selected in the ultrasonic extraction method of horse chestnut shells, the best model expressing the

extraction surface was determined as a reduced cubic model. The industrial expression of this process is as follows:

$$\%ABS = +87.56571 - 4.10625 \cdot \text{temperature} - 1.74625 \cdot \frac{\text{solid}}{\text{liquid}} - 1.14750 \cdot \text{time} - 2.73250 \cdot \frac{\text{solid}}{\text{liquid}} \cdot \text{time} + 2.67679 \cdot \text{time}^2$$

The red regions on the three-dimensional ultrasonic extraction surfaces created using the Design- Expert program refer to the regions with the highest extraction efficiency (Figure 4, 5 and 6). Accordingly, it was found that in order to achieve high efficiency, low solid-liquid ratios required lesser time and high solid-liquid ratios required more time (Figure 4). This may be due to the fact that the antioxidants extracted from the material are not dispersed on the surface, but on the whole. When the other parameters were taken into consideration, it was seen that a better efficiency could be obtained when the temperature and solid/liquid ratio was reduced (Figure 4 and 5). The low temperature indicated that this extraction conditions could be preferred both in terms of low cost and high content of non-degraded antioxidant components.

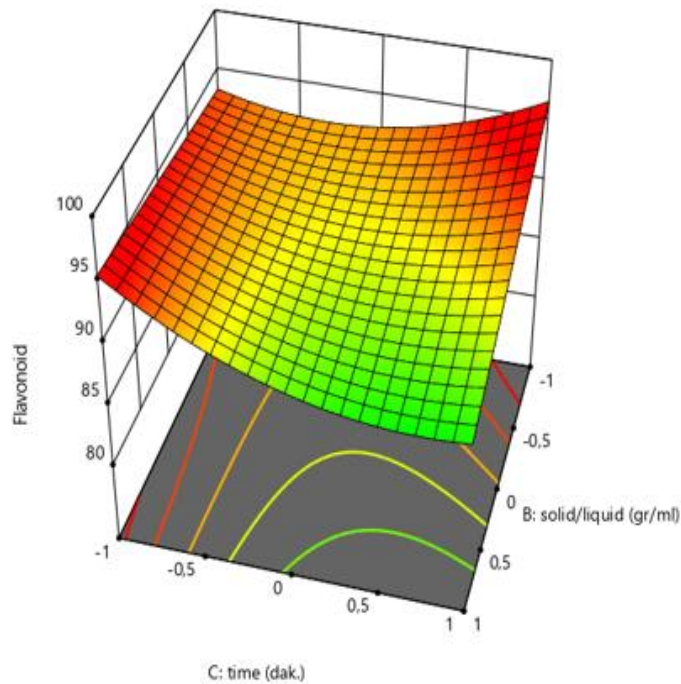


Figure 4. The effect of solid-liquid ratio and time on yield of extraction

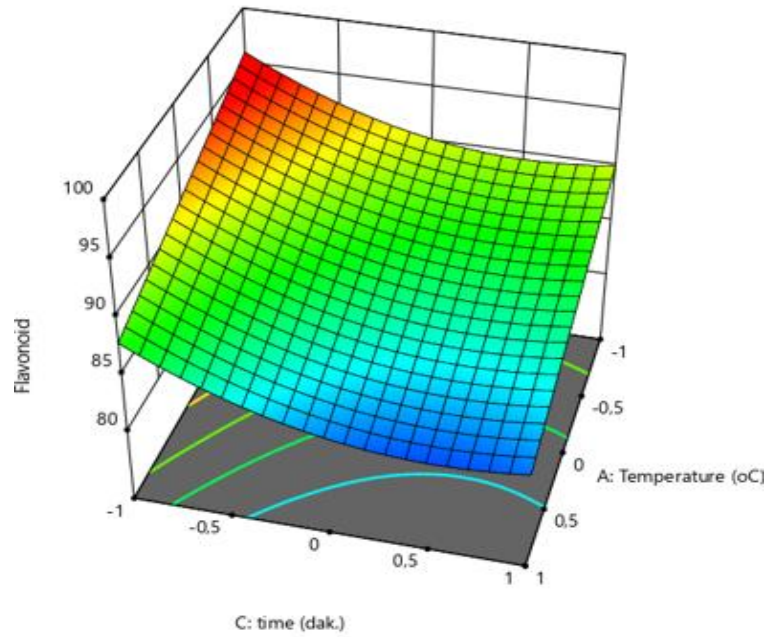


Figure 5. The effect of temperature and time on yield of extraction

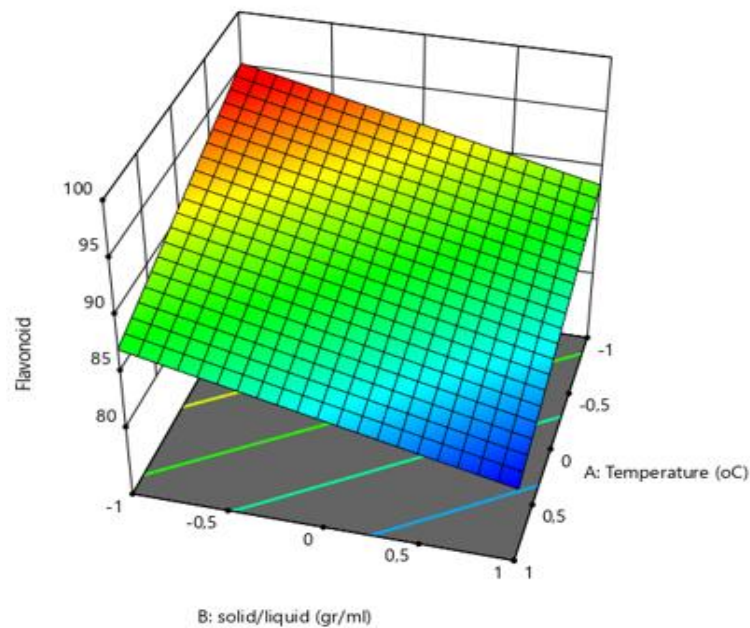


Figure 6. The effect of temperature and solid-liquid ratio on yield of extraction

CONCLUSION

In this study, it was demonstrated that the hand sterilization fluid without alcohol can be produced with extraction of horse chestnut shells, as an alternative to industrial hand disinfection liquid. This will eliminate the disadvantages of alcohol-containing hand disinfectant fluids when used for sterilization. Since horse chestnuts can grow in many geographical areas, spills occur during seasonal changes. Up to now, these materials

considered as waste and disposed of in the trash. Instead of doing this, according to the results of the study, the person appointed by the municipalities should collect the horse chestnuts and forward them to the authorized institutions to turn into useful products. By the way, the cost reduction in the production of sterilization fluids and may be cosmetics also be achieved. In future studies, the effects of the gel on other pathogenic microorganisms, and the usage of other plant sources instead of horse chestnut as antimicrobial materials should be examined and their mechanism of action should be determined. The use of plants in the field of pharmacology, which is increasing in popularity today, may lead to different new studies that may benefit to human health.

REFERENCES

- [1] Erdogan, A.E., Everest, A., 2013. Antimikrobiyal ajan olarak bitki bileşenleri, *Türk Bilimsel Derlemeler Dergisi*, (2), 27-32.
- [2] Ozyurt, M., 2005. Aldehid, Peroksijen ve Perasetik Asit ile Klor Verici Ajan İçermeyen ve Alet Dezenfektanı Olarak Önerilen Diğer Dezenfektanlar, Genel Kullanım Alanları ve Antimikrobiyal Etkinlikleri, 4. Ulusal Sterilizasyon Dezenfeksiyon Kongresi, 180-199.
- [3] Gyawali, R., Ibrahim, S.A., 2014. Natural products as antimicrobial agents. *Food Control*, (46), 412-429.
- [4] Çoban, Ö. E., Patır, B., 2010. Antioksidan etkili bazı bitki ve baharatların gıdalarda kullanımı, *Gıda Teknolojileri Elektronik Dergisi*, 5(2), 7-19.
- [5] Burt, S., 2004. Essential oils: their antibacterial properties and potential applications in foods—a review. *International Journal of Food Microbiology*, 94(3), 223-253.
- [6] Farkas, O., Jakus, J., Héberger, K., 2004. Quantitative structure–antioxidant activity relationships of flavonoid compounds. *Molecules*, 9(12), 1079-1088.
- [7] Büyüktuncel, E., 2012. Gelişmiş ekstraksiyon teknikleri, I. *Hacettepe Üniversitesi Eczacılık Fakültesi Dergisi*, 32(2), 209-242.
- [8] Skrede, G., Wrolstad, R. E., 2002. Flavonoids from berries and grapes. *Functional Foods: Biochemical and Processing Aspects*, 2, 71-133.
- [9] Naczki, M., Shahidi, F., 2004. Extraction and analysis of phenolics in food. *Journal of chromatography A*, 1054(1-2), 95-111.
- [10] Dülger, B., Ceylan, M., Alitsaous, M., Uğurlu, E., 1999. Artemisia absinthium L.(Pelin)'un antimikrobiyal aktivitesi. *Turk. J. Biol*, 23(3), 377-384.
- [11] Kırbağ, S., Zengin, F., 2006. Elazığ yöresindeki bazı tıbbi bitkilerin antimikrobiyal aktiviteleri. *Yüzüncü Yıl Üniversitesi, Ziraat Fakültesi, Tarım Bilimleri Dergisi*, 16(2), 77-80.
- [12] Kırbağ, S., 1999. Hypericum perforatum L.'un değişik ekstraktlarının antimikrobiyal aktivitesi, *Journal of Quafqaz University*, V:II,N:1 102-108.
- [13] Kırbağ, S., Bağcı, E., 2000. Piceae abies (L.) karst. ve Picea orientalis (L.) link uçucu yağlarının antimikrobiyal aktivitesi üzerine bir araştırma” *Journal of Quafqaz University*, V:III,N:1 183-1882.

- [14] Matthews, P., Haas, J.G., 1993. Antimicrobial activity of some edible plants: lotus, coffee and others.” *J.of Food Projection* V:56 N:1 66-68.
- [15] Erkaç, G., Yiğitarıslan, S., 2018. Application of Gallic Acid Produced from Horse Chestnut (*Aesculus hippocastanum*) Shell in Table Olive Maturation. *Eurasian Journal of Food Science and Technology*, 44-52.
- [16] Wilkinson, J. A., Brown, A. M. G., 1999. Horse Chestnut–*Aesculus Hippocastanum*: Potential Applications in Cosmetic Skin- care Products. *International journal of cosmetic science*, 21(6), 437-447.
- [17] Dudek, M.M., Matławska, I., 2011. Flavonoids from the flowers of *Aesculus hippocastanum*. *Acta Pol Pharm*, 68(3), 403-8.
- [18] Stanisavljević, I., Stojićević, S., Veličković, D., Veljković, V., Lazić, M., 2009. Antioxidant and antimicrobial activities of Echinacea (*Echinacea purpurea* L.) extracts obtained by classical and ultrasound extraction. *Chinese Journal of Chemical Engineering*, 17(3), 478-483.
- [19] Balcı, S., Yigitarıslan, S., 2017. Optimization of Ultrasonic Extraction of Total Flavonoids from *Cinnamomum zeylanicum*. *International Journal of Secondary Metabolite*, 4.(3, Special Issue 1), 108-116.
- [20] Ardağ, A., 2008. *Antioksidan kapasite tayin yöntemlerinin analitik açıdan karşılaştırılması (Master's thesis, Adnan Menderes Üniversitesi, Fen Bilimleri Enstitüsü)*.
- [21] Wicks, M.D., Wood, L. K., Garg, L. G., 2006. Methodology for the determination of biological antioxidant capacity in vitro: a review. *Journal of the Science of Food and Agriculture*, 86(13), 2046-2056
- [22] Shirazi, O. U., Khattak, M. A. K., Shukri, N. A. M., Nasyriq, M. N., 2014. Determination of total phenolic, flavonoid content and free radical scavenging activities of common herbs and spices. *Journal of Pharmacognosy and Phytochemistry*, 3(3), 104-108.
- [23] Wang, J., Zhao, Y. M., Tian, Y. T., Yan, C. L., Guo, C. Y., 2013. Ultrasound-assisted extraction of total phenolic compounds from *Inula helenium*. *The Scientific World Journal*, 2013.